1-1-2017

Best Longitudinal Adjustment of Satellite Trajectories for the Observation of Forest Fires (Blastoff): A Stochastic Programming Approach to Satellite System Design

Aaron Bradley Hoskins

Best longitudinal adjustment of satellite trajectories for the observation of forest fires (BLASTOFF): A stochastic programming approach to satellite system design

By

Aaron B. Hoskins

A Dissertation
Submitted to the Faculty of
Mississippi State University
in Partial Fulfillment of the Requirements
for the Degree of Doctor of Philosophy
in Industrial and Systems Engineering
in the Department of Industrial and Systems Engineering

Mississippi State, Mississippi

May 2017

Best longitudinal adjustment of satellite trajectories for the observation of forest fires (BLASTOFF): A stochastic programming approach to satellite system design

By

Aaron B. Hoskins

Approved:

Hugh R. Medal
(Major Professor)

Burak Eksioglu
(Committee Member)

Sandra D. Eksioglu
(Committee Member)

Mohammad Marufuzzaman
(Committee Member)

Stanley F. Bullington
(Graduate Coordinator)

Jason M. Keith
Dean
Bagley College of Engineering

Name: Aaron B. Hoskins

Date of Degree: May 5, 2017

Institution: Mississippi State University

Major Field: Industrial and Systems Engineering

Major Professor: Dr. Hugh R. Medal

Title of Study: Best longitudinal adjustment of satellite trajectories for the observation of forest fires (BLASTOFF): A stochastic programming approach to satellite system design

Pages of Study: 170

Candidate for Degree of Doctor of Philosophy

Forest fires cause a significant amount of damage and destruction each year. Optimally dispatching resources reduces the amount of damage a forest fire can cause. Models predict the fire spread to provide the data required to optimally dispatch resources. However, the models are only as accurate as the data used to build them.

Satellites are one valuable tool in the collection of data for the forest fire models. Satellites provide data on the types of vegetation, the wind speed and direction, the soil moisture content, etc. The current operating paradigm is to passively collect data when possible. However, images from directly overhead provide better resolution and are easier to process. Maneuvering a constellation of satellites to fly directly over the forest fire provides higher quality data than is achieved with the current operating paradigm.

Before launch, the location of the forest fire is unknown. Therefore, it is impossible to optimize the initial orbits for the satellites. Instead, the expected cost of maneuver-

ing to observe the forest fire determines the optimal initial orbits. A two-stage stochastic programming approach is well suited for this class of problem where initial decisions are made with an uncertain future and then subsequent decisions are made once a scenario is realized.

A repeat ground track orbit provides a non-maneuvering, natural solution providing a daily flyover of the forest fire. However, additional maneuvers provide a second daily flyover of the forest fire. The additional maneuvering comes at a significant cost in terms of additional fuel, but provides more data collection opportunities.

After data are collected, ground stations receive the data for processing. Optimally selecting the ground station locations reduce the number of built ground stations and reduces the data fusion issues. However, the location of the forest fire alters the optimal ground station sites. A two-stage stochastic programming approach optimizes the selection of ground stations to maximize the expected amount of data downloaded from a satellite.

The approaches of selecting initial orbits and ground station locations including uncertainty will provide a robust system to reduce the amount of damage caused by forest fires.

Key words: Initial Satellite Orbits, Satellite Maneuvers, Satellite Ground Stations, Stochastic Programming, L-shaped Method, Sample Average Approximation, Forest Fires, Disaster Response

DEDICATION

To Katie, Lori, E.V., and Trey and in memory of Grandma, Grandpa, and K.C.

ACKNOWLEDGEMENTS

This dissertation only has one author listed, but there are many other people that have made significant contributions. First and foremost, I would like to thank my advisor Dr. Hugh Medal. Your assistance in helping me take my notional concepts into functioning models has been incredibly helpful. However, more important than the technical contributions you have made, is the constant support and understanding; while the academics have always been in the forefront, the interest and caring you have shown while I have dealt with the loss of my grandparents and the birth of my first child has been phenomenal. A dissertation is a long journey and it can be easy to lose focus of the bigger picture of life especially if an advisor forgets that their students have more going on than academics. You are the type of advisor I hope to be one day.

My committee has played a vital role in this dissertation as well. When I first enrolled in the program, I was wandering in the wilderness to a certain extent and then Dr. Burak and Dr. Sandra were willing to spend some time serving on a review committee for a class I was taking. (The class should have had a disclaimer in the description that it was the qualifying exam for Chemical Engineering.) After the review was completed, we were talking and that was when I found out that a) I should have an advisor and that b) both of them would be happy to be my advisor. Even after they left MSU, they were willing to

remain on my committee and their feedback and suggestions have helped to strengthen the quality of this dissertation.

Dr. Maruf and I have had a somewhat unusual path. I still remember the first time that we met; I had come to campus for a presentation in Dr. Burak's class and Maruf was also a student in the class and we introduced ourselves. His inputs to the dissertation have always pushed me to try out ideas and algorithms that had not occurred to me and I know that the work is much stronger due to his inputs.

Many of Dr. Medal's other students have helped me out along the way. Mike, Johnathon, and I have been the three distance students going through at the same time and while the proofreading of various papers has been very helpful, just having someone else in a similar situation to reach out to has been even more important. Eghbal and I, being the two "fire guys" in the group, has led to a significant amount of collaboration. As much as I appreciate the technical contributions the three of them have made, the friendships are more important to me. I would also be remiss in not mentioning Chris who ran a number of the simulations for me and completed an independent study course under my supervision.

For any distance student, coworkers at the full-time job also play a critical role in completing a dissertation. Although many of my coworkers have provided support, the two that I am especially indebted to are Michael and Alan. Michael has always been there to let me vent about how a class was going and has never turned me away when I just needed to talk to someone. Alan has been a tremendous support and has verified a number of my derivations and has proctored a number of exams for me (he even chose to work out those problems that were interesting to him).

Even with the support of coworkers, classmates, and faculty, it is not possible to get through the endeavor of a dissertation without unconditional love and support at home. From the very beginning of deciding to enroll in the program, Katie has been with me on every step of the journey and has done as much as she could to help me along the way. I could never have completed this dissertation without everything she has done for me. While becoming a father during the final stages of a dissertation makes an already challenging endeavor more challenging, the smiles from Lori, even when things might not be going exactly how I want them to go, have been invaluable.

TABLE OF CONTENTS

LIST OF TABLES

LIST OF FIGURES

CHAPTER 1

INTRODUCTION

1.1 Introduction

Sputnik 1 was launched in 1957, ushering in the space-age for the human race. In 1960, TIROS-1 was the first weather satellite to be launched. In the decades following, society has become more and more dependent on satellites. The National Aeronautics and Space Administration (NASA) now has multiple constellations of satellites that constantly monitor the Earth to determine weather, land conditions, and other similar types of data. Weather forecasting is more reliable now than it was a generation ago because satellites collect data over the polar regions as well as out in the middle of the ocean and other regions that were not easily monitored before satellites. Satellite images of the coastlines are used to monitor erosion and take appropriate actions to minimize its impact on people and the environment.

This data is especially valuable during a natural disaster. For example, when an area is flooding, knowing how much precipitation to expect with the next storm helps relief personnel to understand if more people need to be evacuated or if it is safe for them to return to their homes. During a forest fire, knowing the moisture content of surrounding vegetation helps in modeling fire behavior and spread. Knowing if a storm is coming or if winds are going to change are additional valuable pieces of information when it comes

to battling the forest fire. A satellite can provide data about soil moisture content by using instruments such as a radiometer at a frequency that is able to pass through vegetation using a variety of polarizations. Precipitation can be measured by analyzing the Doppler frequency of a radar signal. Wind speed can be determined based on multispectral analysis of the data. In general, the various data products can be determined by analyzing different electromagnetic frequencies and satellites are equipped with emitters and detectors for the electromagnetic frequencies that are needed for the data they are designed to collect.

While the satellite data is valuable to the relief personnel, there are obstacles that can prevent them from receiving quality data at the right time. To begin with, the satellite is launched well in advance of the natural disaster and the laws of physics determine where the satellite will be at any point in time. A satellite can be maneuvered, but these maneuvers cost additional fuel. Fuel usage is very important in satellite operations because, to date, there has not been an instance where a satellite has been refueled after launch. For a maneuvered satellite to observe a forest fire, it is critical that the maneuvering is as fuel efficient as possible. However, without knowing where and when the forest fire will occur, an initial orbit must be selected that minimizes the expected maneuver cost. Thus, there is a critical need for tools that can help design initial orbits in preparation of natural disaster observation.

Collection of the data is not the only challenge that is faced for getting information to the relief personnel that need it. Data collected by satellites are transmitted down to the ground at facilities designed to receive and disseminate the data. These facilities are often oversubscribed and there is no guarantee that the capacity will be available to download

the data from the satellite in the most time efficient manner. Because of the potential of a lack of required download capacity, there is value in a critical natural disaster mission having a dedicated set of ground stations to receive the collected data. At the same time, these ground stations are expensive to operate and too many ground stations also leads to a data fusion problem. Because of the cost and the data fusion complication, there is a need to optimally place ground stations in a manner to maximize data collection opportunities.

This dissertation addresses the problems of optimally maneuvering a constellation of satellites and the placement of ground stations. The locations of the forest fires are unknown at the time of the initial decisions (the initial orbits for a constellation of satellites and the locations where ground stations will be constructed) are made. As a result, the problems are solved using stochastic programming techniques. Stochastic programming is used because the problems consist of first-stage decisions that have to be made before the future is known and then subsequent decisions are made to optimize the response to the scenario that is realized. This situation is the problem stochastic programming is designed to solve. In addition, the number of scenarios is substantial and solving the discrete equivalent formulation of the problem is not computationally tractable, so there is a need for a solution approach designed to handle a significant number of potential scenarios. The models are solved to optimize the expected costs over a set of scenarios based on historical data.

1.2 Motivating Example

To illustrate the problems studied in this dissertation, consider the following example. A forest fire has started in Yellowstone National Park. It is currently in the backcountry, but with millions of visitors in the park and the surrounding area, it is imperative to know if the fire is going to head towards the popular areas of the park, such as Old Faithful, or if the fire will remain in the backcountry. The models used to predict the spread of the forest fire do not have enough recent data to accurately predict the spread of the fire. Because the fire is currently deep in the backcountry, it would require personnel driving through rough terrain, which would take too long to get to the area to observe the current conditions. The drones that are available do not have an operating range large enough to fly to the fire, circle while collecting data, and return. Large airplanes with appropriate sensors could fly over the region to collect the data instead of satellites, but the aircraft and crew are unable to perform daily flights for a month due to maintenance requirements and the logistics of rebasing the aircraft and crew. In order to appropriately update the models, higher-resolution data than what will be available from satellites is needed. Even if the satellites were able to collect the required high-resolution images, higher-priority missions are monopolizing the available ground station resources and the capacity is not available in the system to download the data from the satellite and get it to the response team. The only option available to the relief personnel is to use the best data they have, send in resources based on the outdated data, and adjust the plan once it begins to fail. If the location of the forest fire had been known in advance of the fire, then better pre-planning could have been performed to ensure that good data were available.

While that scenario is based on the current paradigm of satellite operations where the satellite has a fixed orbit, there is more that can be done. The satellite has the ability to collect the required data resolution, it just needs to get closer to the forest fire to collect it. A sequence of maneuvers can adjust the satellite's orbit so that rather than being miles to the east or west of the forest fire, it flies directly over the forest fire. If the location of the forest fire were known in advance, then an appropriately equipped airplane and crew would be stationed in the area for the entire duration of the fire.

This dissertation investigates a methodology to determine the optimal initial orbits for a constellation of satellites that will minimize the expected fuel costs required for the satellites to maneuver so as to fly directly over the forest fire. Therefore, the required high-resolution data will be collected and the plan of attack developed by the relief personnel will be based on current data. Also, whereas a drone or airplane would have to expend fuel for each and every flight, once the satellite is in an orbit to fly directly over the forest fire, it will return to the forest fire on a daily basis or more.

In addition, by optimally placing ground station facilities, the capacity will be available for downloading the high-resolution data after it is collected. This dissertation also investigates a methodology to determine the optimal locations of ground station facilities. With ground stations built to handle the data collected by the constellation of satellites, the high-resolution data will be downloaded from the satellites and will be received by the relief personnel to allow for an appropriate attack on the forest fire.

1.3 Statement of the Problem

From the standpoint of a satellite collecting data, a natural disaster can be defined as a latitude and longitude pair with a time-stamp. For most of this dissertation, forest fires are used as a concrete example. The work does extend to the observation of a point on the ground, but forest fires provide an example of a beneficial use of the additional data. In addition, forest fires can last for months and are constantly changing. They benefit more from maneuvering a satellite for active monitoring as compared to an earthquake that does not have the same day-to-day changing dynamics for months after the initiation of the event.

Natural disasters add a level of complexity to the design of a satellite system because decisions have to be made with an uncertain future, If the desire was to monitor, for example, Starkville, MS, then the satellites could be directly launched into an orbit that flew over Starkville every day. The orbit that flew directly over Starkville would not fly over Clemson, SC every day, but if there was no desire to monitor Clemson, then it would be irrelevant that the satellite did not fly directly over Clemson. Conversely, if there was the desire to monitor Clemson and not Starkville, then a different initial orbit could be selected for that mission. However, when there is not that upfront knowledge of what location the satellite has to fly over, then it is not possible to pick an orbit *a priori* that is optimal for the realized scenario.

Rockets do not sit on launchpads fueled and ready to launch at a moment's notice. There is not a warehouse of satellites waiting to be launched. Even under ideal circumstances where a rocket was already at the launch complex, a few days are required to as-

semble the rocket and have it ready for launch. Mounting the satellite to the rocket would require a minimum of three days if it also already happened to be at the launch complex. After launch, a few days are required to deploy the solar panels, checkout and calibrate all of the sensors, communication equipment, and other components of the system. In the best-case scenario, the satellite is collecting data ten days after the natural disaster occurs. However, for routine missions, the time from satellite arrival at the launch complex to collecting data is several months and not ten days. Launching a satellite in direct response to a forest fire is not practical, so maneuvering the satellite is the only feasible option.

The satellites are launched and circle the Earth following their orbital path. Once the forest fire is realized, the satellites optimally maneuver so that they each fly directly over the forest fire once each day. Determining the maneuver sequence once the disaster is realized is a problem that appears in the literature [44], but a key component of the problem remains. In practice, the location and time of the forest fire are unknown when the initial orbits are selected. Therefore, the initial orbits should be selected in such a way as to minimize the expected cost of maneuvering from the initial orbits to the forest fire observing orbits. Thus, the first problem this dissertation addresses is determining a means to optimally select the initial orbits given an unknown future fire location.

The second problem of this dissertation aims to increase the amount of data collection for a satellite by utilizing both the ascending and descending components of the satellite's orbit. A significant amount of data is collected as the constellation of satellites fly over the forest fire, but there is the potential for even more data to be collected. During each revolution, the satellite first flies from the south, crosses the latitude of the forest fire, and

then continues northward. During one revolution each day, the forest fire is directly under the satellite as it flies towards the north. However, during each revolution the satellite flies from the north, crosses the latitude of the forest fire, and then continues southward. It is possible to maneuver the satellite so that it is flying south over the latitude of the forest fire at the same instant that the forest fire is under the orbital path resulting in two contacts per day rather than only one. While the maneuvering required to synchronize the forest fire and satellite's movements will require fuel, it will also provide for a greater amount of collected data. The second problem of this dissertation addresses optimally choosing the initial orbit of a constellation of satellites to allow for each satellite to collect data twice per day.

The last problem of this dissertation considers the ground stations used to download data. Satellites collect data as they fly over a forest fire and download the data to facilities on the ground. There is a limited capacity of the amount of data that the satellite can store, so having sufficient download capacity is the only means of preventing data from being lost. The location of the forest fire impacts the optimal location of a ground station. For example, if the forest fire surrounded the ground station, then the satellite would not be able to collect data of the forest fire while simultaneously downloading data to the ground station; as a consequence, either the full capacity of the ground station will not be used or less data will be collected. Also, if the satellite is flying from the south to the north and the ground station is south of the forest fire, then the satellite will have download capacity before it has data and will have data when it does not have download capacity. Unfortunately, the ground stations must be built prior to knowing the location

of the forest fire. The third problem addressed by this dissertation closes the loop on the satellite system; it optimally places satellite ground stations based on historical forest fire and hurricane data.

1.4 Purpose of the Study

Uncertainty introduces complications into an optimization problem because a solution does not need to be found for one discrete case, but instead needs to best handle a wide variety of scenarios. In the literature concerning satellite collection of natural disaster data, uncertainty has before now been ignored and the location of the satellites and natural disaster are known at epoch. While that approach does provide a methodology that can be used once a natural disaster occurs, it is not ideal for mission managers attempting to design a mission that must respond to an unknown forest fire location. This dissertation is the first to include uncertainty in the location of the forest fire and thus fills a gap in the literature.

The aerospace community uses metaheuristics to solve this class of problems and metaheuristics do provide good upper bounds to minimization problems. At the same time, an upper bound is not necessarily optimal and its quality can only be determined by establishing a lower bound demonstrating how close the solution is to the true optimal solution. This dissertation introduces techniques from the operations research (OR) community to the aerospace community that produce solutions that are provably optimal or at least provide an optimality gap. When millions, if not billions, of dollars are going to be spent building and operating a system, it is important to understand if the solution is optimal, or

at least close to the optimal solution, or if it is potentially far from the optimal solution, but just happens to be the best solution found so far.

1.5 Significance of the Study

The aerospace community has a variety of complex problems that could benefit from algorithms developed by the OR community. However, the two communities do not have a significant amount of communication; at the INFORMS Annual Conference in 2016 there were only two presentations concerning satellites and one of the two was work done as part of this dissertation. As a result, the aerospace community cannot exploit algorithms to more efficiently solve their problems or to demonstrate the quality of their solutions through concepts such as an optimality gap. At the same time, the OR community will benefit from a new set of complex domain problems that require better algorithms.

This dissertation desires to help to provide a bridge between the two communities. The dynamics modeled in this dissertation are more advanced than what is typically studied in the OR literature and while algorithms have been modified and applied, there is still the potential for more development to improve solution run times. The algorithms being applied have allowed for a class of problems that has up until now not been addressed by the aerospace community in large part due to the intractable nature of the formulation of problems with uncertainty using other solution algorithms.

The significance of this dissertation is its solution of a class of problems that has not been previously solved in the aerospace community while introducing more complex dynamics into models solved with algorithms from the OR community. It provides a starting

point for researchers from both communities to advance their fields due to interactions with the other community.

The potential practical impact of this dissertation is significant. Earth reconnoissance missions are common and the ability to be operationally responsive to changing satellite missions is an active area of research. Designing initial orbits that can efficiently change to allow for high-resolution imagery of a location has the potential to increase the amount of data collected. The techniques developed as a part of this dissertation could be used to monitor any location on the ground whether the location of interest is a forest fire or a building. The optimal selection of ground stations can be extended to a variety of ground assets as well. For example, the same methodology could be used to select the optimal location of sensor sites to detect satellites flying over. The dissertation has the ability not only to improve the collection of data for forest fires as a means to help to optimally use fire suppression resources, but the techniques can be extended to related missions.

1.6 Definition of Terms

1.6.1 Astrodynamics Primer

An orbit is the path the satellite follows around a central body; for this dissertation, the central body is the Earth. The orbit is fixed in an inertial Cartesian coordinate system which is centered at the center of the Earth with the positive z-axis extending through the North Pole, the positive x-axis pointing towards the First Point of Ares (the vernal equinox), and the y-axis producing a right-handed coordinate system. Figure 1.1 gives a graphical representation of the coordinate system as well as the orbital elements that will be described below.

At every instant in time, the satellite has a position and velocity that can be defined in terms of this coordinate system. By integrating over time, the orbit of the satellite can be determined. Two satellites at the same location with different velocities are on two different orbits and as a result, performing a maneuver by expelling propellent changes the satellite's velocity and thus changes its orbit.

Six elements uniquely describe an orbit and the inertial position and velocity Cartesian state are not the most ideal set to use due to the fact that all six elements are constantly changing. An alternative set of six elements are the classical (or Keplerian) elements. The six elements are: semi-major axis (a), eccentricity (e), inclination (i), right ascension of the ascending node (Ω), argument of perigee (ω), and true anomaly (ν). A majority of textbooks agree on the variable representing the first five elements, but ν, f, and θ are all commonly used for the true anomaly. This dissertation uses the convention that the true anomaly is represented by ν.

All orbits follow conic sections with the center of the Earth at a focus with ellipses and circles being orbits that remain orbiting the Earth. Satellites sent to other planets, such as the Voyager spacecraft, are placed on hyperbolic orbits and do not remain orbiting the Earth. This dissertation does not include interplanetary travel, so all orbits are either circular or elliptical. Two properties of an ellipse are the semi-major axis and eccentricity. The semi-major axis is the line that passes through the two foci of the ellipse with end points on the ellipse; the eccentricity, a number between 0 and 1 for an ellipse, is the ratio of the distance from the center of the ellipse to the focus divided by the semi-major axis; it is a measure of how elongated the ellipse is. These two elements (semi-major axis and

eccentricity) describe the shape of the orbit and are represented by a and e respectfully. A circle is a special case of an ellipse where the two foci are coincident and the eccentricity is 0. The relationship between a circle and an ellipse is analogous to the relationship between a square and a rectangle.

The orientation of the orbit is three of the other required six elements. The inclination of the orbit is the angle between the equatorial plane and the orbital plane (equivalently, it is the angle between the angular momentum vector and the z-axis) and is represented by i. For every orbit with an inclination greater than 0 , there is a unique point in the orbit where the satellite crosses the equator coming from the southern hemisphere; this point is the ascending node. The angle from the x-axis to the ascending node is the right ascension of the ascending node and is represented by Ω. The two points where the semi-major axis intersects the orbit are called perigee and apogee. Perigee is the point of the orbit where the satellite is closest to the Earth; apogee is the point on the orbit where the satellite is furthest from the Earth. The perigee distance is calculated with equation (1.1) while the apogee distance is calculated with equation (1.2) The angle from the ascending node to perigee is the argument of perigee (ω) and is the third angle that describes the orbit's orientation.

$$r_p = a(1 \quad e) \tag{1.1}$$

$$r_a = a(1 + e) \tag{1.2}$$

The sixth element is the true anomaly and it is defined as the angle from perigee to the satellite's location on the orbit and is represented as ν. Note that the advantage of the

Keplerian elements is that five of the elements are constant and only one is time-varying because the orientation and shape of the orbit are constant and only the position on the orbit changes with time. The primary advantage to working in Keplerian element space rather than Cartesian space is the simplicity introduced by the time-invariant nature of five of the six values.

An orbital period is the amount of time required for the satellite to travel 360 (one complete revolution) in true anomaly and is only a function of the semi-major axis and the gravitational parameter of the Earth (μ) and is calculated using equation (1.3). Other important quantities that are derived from the orbital elements are the distance from the center of the Earth to the satellite with equation (1.4) and the speed of the satellite using the vis viva equation (equation (1.5)).

$$P = 2\pi\sqrt{\frac{a^3}{\mu}} \tag{1.3}$$

$$r = \frac{a(1 \quad e^2)}{1 + e\cos(\nu)} \tag{1.4}$$

$$V = \sqrt{\frac{2\mu}{r} \quad \frac{\mu}{a}} \tag{1.5}$$

When a satellite passes over a point coming from the south, that is an *ascending-pass* over the point. On the other hand, if the satellite is coming from the north, that is the *descending-pass*. As an example, a satellite flying over the Gulf of Mexico and then flying over Starkville, MS is on an ascending-pass over Starkville, but a satellite flying over Tennessee and then Starkville is on a descending-pass over Starkville. Figure 1.2 shows the ascending- and descending-passes over the equator for a satellite. The orbit is fixed in

inertial space, so the inertial positions do not change. However, the Earth rotates, so the location on the ground below the satellite changes.

The previous discussion is true for all satellites and is independent of additional satellites. This dissertation includes constellation of satellites; constellations of satellites are groups of satellites that operate in combination to achieve a mission objective. One of the best known constellation of satellites is the Global Positioning System (GPS) constellation. The GPS constellation uses signals from multiple satellites as a means to determine the location of a GPS receiver; a single satellite could not be used to determine the location of the receiver so the system requires multiple satellites in the constellation.

Typically constellations of satellites consist of virtually identical satellites in similar orbits. The members of the constellation usually have a majority of the orbital elements identical, but differ in one or two elements. One common design are for the members of the constellation to all have different true anomaly values, but the other five elements are identical. A second common design is for there to be a difference in the right ascension of the ascending node and potential a difference in true anomaly as well. This dissertation employs the second type of constellation because it allows for up to two direct flyover opportunities per constellation member per day. The other common constellation design would only allow for two total direct flyover opportunities per day.

At every instance in time, the satellite is directly over a location on the ground. The time history of the collection of latitude, longitude pairs can be plotted on a map to produce the satellite's ground track. The maximum latitude of all of the points on a satellite's ground track is equal to the orbit's inclination. The position vector from the center of the Earth to

the satellite is always contained in the orbital plane that is rotated i above the equatorial plane. The maximum angle of the position vector above the equatorial plane is i . Latitude is defined as the angle above the equatorial plane. Therefore, the maximum latitude of the ground track is the inclination of the orbit. A consequence of this relationship is that the minimum inclination of an orbit in this dissertation must be at least the maximum latitude of all forest fires of interest.

A satellite performs a maneuver by having fuel pass from its storage tanks and out through a nozzle. The change in the velocity of the satellite (V) is based on the exit velocity of the gas leaving the nozzle (V_e), the initial mass of the satellite (m_0), and the mass of the satellite after the propellant has been expelled (m_f) and is most commonly referred to as the *rocket equation*.

$$V = V_e \ln \frac{m_0}{m_f} \tag{1.6}$$

The exhaust velocity is different for different types of propellants and the design of different aspects of a satellite system are usually proceeding concurrently. Therefore, the team designing the orbit will commonly design maneuvers around the value of V rather than the amount of fuel consumed. This dissertation does not take into consideration the amount of propellant consumed by the maneuver. It uses the change of orbital period as a measure of the amount of fuel consumed; the relationship between the orbital period and V is described later.

A *solar day* is exactly 24 hours (1,440 minutes) long and is based on the sun's position in the sky. The *sidereal day* is based on the location of the stars and is based on the Earth's rotation rate. Because this dissertation desires to fly directly over the same ground location every day, the sidereal day is used as the time unit. If the solar day were to be used, then the rotation rate of the satellites and the rotation rate of the Earth would not be synchronized. The difference between the solar and sidereal day can be explained by an example. Assume that the Earth did not rotate and on the first day of the year the sun was directly overhead of a location on the Earth. Six months later, since the Earth is not rotating, the same spot on the Earth no longer has the sun directly overhead; the sun is directly overhead of a location on the opposite side of the Earth. On the first day of the next year, the sun is again directly overhead. During the course of one year, the location on the Earth has experienced one day even though the Earth is not rotating. This extra day due to the Earth revolving around the sun is the difference between a solar and a sidereal day.

At any instant in time, a line can be drawn from the center of the Earth to the satellite and the line will intercept the surface of the Earth at a single point. The time history of these points on the surface of the Earth create the satellite's *ground track*. Figure 1.3 is an example ground track for a circular orbit with a 60 inclination and an altitude of 600 km. An important feature to note is that the sample ground track never goes to a latitude greater than 60 N and never goes to a latitude less than 60 S; for all orbits, the inclination is the limit on the minimum and maximum latitude of the ground track. An equatorial orbit (an orbit with an inclination of 0) has a ground track that never goes above or below the equator.

An important circular, equatorial orbit is a geostationary orbit. The semi-major axis of a geostationary orbit is determined by setting the period equal to one sidereal day in equation (1.3). Because the period is equal to one day and the circular orbit has a constant angular rate, the satellite is rotating at the same rate as the surface of the Earth. The ground track of a geostationary orbit is a single point. Geostationary orbits are beneficial for many applications because being in the same position relative to the surface of the Earth means that they can collect and transmit data continuously. For example, the reason that people can watch satellite TV without needing to constantly move their satellite dish to track a satellite is that the broadcast satellite is in a geostationary orbit. One disadvantage of geostationary satellites are that at an altitude of 35,786 km, they are significantly further from the surface of the Earth than Low Earth Orbit (LEO) satellites. A second disadvantage is that while a geostationary satellite at -90 longitude will have a continuous view of the United States, it will never be able to observe China on the opposite side of the Earth. A third disadvantage is that the GEO satellite cannot observe the regions near the poles due to their stationary positions and the curvature of the Earth. As a comparison Figure 1.4 has the ground track of the same sample satellite mentioned above over one month. As is seen in the figure, over the course of the month, the satellite flies over almost every point on the surface of the Earth between 60 N and 60 S.

The research in this dissertation investigates LEO satellites because the lower altitude provides more detailed images than the geostationary images. In addition, the ground track can be adjusted to best serve the needs of the realized disaster scenario whereas a geostationary satellite would maintain a stationary position.

1.6.2 Operations Research Concepts

All parts of this dissertation include optimization with uncertainty; that is, there are decisions (i.e., first-stage decisions) that must be made with uncertain knowledge of the future. After these first-stage decisions are made, a scenario is realized and subsequent decisions are made as part of the second-stage. The problem is thus to select the first-stage solution that minimizes the expected cost over all second-stage problems. This optimal first-stage solution may not be the optimal solution for any scenario, but it is associated with the lowest expected cost.

As an example, define the first-stage variables as x and the second-stage variables as y. The objective coefficients are c and q respectfully and the constraint matrices are T and W. The constant terms in the constraints is the vector h.

$$\text{Minimize } q^T y + c^T x \tag{1.7}$$

st

$$Wy + Tx = h \tag{1.8}$$

The second-stage problems are independent of each other; only one scenario will be realized. Phrased differently, in the discrete equivalent formulation of the problem, the columns of the W matrix are zero for all variables associated with a scenario other than the scenario associated with the constraint. Therefore, the general model can be rewritten in terms of each scenario s out of the set of scenarios S with the associated probability of the realization of a particular scenario being p_s.

$$\text{Minimize} \sum_{s=1}^{S} p_s q^T y_s + c^T x \tag{1.9}$$

st

$$W_s y_s + T_s x = h_s \qquad \forall s \in S \tag{1.10}$$

The problem is thus decomposed into smaller problems with each scenario being a single problem instance. A decomposition strategy, such as the L-shaped method is capable of solving problems with large numbers of scenarios that cannot be reasonably solved with a discrete equivalent formulation. However, as the number of scenarios approaches infinity, then decomposition strategies are unable to solve the problem in a reasonable amount of time. Sample Average Approximation (SAA) is a method that randomly samples from the set of potential scenarios and determines a statistical upper and lower bound of the problem. This dissertation includes a problem where the number of scenarios becomes intractable for reasonably sized discrete approximation of continuous scenario parameters. For a minimization problem, the lower bound is calculated by solving n random samples of scenarios and taking the mean of the samples. The upper bound is calculated by taking the n first-stage solutions from the lower bound problems and solving n' randomly generated second-stage problems for each of the n first-stage solutions and determining the mean objective value.

There are a variety of ways to sample the scenarios within the SAA approach. A pure Monte Carlo selection selects an independent, identically distributed (iid) value for each scenario parameter for each sample. However, this approach can result in a prohibitively

large estimator variance. One approach to reduce estimator variance is to induce correlation into the sampling procedure. The samples can be negatively correlated using the antithetic variates approach; randomly sample a scenario and then create its mirror scenario. In the Latin hypercube approach one creates a grid of scenarios and randomly samples the grid and eliminates all other cells that have a common index with the selected cell. Stratified sampling also breaks the scenarios into a grid, but requires that each set of scenarios consists of one scenario from each grid cell.

As a means of evaluating the solutions to the stochastic programming model, the expected value with perfect information (EVWPI) and the resulting expected value of perfect information (EVPI) for each of the test cases is calculated. The EVWPI is calculated by solving the *wait-and-see* problem for each scenario (the entire problem, including the first-stage variables, is solved given that the random realization is known) and calculating the weighted average of the objective values of the deterministic solutions, equation (1.11) is the EVWPI value and the EVPI value is the difference between the EVWPI and the two-stage optimal objective value; it is calculated with (1.12).

$$EVWPI = \mathbb{E}\left[\left(\text{Maximize } \sum_i \left(\sum_j \left(c_{i,j}(s)y_{i,j}(s) \qquad z_i(s)\right)\right)\right]\left(\right. \tag{1.11}$$

$$EVPI = EVWPI \quad Cost \tag{1.12}$$

$$\%Difference = \frac{EVPI}{EVWPI} \tag{1.13}$$

There is not usually a single solution to the wait-and-see problem, so while it is used to create a metric, it does not provide an implementable solution. As a first attempt at analysis of a problem, rather than solving the large instance of the problem, a small instance can be

solved. A reasonable initial problem to solve is the *expected-value* problem; the problem is solved using the expected value of all of the scenarios. The result of the expected-value problem is a first-stage solution that is implementable. The value of the stochastic solution (VSS) is calculated by using the optimal set of first-stage variables for for the expected-value problem and calculating the expected cost over all scenarios using those first-stage variable values. The VSS is the difference between that expected value and the expected value of the complete problem.

A portion of this dissertation requires solving for the minimum and maximum of unimodal functions. While linear programming could be used to minimize and maximize the functions, the *Golden Ratio Search* algorithm [32] is more efficient and is implemented. The equations do not have analytical derivatives, so search algorithms based on gradients are not ideal candidates. The equations are unimodal, but not linear. The search procedure works by evaluating the function at two end points and at two points that are a Golden Ratio fraction of the distance between the end points. Based on the function evaluations for the mid points, one of the two replaces an end point. The process iterates until the algorithm converges on the optimal solution.

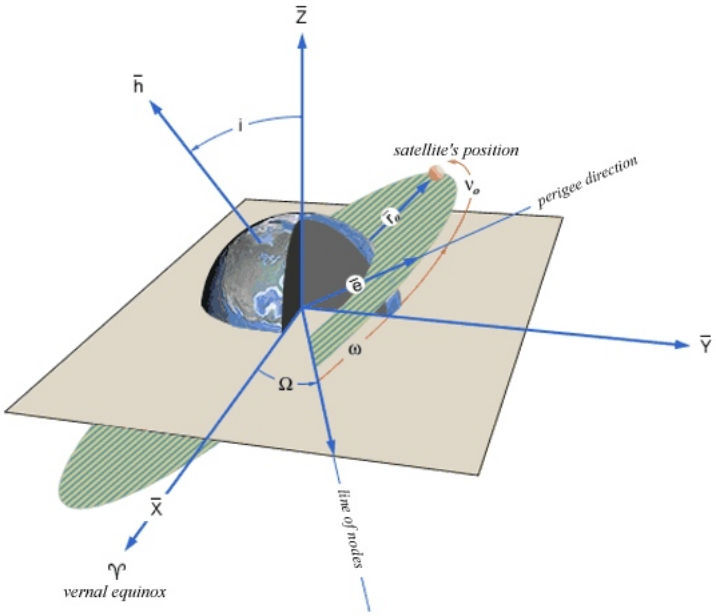

a - defines the size of the orbit
e - defines the shape of the orbit
i - defines the orientation of the orbit with respect to the Earth's equator.
ω - defines where the low point, perigee, of the orbit is with respect to the Earth's surface.
Ω - defines the location of the ascending and descending orbit locations with respect to the Earth's equatorial plane.
ν - defines where the satellite is within the orbit with respect to perigee.

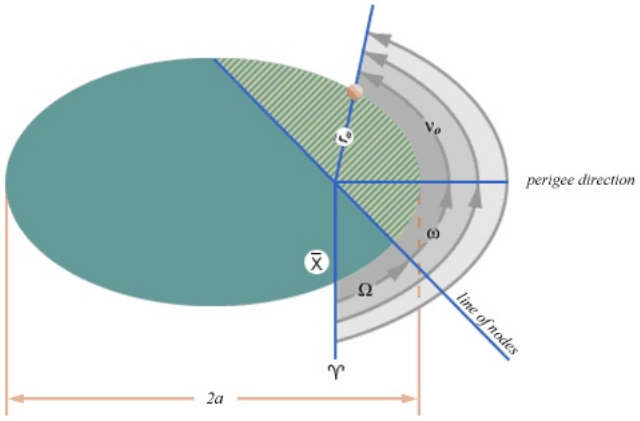

Figure 1.1

Orbital Elements

(Image from http://spaceflight.nasa.gov/realdata/elements/graphs.html)

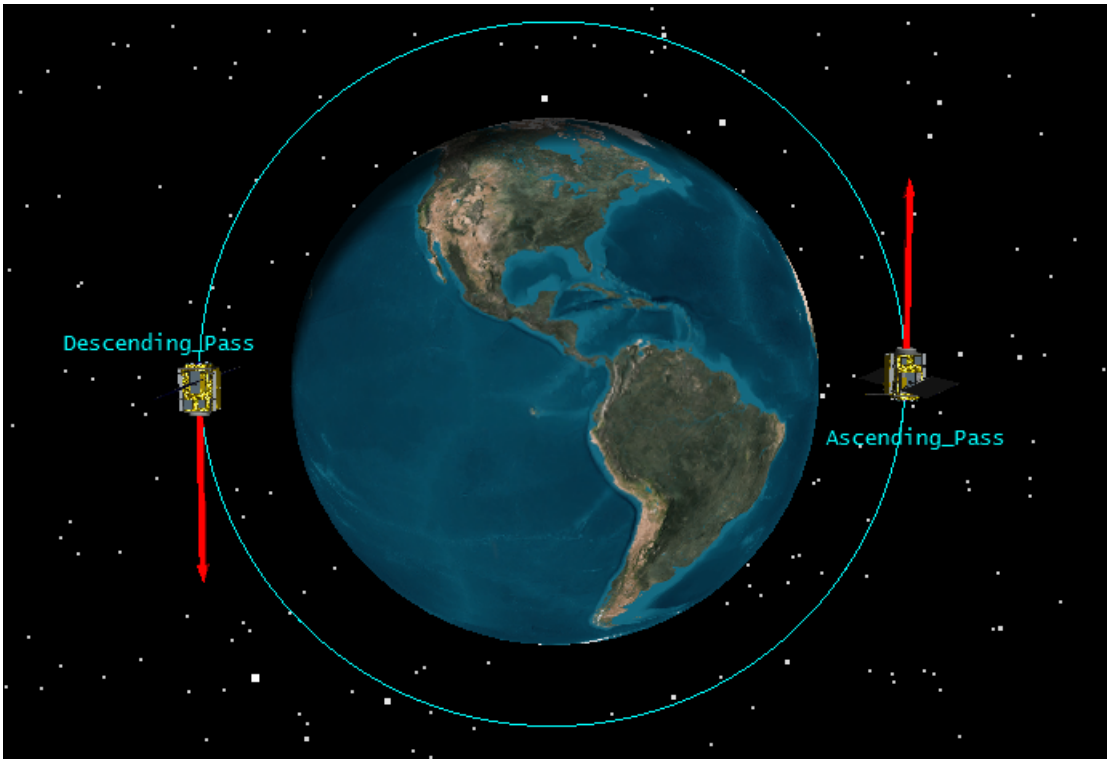

Figure 1.2

Ascending and Descending-Passes

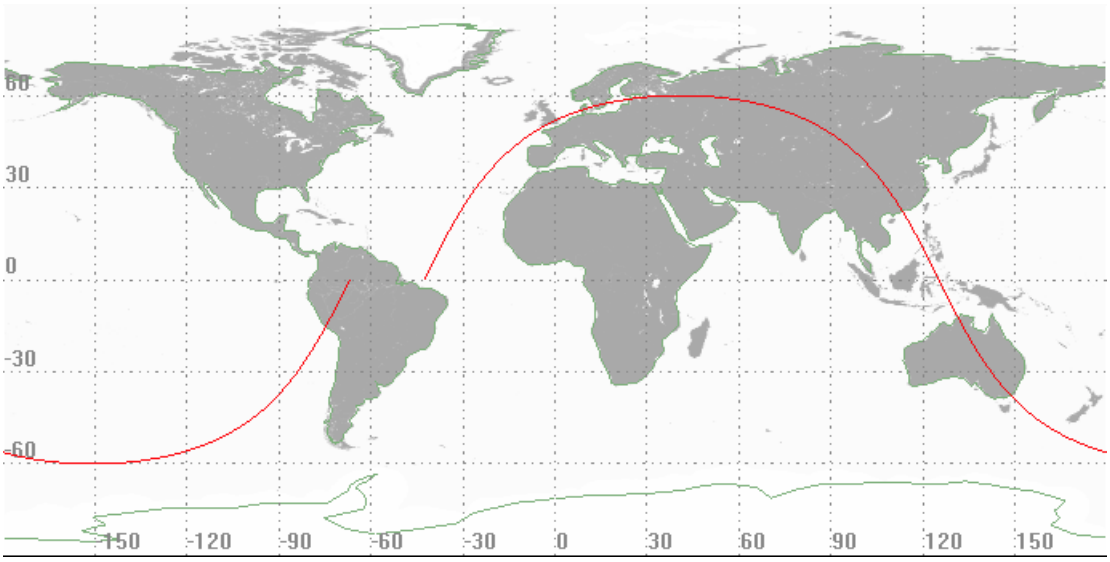

Figure 1.3

60 Inclination Ground Track

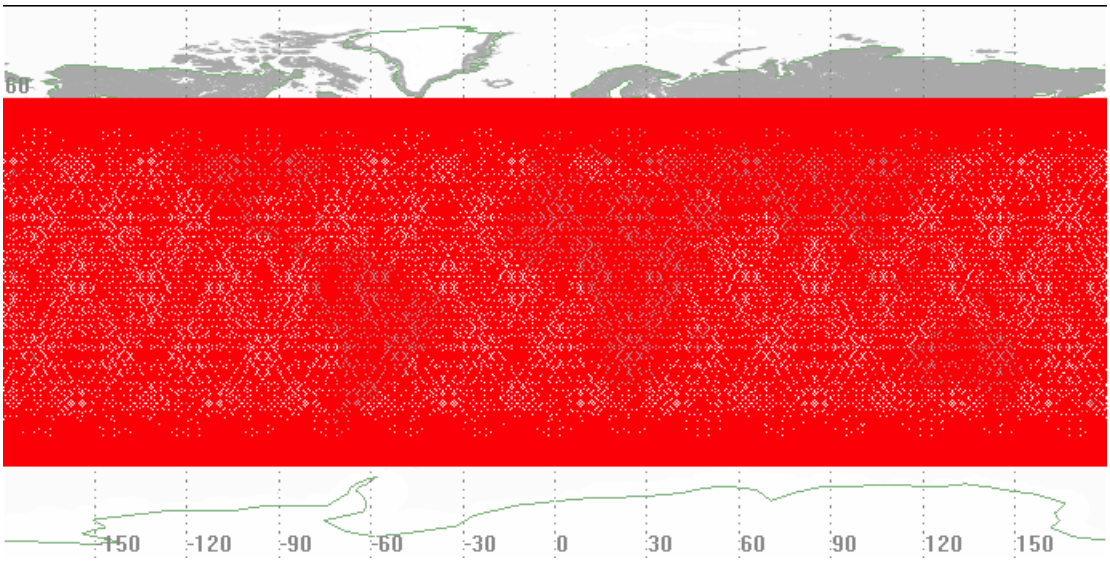

Figure 1.4

60 Inclination Ground Track 1 Month

CHAPTER 2

REVIEW OF THE LITERATURE

2.1 Introduction

This dissertation consists of interdisciplinary research of applying operations research (OR) algorithms to the domain of satellite mission design. The overlap that does exists between these two communities primarily occurs with the scheduling of image collection by satellites. The first component of the forthcoming literature review is focussed on that particular topic. The research that compromises this dissertation does involve image collection. However, the difference between this dissertation and the scheduling of image collection is that this dissertation focusses on the orbit design and the collection and dissemination of data while the image scheduling does not try to adjust or select the orbit and is not concerned with data storage limits and data transmission. Because of the importance of having a starting point in the discussion of the interaction between the two communities, the review is included.

The next sections are concerned with initial orbit selection and maneuver planning. The most common algorithms for these two areas are metaheuristics and brute force enumeration. In comparison, this dissertation uses stochastic programming to join the two problems of orbit design and satellite maneuvering. The review is not a review of all orbit

design and maneuver planning studies, but is focused on concepts that are incorporated into the models designed in this dissertation.

There have been some entries in the literature devoted to satellite orbits and disaster response. These papers set the framework for where this research belongs in the overall landscape. Many of the papers address an area covered by this dissertation, but do not cover the combined problem addressed by this dissertation.

A component of this dissertation involves the construction of ground stations for the receiving of satellite data. While this problem has not been addressed with rigor in the literature prior to this dissertation, the location of facilities and supplies for emergency response has been studied extensively. The final component of this review is focussed on the topic of facility location and disaster preparedness and response.

2.2 Review of Research

2.2.1 Satellite Data Collection Scheduling

At one point, each instrument on each National Aeronautics and Space Administration (NASA) satellite was independently scheduled and the resulting schedules were manually merged [40]. However, this methodology does not guarantee a globally optimal solution and the methodology becomes intractable as the number of available satellites and sensors grows. The problem of satellite data collection is not a classical scheduling problem due to the fact that not all tasks will be scheduled [28]; both the images to be collected and the order of image collection must be determined. There has been a significant amount of research in the area of scheduling image collection for satellite reconnaissance. The scheduling of satellite image collection is a complex problem, and methodologies such

as: heuristics [9], binary programming [38], genetic algorithms [56], local search [82], network theory [93], two-phase task clustering [96], and task merging [99] have been applied. Regardless of the optimization algorithm used, consideration of image priority and onboard storage must be considered [100]. Gabrel [27] introduced a decomposition and flow formulation with binary programming to improve the optimality gap. Wolfe et al. [95] solved the scheduling problem with three different algorithms and determined that the genetic algorithm performed the best, the look ahead algorithm was the second best performer, and the priority dispatch algorithm returned acceptable solutions, but performed the worst. Data fusion is also a key technology with satellite data and it is possible to extract data from a set of observations that are not possible with a single observation [103].

A NASA mission had a constellation of satellites replan the collection and download of data based on observations of the previous revolution [76]. As an additional means to increase the flow of data to researchers, satellite sensors are being web enabled to increase the timeliness and availability of data [12]. However, the problem can morph into the systems of systems domain that crosses both organizational and political boarders [47, 86].

2.2.2 Orbit Design

Previous studies have looked at the design of satellite orbits to perform reconnaissance on a set of locations over a specified amount of time [1] and have included consideration of the Earth-sun vector at the observation times [29]. However, these previous studies designed initial orbits for the satellites with a set of known observation locations. The works did show the importance of appropriately designing initial orbits, but since the location of

the natural disaster is not known before launch, the techniques cannot be readily applied to disaster response. Other work has considered maneuvering satellites to collect data after a natural disaster occurred [14]. However, this work only solved the second half of the complete two-stage problem. The first decision that must be made is what orbits to launch the satellites into and then, after the disaster is realized, the second decision is the maneuver sequence to move the satellites from their initial orbits to the orbits required to collect the data of the natural disaster. The locations of the satellites at the epoch of the forest fire will impact the maneuver sequence required for monitoring the forest fire, so selecting the initial orbits that minimize the expected maneuver cost is desirable.

Previous investigations considered the use of repeat ground tracks for reconnaissance missions using both sliding ground tracks [15] and successive coverage [26]. Efficient methods of selecting repeat ground tracks have been investigated for use inside of metaheuristics [88]. The allure of repeat ground tracks for reconnaissance missions is the fact that the same location is viewed on a consistent basis without the need to expend fuel. Repeat sun-synchronous orbits including perturbing forces have also been investigated [54].

Recovery from natural disasters can take months of cleanup and a natural disaster, such as a forest fire, can last for months. These long-term disaster scenarios require prolonged monitoring and are candidate scenarios for maneuvering satellites for continual observation. Therefore, the models presented in this dissertation include a data collection phase for prolonged monitoring of a forest fire. A circular revisit orbit is a repeat ground track orbit that passes directly over a location of interest twice per day. Analytical methods determining the required conditions for a circular revisit orbit have been established [51].

However, this analytical method requires *a priori* knowledge of the location of interest. The circular revisit orbit is not the only design paradigm that takes the descending-pass into consideration [72]. Similarly, a geometric approach has been applied to determine the revisit time over the course of up to two revolutions for a constellation of satellites [84].

Satellite constellation design can include discontinuous and non-differentiable objective functions that can only be solved using metaheuristics [22]. Research has also used genetic algorithms to design constellations that minimize the average and maximum revisit times [94]. Other researchers have developed a semi-analytical approach based on orbital elements to determine coverage [74]. Research has also found constellation designs with consistent revisit times over all latitudes [58]. Analytical methods have been developed for determining discontinuous coverage of latitude bands [66] and optimization of constellation design [67]. In addition to orbital constraints, research has also looked at including other mission requirements [61].

This dissertation is mainly concerned with having the satellite revisit locations for data collection and transmission. However, other researchers have taken other criteria such as the lifetime of the satellite and the image resolution into consideration during the designing of the orbit [70].

2.2.3 Satellite Maneuvering

This dissertation will present a design that manipulates the ground tracks of a satellite constellation for the observation of a forest fire. Previous research has investigated the concept of manipulating the ground track of a satellite while also considering relative

position to other satellites [48]. In addition, researchers have considered manipulating the ground track by maneuvering for observation of a particular region [77] and maneuvers considering keep-out cones [80]. However, these works have not taken into consideration the combined problem of both selecting the initial orbits and performing maneuvers. Other research has also investigated the optimization of a constellation through reconfigurable maneuvers [2], with other work focusing on the selecting of maneuvers based on technological constraints [17]. Another study did not consider the ground track of the satellite constellation, but considered the relative spacing between satellites to maximize the collection of scientific data [35]. In addition, researchers have investigated the concept of maneuvering satellites in response to a natural disaster such as an earthquake [44]. None of the before mentioned work has investigated the complete problem of initial orbit selection and maneuver planning for an *a priori* unknown location.

Research has investigated the reconfiguration of a satellite constellation due to the addition or subtraction of a satellite [23], but the complexity of the model required the use of a metaheuristic rather than an exact solution method. Other researchers have used traditional nonlinear control techniques to reconfigure a constellation of satellites [21].

Previous research [44, 104] has taken the approach that the natural disaster occurs at some epoch and assigns the states of the satellites at that epoch. To create a maneuver plan to optimize the collection of data for the disaster site, metaheuristics are then used. The results demonstrate that it is possible to design a low cost maneuver sequence to increase the amount of collected data. However, there is no investigation of how the cost changes if the states of the satellites are different at epoch or if the site of the natural disaster is differ-

ent than the one considered. Thus, a gap is present in the literature in the design of initial orbits that will minimize the expected cost of maneuvering the constellation of satellites to monitor a natural disaster. The research presented here helps to fill this gap in the literature. Selecting both the initial satellite orbits and the subsequent maneuvers is requires very large problem instances when uncertainty is included. Our approach, Best Longitudinal Adjustment of Satellite Trajectories for the Observation of Forest Fires (BLASTOFF), described in the remainder of this dissertation, is able to overcome this challenge by using efficient decomposition strategies and exploiting linear relationships to avoid nonlinear solution techniques.

2.2.4 Satellite Collection of Disaster Data

Researchers have examined the general problem of task scheduling for satellites after a natural disaster using heuristics [91] as well as robust methods [102]. There has been work that investigated the tradeoff between observation time and fuel usage [104] after a disaster and as part of mission design [35], but these works assumed *a priori* knowledge about the state of the system that would not be known before a disaster situation. It is also possible to adaptively readjust the tasking part way through a task list in response to a natural disaster [50]. Similarly, Wu et al. [97] used an ant colony optimization algorithm to have disaster data required to be collected and use any remaining resources to collect standing collection requests.

NASA performed an experiment where a forest fire was detected by one satellite and then a trailing satellite in the constellation was tasked with collecting more data of the for-

est fire [55]. Other researchers have investigated the collection of data after an event in order to maximize the amount of data collected, but did not focus on the selection of the ground station locations. Zhu et al. [104] considered observing a site after an earthquake with a sun-synchronous satellite and optimized the amount of collected data using a Particle Swarm Optimization (PSO) algorithm teamed with a Differential Evolutionary (DE) algorithm. Chen et al. [13] used a Self-Adaptive DE Algorithm to take into consideration both the priority of the site as well as the amount of time the site was in view.

Rather than attempting to optimize the collection of data by adjusting the orbit, some researchers have investigated the use of scheduling algorithms to maximize the collection of disaster data by satellites. Wang et al. [92] solved the problem of scheduling for a constellation of satellites tasked for disaster relief using nonlinear programming. Wang et al. [89] use a task-merging scheme to create a dynamic schedule for taking pictures of a disaster site using a constellation of satellites.

Wu et al. [98] identify the benefit of surveillance data after a natural disaster and note the fact that the high demand for data cannot be met with standard operating procedures. Their solution is to cooperatively schedule a heterogeneous set of resources including satellites using a tabu list simulated annealing approach. The authors provide a solution to the problem of the need to increase the amount of collected data after a natural disaster, but use a metaheuristic solution technique. A two-stage approach has also been investigated where the visibility of a location, such as a natural disaster, is first maximized and then the solution is refined by a combination of maximizing collection time while minimizing the coverage gaps [63]; the method relies on *a priori* knowledge of the location to be observed.

Natural disasters occurring near international borders can be of interest to more than one country and fusing data from different information systems can be a challenge. However, it is a challenge that has been researched [46].

The research on satellite motion optimization for disaster relief data collection that has been done previously assumes a static disaster site that is being viewed and does not take into consideration the location of ground stations. Thus, an important research question remains: how to select the locations of ground stations given uncertainty in the location of the disaster? This dissertation seeks to answer this research question by solving a corresponding stochastic optimization problem.

2.2.5 Disaster Preparedness and Response

A problem addressed by this dissertation is a variant of the stochastic capacitated facility location problem [81] and lends itself well to stochastic programming. The problem of this dissertation is related to the facility location problem in that a disaster "generates" data, a satellite collects the data in the form of images and atmospheric readings, and the ground station "consumes" the data.

While not much work has been done by the aerospace community in terms of satellite usage during a disaster, the OR community has performed a significant amount of research concerning disaster relief activities, especially in the area of facility location. Galindo and Batta [30] used a capacitated facility location approach for the selection of disaster relief supplies for distribution following a hurricane. In addition to the location of emergency supplies, Pacheco and Batta [62] added the ability to reposition supplies based on updated

advisories by implementing a combination of stochastic programming and decision theory. Lodree et al. [41] used a two-stage stochastic programming approach to show that pre-positioning supplies is superior to the wait-and-see approach often employed. The optimal selection of hurricane evacuation locations was investigated by Sherali et al. [75] using both a heuristic and an enumeration algorithm. A dynamic allocation model is used by Rawls and Turnquist [65] to pre-locate supplies before a hurricane. Jia et al. [39] investigated the more general problem of a planning for a generic large-scale disaster and used three different heuristic techniques to independently arrive at optimal locations for medical supplies. For the case of an anthrax attack, Murali et al. [60] used a locate-allocate heuristic to decide which locations to open and the corresponding supply and demand.

In somewhat similar research to this dissertation, Averbakh and Berman [3] studied a weighted p-center problem with uncertain node weights and were able to achieve an analytical solution. Berman et al. [6, 7] built on this work investigating centralizing resources and locating facilities in the presence of incomplete information. Lu and Sheu [53] built on that work by investigating the placement of urgent relief centers as a robust p-center model using a heuristic method to solve the NP-hard problem. Drezner [20] used a heuristic approach to solve the p-median problem where it is assumed that the facility may not be operational all of the time and that demand may need to be met by the second closest facility. In similar work, Huang et al. [36] observed that while the p-center problem assumes that each facility is able to meet all demand, this is not necessarily true during a large scale emergency; they used dynamic programming to solve the problem where each facility cannot meet all demand.

CHAPTER 3

INITIAL ORBIT SELECTION FOR FOREST FIRE MONITORING

3.1 Introduction

Currently satellites fly passively and collect data about natural disasters on a happenstance occurrence. As a result of this practice, the amount of collected data is less than could be if the satellites maneuvered to increase their data collection opportunities of a disaster location. This chapter presents a methodology for selecting the initial orbits for a satellite constellation in order to minimize the expected maneuver cost over a variety of disaster scenarios. The goal of the chapter is to identify a methodology for initial orbit selection and subsequent maneuvering that will minimize the expected fuel costs of the maneuvers while providing significantly more data than is available with the standard operating procedures.

3.1.1 Motivation

Satellites have conducted reconnaissance since the earliest days of the space program [16]. After a natural disaster, satellite data can be a valuable asset to the relief effort, whether the disaster is a volcanic eruption [43], a hurricane [5], a tsunami [101], an earthquake [68], or a forest fire [31]. Due to the value satellite data can provide during an emergency, being able to collect as high of quality data as frequently as possible is ad-

vantageous. Because the time and location of a natural disaster are not known at the time satellites are launched, the quantity and quality of the collected data is a random quantity. The satellites are able to view the disaster location at some point in time from some distance away, but there can be significant time between viewing opportunities and all viewing opportunities can be from a significant distance away.

The shorter the distance between the satellite and the disaster location, the higher the image resolution will be. After a disaster occurs, it is important for planners to have access to high-resolution data products. With a passive system, such as the current operating paradigm for Earth observing satellites, there is no ability to increase the resolution of the collected images of the disaster location or the frequency of the image collection. To date, researchers have focused on data fusion as a means to increase the resolution of images, seeking to identify more fires from orbit [73]. However, there are limitations to the improvement of the resolution with this technique. A more direct way to increase the image resolution is to decrease the distance between the satellite and the fire. Combining the data fusion and the decreased distance will even further enhance the image resolution.

There are dozens of satellites currently in orbit with the task of observing the Earth. The various satellites have different types of sensors and are able to detect a wide range of natural occurrences. For example, the National Aeronautical and Space Administration's (NASA) Landsat program has been continually using a series of satellites starting in the 1970s. NASA initially launched Earth Observer 1 (EO-1) as a one-year experiment, but the data collected by EO-1 proved to be so valuable that, rather than decommissioning the satellite at the end of its one-year mission, EO-1 is still collecting data. By collecting

satellite data at various wavelengths, it is possible to detect measurements such as wind speed, temperature, moisture, etc. However, currently none of these satellites is actively maneuvered to collect data due to a natural disaster or other significant event. As a result, the data is available to the end users whenever the satellite happens to fly over a location of interest.

This chapter proposes an approach of actively maneuvering the satellites of a constellation to increase both the resolution of images collected of a disaster site as well as the frequency of image collection. A constellation of satellites is a group of satellites that work together for a common goal; a well-known example is the Global Positioning System (GPS) constellation. For this chapter, the satellites are maneuvered in such a way that each satellite flies directly over the disaster location once per day providing the highest possible image resolution at a high collection cadence.

While satellite data is important for all natural disasters, this dissertation focuses on its use for forest fires as a motivating example; however, it would be possible to expand the techniques developed in this chapter to monitor any natural disaster. Forest fires are a concrete base case for this dissertation because of the significant number of different uses for satellite data [19]. Satellite data can help determine the vegetation of an area before a fire [42, 45], detect and monitor forest fires [52, 73], help predict the spread of a forest fire [10, 25, 24], and determine its environmental impacts [59, 79]. A shortcoming of satellite data for forest fires is the ability to detect smaller fires [64], but our approach, Best Longitudinal Adjustment of Satellite Trajectories for the Observation of Forest Fires

(BLASTOFF), of flying directly over the disaster site will increase the image resolution and thus make even smaller fires capable of benefiting from the use of satellite data.

This chapter uses an exact solution method rather than a metaheuristic method and that provides for a provably optimal solution. By using a decomposition strategy, we are able to ensure that the problem remains tractable even with a large number of scenarios and, as a result, are able to solve problem instances that are large enough to realistically capture the uncertainty in the location of a natural disaster. Modifications of the L-shaped method are included in the solution methodology to increase the speed of convergence of the algorithm. The chapter also introduces a new way to model the problem that takes advantage of linear relationships that exist in the complex dynamics of a satellite's motion. We show through empirical analysis that our proposed solution technique significantly increases the quantity and quality of data collection opportunities. Analysis also shows that our proposed solution is robust over a wide array of scenarios. As an additional significant contribution of this chapter, we show that our solution enhances the current practice by providing both higher quantity and quality data for forest fire observation.

3.1.2 Contributions

This dissertation is the first to address the problem of selecting initial satellite orbits while minimizing the expected fuel costs for observation of an unknown disaster location. While previous research has examined maneuvers from an arbitrarily selected epoch, the research presented here removes the assumption of a known epoch to fill the gap in the literature created by the assumption. It also presents a class of algorithms that has not been

utilized by the aerospace community to solve this class of problem. The use of an exact solution technique and the accompanying model provide for a computationally efficient solution. The end goals of this chapter are to: 1) Demonstrate the ability to solve the problem of initial orbit selection under uncertainty using a stochastic programming algorithm. 2) Provide a model that accurately and efficiently represents the complex dynamics of satellite motion for observation of a ground location. 3) Present a solution that provides more data with better resolution than the current operating procedures. To reach those goals we provide the following contributions: 1) We solve the problem of satellite orbit selection and maneuvering with uncertain future events using an enhanced L-shaped method. 2) We take advantage of certain linear relationships that exist in the dynamics of the problem to linearize our model. 3) We show through independent simulation that the solution resulting from our model produces more images at higher levels of quality as compared to existing methods used in practice.

3.2 Model Description and Formulation

3.2.1 Underlying Dynamic Relationships

The purpose of this chapter is to design a constellation of satellites in such a manner that minimizes the expected cost of maneuvering the satellites to all fly directly over a forest fire once per day. The location of the forest fire is not known in advance of the launch of the satellites. The model includes a few assumptions. First, there is no consideration of the time of day. The constellation of satellites will have a variety of collection opportunities throughout the day, so there will be some night observations and some daytime observations. However, a forest fire admits a large amount of light, so visual night images

might still be valuable. In addition, satellite sensors detect more than the visible wavelengths of light (as an example, infrared wavelengths can be measured), so data collected during the nighttime does have value and, depending on the wavelength collected, can be more valuable than daytime collections. Second, forest fires are more likely to occur during the summer than during the winter, but the model does not specify the launch date nor the amount of time between launch and the forest fire epoch; therefore, the model is indifferent in terms of the time of the year. The model starts at the epoch of the forest fire and maneuvers the satellite constellation for monitoring once the location of the forest fire is realized. Third, maneuvers are impulsive; the satellite travels along an orbital path and then it exhausts gas out of a thruster and the position does not change, but the velocity does change. With a change in velocity, the satellite now follows a different orbital path. Fourth, the only force acting on the satellite, other than its impulsive maneuvers, is Earth with a uniformly distributed mass. These last two assumptions are common assumptions made during initial mission planning and are reasonably accurate [85].

A satellite performs a maneuver by having fuel pass from its storage tanks and out through a nozzle. The change in the velocity of the satellite (V) is based on the exit velocity of the gas leaving the nozzle (V_e), the initial mass of the satellite (m_0), and the mass of the satellite after the propellant has been expelled (m_f) [83] and is most commonly referred to as "the rocket equation".

$$V = V_e \ln \frac{m_0}{m_f} \tag{3.1}$$

The exhaust velocity is different for different types of propellants and the design of different aspects of a satellite system are usually proceeding concurrently. Therefore, the team designing the orbit will commonly design maneuvers around the value of V rather than the amount of fuel consumed. This dissertation will likewise be concerned with only the change in velocity rather than the expelling of propellant. The velocity (V) of a satellite at any point can be calculated if the distance from the center of the Earth to the satellite (r), the satellite's orbit's semi-major axis (a), and the gravitational parameter of the Earth ($\mu = 398,600.4415 \frac{\mathrm{km}^3}{\mathrm{s}^2}$) [85] are known. The satellite's orbit is an ellipse; the semi-major axis is the line from the center of the ellipse through a focus to the perimeter; it is a measure of how big the ellipse is. The gravitational parameter of the Earth is the gravitational constant multiplied by the mass of the Earth.

$$V = \sqrt{\left(\frac{2\mu}{r} - \frac{\mu}{a}\right)} \tag{3.2}$$

The maneuvers performed as part of this dissertation are assumed to be impulsive and do not change the orbital plane of the satellite. Impulsive maneuvers are a very common assumption made during the initial trade studies of potential maneuver sequences and is a reasonable assumption for this dissertation. Therefore, to calculate the V of the maneuver, equation (3.2) can be used to calculate the pre- and post-maneuver velocities with the difference being the value of V where the final semi-major axis value (a_f) and the initial semi-major axis value (a_0) are the only differences between the two values obtained.

$$V = \sqrt{\left(\frac{2\mu}{r} - \frac{\mu}{a_f}\right)} \quad \sqrt{\left(\frac{2\mu}{r} - \frac{\mu}{a_0}\right)} \tag{3.3}$$

The amount of time required for a satellite to make one complete revolution of its orbit is the orbital period (P); π is the normal geometry value where there are 2π radians in a circle [85].

$$P = 2\pi\sqrt{\left(\frac{a^3}{\mu}\right)} \tag{3.4}$$

The period is only a function of the semi-major axis. The only value that changes in equation (3.3) is the semi-major axis. Therefore, we use the change in period ( ) as a surrogate for the maneuver cost.

$$= 2\pi \left(\sqrt{\left(\frac{a_f^3}{\mu}\right)} \quad \sqrt{\frac{a_0^3}{\mu}}\right)\left(\right) \tag{3.5}$$

3.2.2 Objective Function

The objective function of the model is the expected value of the summation of all maneuvers over all revolutions ($j \in J$) for all satellites in the constellation ($k \in K$) for all scenarios ($s \in S$). The summation is of the absolute value because fuel has to be expelled to either increase or decrease the semi-major axis; it is similar to driving your car in reverse consumes gas rather than putting gas into your tank. Minimizing the amount of fuel used during the maneuvers will allow for a longer mission lifetime and minimizing the magnitude of the maneuvers determined by the model will minimize the amount of fuel used by the satellite. There would be benefit in balancing the amount of fuel used by each

satellite in the constellation, but that complexity is outside of the scope of this dissertation. The value of for satellite k on revolution j for scenario s is $_{j,k}(s)$.

$$\text{Minimize } \mathbb{E}_S \sum_{j=0}^{J} \sum_{k=1}^{K} \left(\quad _{j,k}(s) \right| \tag{3.6}$$

3.2.3 Scenario Definition

The location and epoch of the forest fire are unknown at the time of launch; selecting the initial orbits takes place before knowing the location and epoch of the forest fire. Then, the forest fire occurs and the satellites maneuver to maximize data collection. The problem consists of a set of decisions made with an uncertain future, then an event is realized and subsequent decisions are made. This problem lends itself well to a two-stage stochastic program with scenario uncertainty.

Each of the scenarios is defined based on the geometry between the anchor satellite and the forest fire at the epoch of the realization of the forest fire. The difference in the longitude of the forest fire and the longitude of the location directly below the orbit at the latitude of the forest fire ($_0$) is one component of the geometry of the scenario as is seen in Figure 3.1. The other component is the difference in true anomaly between the anchor satellite's current location and the location of the first maneuver (ν_0) as is seen in Figure 3.2.

3.2.4 First-Stage Variables

The optimal cost maneuver sequence between two co-planer orbits is a Hohmann transfer [34] that performs two maneuvers with one being at apogee (the point on the orbit fur-

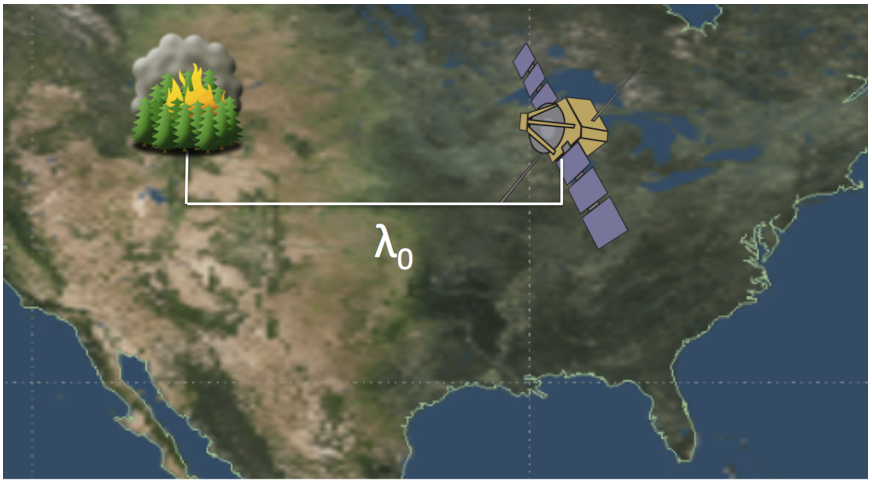

Figure 3.1

Illustration of $_0$

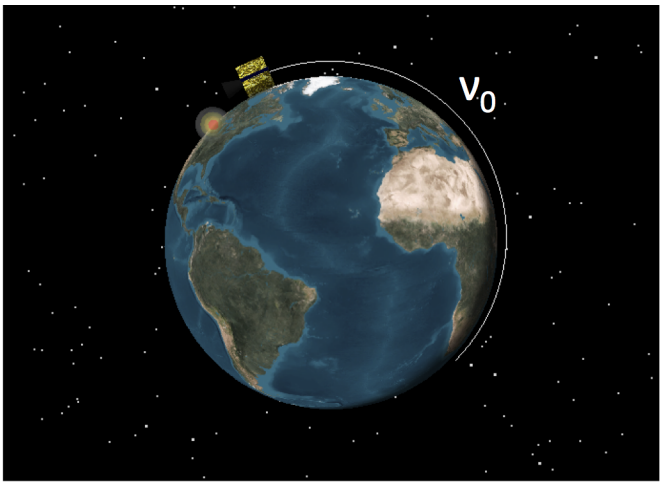

Figure 3.2

Illustration of ν_0

thest from the Earth) and the other at perigee (the point on the orbit closest to the Earth). The initial orbits of the constellation are circular. For Earth observing missions, circular orbits are primarily chosen because, as can be seen from equation (3.2), a circular orbit has a constant speed because the distance from the Earth to the satellite is constant. Apogee and perigee can be any points of a circular orbit that are 180 apart. For this dissertation, the first maneuver is performed 180 away from the ascending-pass over the latitude of the forest fire location and subsequently the second maneuver is directly above the latitude of the forest fire location during the ascending-pass. The elapsed time between two points of an orbit is nonlinear. An exception to this is that apogee and perigee are half of the orbital period away from each other. Therefore, by constraining the maneuvers and the viewing of the forest fire to occur at either apogee or perigee, there is a linear relationship in time between all points of interest. Because the orbit is circular, there is no fundamental difference in the orbital location that is designated as the point that will align the satellite with the latitude of the forest fire. Since it does not matter, in terms of the dynamics, which orbital location views the forest fire, it is beneficial to choose a location that has a desirable mathematical characteristic.

The constellation consists of K satellites and the differences between the satellites are the *longitudinal spacing* and the *true anomaly*. These two differences are the first-stage design variables of the constellation. The other first-stage design variable is the initial orbital period (P_0). The longitudinal spacing between satellite k and the anchor satellite is Ω_k and is constrained between a minimum (Ω_{min}) and a maximum (Ω_{max}) parameter. The

difference in true anomaly is represented by the difference in time (t_k), and is constrained to be less than the initial orbital period.

3.2.5 Second-Stage Variables and Constraints

Once the forest fire has occurred, the anchor satellite will have an amount of time (τ) to transition from the initial orbit to the data collection phase where the satellite will pass directly over the forest fire once per day. The number of revolutions required for the transition phase ($g_k(s)$) is dependent on both the satellite and scenario.

The model includes a constraint that requires each satellite to be in the data collection location at the exact instant that the forest fire will be passing below the orbit.

$$\left(\sum_{j=1}^{g_k(s)} \frac{2P_{j,k}(s) + \quad_{j,k}(s)}{2}\right)\left(+\frac{1}{2}P_{g_k(s)+1,k} + \frac{\nu_0(s)}{360}P_0\right.$$

$$\left(\ {}_0(s) + \Omega_k\right)\frac{1,436.07}{360} = \tau \quad t_k \qquad \forall k \in K, s \in S \qquad (3.7)$$

$$0 \leq t_k < P_0 \qquad \forall k \in K \qquad (3.8)$$

$$\Omega_{min} \leq \Omega_k \leq \Omega_{max} \qquad \forall k \in K \qquad (3.9)$$

A maneuver is performed at the beginning of an orbit and the same maneuver is performed halfway through the orbit to perform a Hohmann-like transfer from one orbit to the next. Therefore, the period of the next orbit for a satellite/scenario pair ($P_{j+1,k}(s)$) is the period of the current orbit for the satellite/scenario pair ($P_{j,k}(s)$) plus the maneuver performed at the halfway point of the current orbit ($\quad_{j,k}(s)$) plus the maneuver performed at the start of the next orbit. The maneuvers are bounded by a maximum magnitude of

an allowable maneuver ($_{max}$) and the period is bounded by a minimum (P_{min}) and a maximum (P_{max}) value.

$$P_{j+1,k}(s) = P_{j,k}(s) + \ _{j,k}(s) + \ _{j+1,k}(s) \qquad \forall j \in J, k \in K, s \in S \qquad (3.10)$$

$$_{max} \leq \ _{j,k}(s) \leq \ _{max} \qquad \forall j \in J, k \in K, s \in S \qquad (3.11)$$

$$P_{min} \leq P_{j,k}(s) \leq P_{max} \qquad \forall j \in J, k \in K, s \in S \qquad (3.12)$$

To better understand constraint (3.10), consider the example illustrated by Figure 3.3 and Table 3.1. The satellite is flying in the outer circular orbit with a period P_0. Then, the forest fire occurs and the first maneuver is at location A changing the orbital period to P_1. The satellite is now on an elliptical transfer orbit for half of a revolution at which time it is directly over the latitude of the forest fire at location B. To circularize the orbit, the same maneuver is performed at B that was performed at A. The P variables are defined to start at the commencement of a full revolution and the satellite has not traveled a full revolution, so there is no new P variable. The satellite continues on the middle circular orbit until it reaches location C and performs maneuver $_2$ to change to the elliptical transfer orbit between the middle and inner circular orbits. Between the setting of the values for P_1 and P_2, two maneuvers have occurred, so both maneuver values must be added to P_1 in order to calculate P_2. Similar to before, a maneuver is performed at location D to circularize the orbit. When the satellite reaches location E, P_3 has begun, so the value is calculated. Since no maneuver is performed at location E, $_3 = 0$.

During the collection of data phase, the satellites are constrained to make exactly 15 revolutions over the course of a day. By requiring exactly 15 revolutions, each satellite is

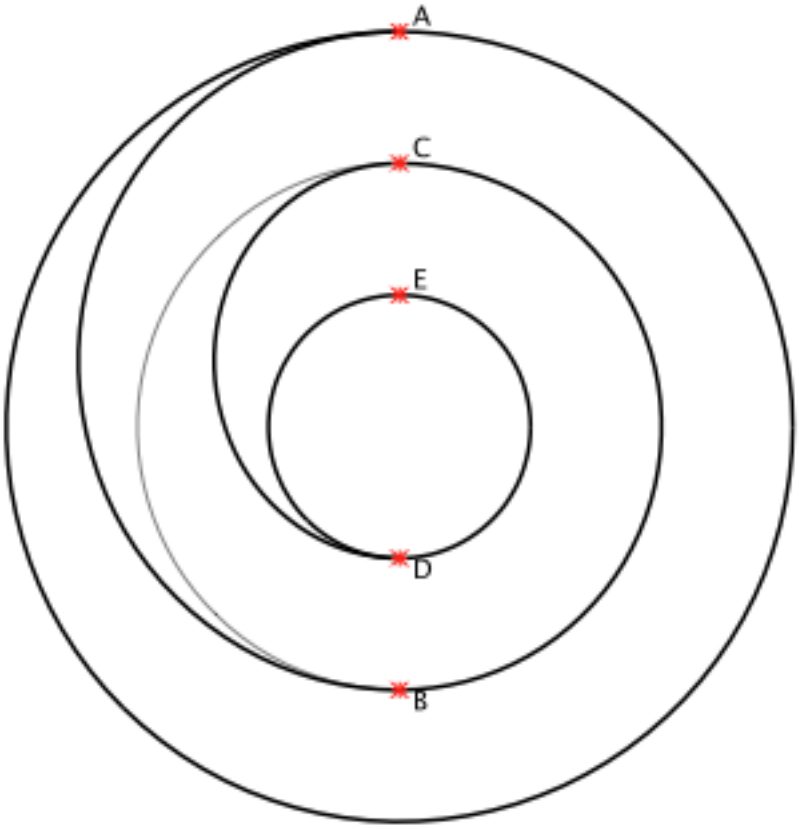

Figure 3.3

Maneuver Locations for Example

Table 3.1

Maneuver Sequences for Example

Location	**P Before**	**Maneuver**	**P After**	**Time to Next Maneuver**
A	P_0	$_1$	$P_1 = P_0 +$ $_1$	$\frac{1}{2}P_1$
B	P_1	$_1$	$P_1 +$ $_1$	$\frac{1}{2}(P_1 +$ $_1)$
C	$P_1 +$ $_1$	$_2$	$P_2 = P_1 +$ $_1 +$ $_2$	$\frac{1}{2}P_2$
D	P_2	$_2$	$P_2 +$ $_2$	$\frac{1}{2}(P_2 +$ $_2)$
E	$P_2 +$ $_2$	$_3$	$P_3 = P_2 +$ $_2 +$ $_3$	$\frac{1}{2}P_3$

directly over the forest fire once per day. The day index (d) is an integer and there are D days of collection. The amount of time that it takes to rotate 360 relative to the stars is the sidereal day and is 1,436.07 minutes.

$$\sum_{j=1}^{14} \frac{2P_{g_k(s)+1+15d+j,k}(s) + \quad _{g_k(s)+1+15d+j,k}(s)}{2}\Bigg)\Bigg(+ \frac{1}{2}P_{g_k(s)+1+15d,k}(s) + \frac{1}{2}P_{g_k(s)+1+15d+15,k}(s) = 1,436.07 \qquad \forall d \in D, k \in K, s \in S \tag{3.13}$$

For notational simplicity, the set $\mathcal{I}$ is introduced.

$$\mathcal{I}_k(s) = g_k(s) + 1 + 15d \qquad \forall d \in D \tag{3.14}$$

Performing a maneuver during data collection can prevent data collection. The orientation of the satellite for collecting the image and the orientation for performing the maneuver might not be identical; therefore, the satellite can only achieve one of the orientations. Even if the orientations happen to be identical, the expelled gas of the maneuver could interfere with the data collecting sensors. Performing the maneuver can also cause the satellite to shake and this could smear the images as well. Therefore, an additional constraint requires no maneuvers are performed during imaging opportunities.

$$_{j,k}(s) = 0 \qquad \forall j \in \mathcal{I}_k(s), k \in K, s \in S \tag{3.15}$$

The problem consists of a set of decisions made (P_0, Ω_k, and t_k) followed by a scenario being realized ($_0$ and ν_0) and then the response ($P_{j,k}(s)$ and $_{j,k}(s)$) being scenario dependent. The problem can therefore be broken into a first-stage problem with supporting second-stage problems. Because the Earth rotates at a constant speed and because the anchor satellite's speed is constant for the initial orbit, the scenarios will be uniformly distributed values between 0 and 360 for each of the scenario parameters. The scenarios are all equally likely. In the subsequent section, we describe how this model can be solved using an enhanced L-shaped method.

3.3 Solution Method

3.3.1 Reformulation

The issue that arises in using the L-shaped method to solve the model is the fact that the objective function of the second-stage is not linear. To address this issue, we linearize the second-stage objective function. The variable $_{j,k}(s)$ is replaced in the constraints

with the set of variables ($^{+}_{j,k}(s)$ $_{j,k}(s)$) where $^{+}$ is the positive component of the maneuver and is the negative component of the maneuver. Because both variables are magnitudes, neither can be negative. We also replace the objective function (equation (3.6)) with the following:

$$\text{Minimize } \mathbb{E}_S \sum_{j=0}^{J} \sum_{k=1}^{K} \left(\; ^{+}_{j,k}(s) + \; _{j,k}(s) \right. \tag{3.16}$$

$$0 \leq \; ^{+,}_{j,k} \; (s) \leq \; _{max} \qquad \forall j \in J, k \in K, s \in S \tag{3.17}$$

In addition to reformulating the model as described above, cuts are added to the model to improve the efficiency of solving the model. The L-shaped method adds cuts to the model if a solution to the first-stage does not have a feasible solution in one of the second-stage problems. Before implementing the L-shaped method, we determine the range of values of P_0 that are feasible for all scenarios for the anchor satellite. There is a minimum ($P_{min,g}$) and a maximum ($P_{max,g}$) orbital period that allows the 15 revolutions to be completed in exactly one day. The first orbital period of the data collection phase is defined as P_g. These worst-case values assume that the maximum magnitude maneuver is performed on all of the 15 orbits (until the minimum or maximum allowable period is reached). As a result, the bounds on the minimum and maximum period at the beginning of the data collection phase can be calculated by the following two linear programs (LP).

$$P_{min,g} = \text{Minimize } P_g \tag{3.18}$$

st

$$P_{j+1} = P_j + \; _j + \; _{j+1} \qquad \forall j \in J \tag{3.19}$$

$$\frac{1}{2}P_g + \sum_{j=g+1}^{g+14}\left(P_j + \frac{1}{2}\quad_j\right) + P_{g+15} = 1,436.07 \tag{3.20}$$

$$P_{min} \leq P_j \leq P_{max} \qquad \forall j \in J \tag{3.21}$$

$$_{max} \leq \quad_j \leq \quad_{max} \qquad \forall j \in J \tag{3.22}$$

$$_g = 0 \tag{3.23}$$

$$_{g+15} = 0 \tag{3.24}$$

$$P_{max,g} = \text{Maximize } P_g \tag{3.25}$$

st

$$P_{j+1} = P_j + \quad_j + \quad_{j+1} \qquad \forall j \in J \tag{3.26}$$

$$\frac{1}{2}P_g + \sum_{j=g+1}^{g+14}\left(P_j + \frac{1}{2}\quad_j\right) + P_{g+15} = 1,436.07 \tag{3.27}$$

$$P_{min} \leq P_j \leq P_{max} \qquad \forall j \in J \tag{3.28}$$

$$_{max} \leq \quad_j \leq \quad_{max} \qquad \forall j \in J \tag{3.29}$$

$$_g = 0 \tag{3.30}$$

$$_{g+15} = 0 \tag{3.31}$$

Once the minimum and maximum values for the orbital period at the beginning of the data collection phase has been established, it is then possible to calculate the minimum and maximum initial orbital periods for the anchor satellite for each scenario. The lower bound on the initial orbital period ($P_{min,0}$) is the maximum of the minimum values and the upper bound on the initial orbital period ($P_{max,0}$) is the minimum of the maximum values.

$$P_{min,0} = \text{Maximize}\left(\text{Minimize}_S\ P_0\left(s\right)\right) \tag{3.32}$$

st

$$P_{j+1}(s) = P_j(s) + \quad_j(s) + \quad_{j+1}(s) \qquad \forall j \in J \qquad (3.33)$$

$$\sum_{j=1}^{g_0(s)} \left(P_j(s) + \frac{1}{2} \quad_j(s) \right) \left(= \tau + \quad_0(s) \frac{1,436.07}{360} \quad \nu_0(s) \frac{P_0(s)}{360} \right. \qquad (3.34)$$

$$P_{min} \leq P_j(s) \leq P_{max} \qquad \forall j \in J \qquad (3.35)$$

$$_{max} \leq \quad_j(s) \leq \quad_{max} \qquad \forall j \in J \qquad (3.36)$$

$$P_{min,g} \leq P_g(s) \leq P_{max,g} \qquad (3.37)$$

$$P_{max,0} = \text{Minimize}\left(\text{Maximize}_S \; P_0(s)\right) \qquad (3.38)$$

st

$$P_{j+1}(s) = P_j(s) + \quad_j(s) + \quad_{j+1}(s) \qquad \forall j \in J \qquad (3.39)$$

$$\sum_{j=1}^{g_0(s)} \left(P_j(s) + \frac{1}{2} \quad_j(s) \right) \left(= \tau + \quad_0(s) \frac{1,436.07}{360} \quad \nu_0(s) \frac{P_0(s)}{360} \right. \qquad (3.40)$$

$$P_{min} \leq P_j(s) \leq P_{max} \qquad \forall j \in J \qquad (3.41)$$

$$_{max} \leq \quad_j(s) \leq \quad_{max} \qquad \forall j \in J \qquad (3.42)$$

$$P_{min,g} \leq P_g(s) \leq P_{max,g} \qquad (3.43)$$

This set of LP solutions adds two cuts to the model that ensures that there is a feasible solution for the anchor satellite for any given selection of the initial orbital period.

$$P_{min,0} \leq P_0 \leq P_{max,0} \qquad (3.44)$$

Bounding the initial orbital period to the feasible range does require solving two LP's per scenario in addition to two LP's to determine the minimum and maximum orbital pe-

riod at the beginning of the data collection phase. These cuts remove infeasible solutions and speed up the algorithm by increasing the likelihood that all second-stages are feasible. However, there is no guarantee of relatively complete recourse due to the two first-stage satellite specific variables. To create a model with relatively complete recourse, we add the feasibility variables $^{+,}_{k}\ (s)$ and include them in the cost with a large penalty coefficient $\mathcal{M}$. A model with relatively complete recourse is desirable due to the significant computation time required to check the first-stage solution for feasibility. The complete model for the problem is:

$$\text{Minimize}\ \mathbb{E}_S \sum_{j=0}^{J}\sum_{k=1}^{K}\Bigg({}^{+}_{j,k}(s) + \quad {}_{j,k}(s) + \mathcal{M}\quad {}^{+}_{k}(s) + \quad {}_{k}(s) \tag{3.45}$$

st

$$P_{j+1,k}(s) = P_{j,k}(s) + \quad {}^{+}_{j,k}(s) \quad {}_{j,k}(s) + \quad {}^{+}_{j+1,k}(s) \quad {}_{j+1,k}(s) \qquad \forall j \in J, k \in K, s \in S \tag{3.46}$$

$$\left(\sum_{j=1}^{g_k(s)} \frac{2P_{j,k}(s) + \quad {}^{+}_{j,k}(s) \quad {}_{j,k}(s)}{2}\right)\Bigg(+ \frac{1}{2}P_{g_k+1,k}(s) + \frac{\nu_0(s)}{360}P_0 \left(\ {}_0(s) + \Omega_k\right)\frac{1,436.07}{360} = \tau \quad t_k + \ {}^{+}_{k}(s) \quad {}_{k}(s) \qquad \forall k \in K, s \in S \tag{3.47}$$

$$\sum_{j=1}^{14}\frac{2P_{\mathcal{I}_k(s)+j,k}(s)}{2}$$

$$\frac{\left(\left(\begin{smallmatrix}+\\ \mathcal{I}_k(s)+j,k\end{smallmatrix}(s) \qquad \mathcal{I}_k(s)+j,k\,(s)\right)\right)}{2}\Bigg)\Bigg($$

$$+\frac{1}{2}P_{\mathcal{I}_k(s),k}(s)+\frac{1}{2}P_{\mathcal{I}_k(s)+15,k}(s)=1,436.07 \qquad \forall k\in K, s\in S \quad (3.48)$$

$$P_{min,0}\leq P_0\leq P_{max,0} \quad (3.49)$$

$$P_{min}\leq P_{j,k}(s)\leq P_{max} \qquad \forall j\in J, k\in K, s\in S \quad (3.50)$$

$$0\leq \begin{smallmatrix}+,\\ j,k\end{smallmatrix}(s)\leq \quad max \qquad \forall j\in J, k\in K, s\in S \quad (3.51)$$

$$\begin{smallmatrix}+,\\ j,k\end{smallmatrix}(s)=0 \qquad \forall j\in \mathcal{I}_k(\omega), k\in K, s\in S \quad (3.52)$$

$$0\leq t_k<P_0 \qquad \forall k\in K \quad (3.53)$$

$$\Omega_{min,k}\leq\Omega_k\leq\Omega_{max} \qquad \forall k\in K \quad (3.54)$$

$$\begin{smallmatrix}+,\\ k\end{smallmatrix}(s) \quad 0 \qquad \forall k\in K, s\in S \quad (3.55)$$

3.3.2 Enhanced L-Shaped Method

The model is solved using the L-shaped method [87] along with several enhancements. The L-shaped method consists of solving a LP consisting of only the first-stage variables (P_0, Ω_k, and t_k) and a variable representing an estimate of the second-stage cost. The solution of this first-stage LP is checked to see if it is feasible for all of the second-stage problems. If the solution is not feasible for all second-stage problems, then a cut is made to the first-stage model based on the simplex multipliers of the infeasible second-stage problem. The first-stage LP is then solved and the new optimal solution is found. This process iterates until a first-stage solution is found that is feasible for all second-stage problems. Next, each of the second-stage LP's are solved using the first-stage solution. The

results provide the cost and simplex multipliers. The cost is checked against the estimated cost solved for using the first-stage LP. If the algorithm has converged, then it terminates. If the algorithm has not converged, then a cut is made to the first-stage problem based on the simplex multipliers from the second-stage LP's and the entire process iterates until convergence.

Because of the unique nature of this model, the L-shaped method has been modified to more efficiently determine the optimal solution. First, all values of Ω_k are independent and do not interact with each other (the same is also true for all values of t_k). Therefore, rather than decomposing the problem based on only the scenario, our modified implementation decomposes the second-stage LP's based on both scenario and the satellite constellation index. Second, because of the weak interaction between all of the different scenarios and the different satellites in the constellation, the feasibility cuts do not encourage rapid convergence on a feasible solution. To encourage convergence, we add the strongest cuts (the P_0 bounds described above) to the first-stage model *a priori* to eliminate as many infeasible solutions as possible. The model can be solved without these first-stage *a priori* cuts, but the amount of run time for the algorithm increases. To avoid the significant time penalty with adding the weaker feasibility cuts and checking for feasibility, a penalty term is added to the second-stage guaranteeing relatively complete recourse. Because the model has relatively complete recourse, the feasibility check is bypassed.

The first-stage model determines the initial orbital parameters and includes θ as a lower bound estimate of the second-stage cost. Each iteration ℓ adds a cut to the first-stage to refine the lower bound of the second-stage cost.

Minimize θ (3.56)

st (3.57)

$$P_{min,0} \leq P_0 \leq P_{max,0} \tag{3.58}$$

$$0 \leq t_k < P_0 \qquad \forall k \in K \tag{3.59}$$

$$\Omega_{min,k} \leq \Omega_k \leq \Omega_{max} \qquad \forall k \in K \tag{3.60}$$

$$E_\ell\left(P_0, t, \Omega\right) + \theta \quad e_\ell \qquad \forall \ell \leq L \tag{3.61}$$

where (P_0, t, Ω) is a vector of all first-stage variables, the values of E_ℓ and e_ℓ depend on the second-stage Simplex multipliers and will be discussed shortly, and L is an index from Algorithm 1.

The second-stage model is solved for a single scenario and a single satellite. The solver does not change the provided first-stage variable values. The k and s terms are not included in the model because only a given set of values is used for each second-stage subproblem.

$$\text{Minimize} \sum_{j=0}^{J} \left(\quad {}_j^{+} + \quad {}_j + \mathcal{M} \quad {}^{+} + \right. \tag{3.62}$$

st (3.63)

$$P_{j+1} = P_j + \quad {}_j^{+} \quad {}_j \quad + \quad {}_{j+1}^{+} \quad {}_{j+1} \qquad \forall j \in J \tag{3.64}$$

$$\left. \sum_{j=1}^{g} \frac{2P_j + \quad {}_j^{+} \quad {}_j}{2} \right) \left(+ \frac{1}{2} P_{g+1} = \tau \quad t + \quad {}^{+} \quad \frac{\nu_0}{360} P_0 \right.$$

$$+ \left(\quad {}_0 + \Omega \right) \frac{1,436.07}{360} \tag{3.65}$$

$$\sum_{j=1}^{14} \frac{2P_{\mathcal{I}+j} + \quad {}^{+}_{\mathcal{I}+j} \quad \mathcal{I}+j}{2} \Bigg) \Bigg(+ \frac{1}{2}P_{\mathcal{I}} + \frac{1}{2}P_{\mathcal{I}+15} = 1,436.07 \tag{3.66}$$

$$P_{min} \leq P_j \leq P_{max} \qquad \forall j \in J \tag{3.67}$$

$$0 \leq \quad {}^{+,}_{j} \quad \leq \quad _{max} \qquad \forall j \in J \tag{3.68}$$

$${}^{+,}_{j} \quad = 0 \qquad j \in \mathcal{I} \tag{3.69}$$

$${}^{+,} \qquad 0 \tag{3.70}$$

For notational simplicity, we can rewrite the second-stage problem to consist of a recourse matrix (W) that contains all of the coefficients for the second-stage variables, a technology matrix (T) that consists of all of the coefficients for the first-stage variables, and a vector (h) that consists of all of the constant terms.

$$\text{Minimize } \sum_{j=0}^{J} \Bigg(\quad {}^{+}_{j} + \quad _{j} + \mathcal{M} \quad {}^{+} +$$

st

$$W\left(P, \quad , \quad \right) = h \quad T\left(P_0, t, \Omega\right)$$

The following pseudo code in Algorithm 1 presents our implementation of the L-Shaped algorithm.

3.4 Numerical Results

The forthcoming analysis is broken into two sections. In the first section, we present representative experiments that detail the optimal initial orbital configuration of the constellation of satellites. In the second section, we compare the solution quality achieved by our constellation as compared to using the current paradigm of non-maneuvering satellites.

Algorithm 1 Modified L-shaped Method

1: $L = v = 0$

2: Set $v = v + 1$

3: Solve first-stage

4: Define first-stage solution as $(P_0, t, \Omega)^v$

5: **for** $s \in S$ **do**

6: **for** $k \in K$ **do**

7: Solve second-stage

8: Determine second-stage simplex multipliers $\pi_k^v(s)$

9: **end for**

10: **end for**

11: Set $E_{L+1} = \frac{1}{S} \sum_{s=1}^{S} \sum_{k=1}^{K} \pi_k^v(s) T(s)$

12: Set $e_{L+1} = \frac{1}{S} \sum_{s=1}^{S} \sum_{k=1}^{K} \pi_k^v(s) h(s)$

13: Set $w^v = e_{L+1}$ $E_{L+1}(P_0, t, \Omega)^v$

14: **if** θ^v w^v **then**

15: Stop; have optimal solution

16: **else**

17: Set $L = L + 1$

18: GOTO 2

19: **end if**

3.4.1 Initial Orbital Parameters

Tables 3.2–3.6 below describe a variety of test cases and the corresponding results. For all test cases, the maximum maneuver magnitude is set to a value of 0.25 minutes ($_{max} = 0.25$). The initial orbital period is bounded between 91.5381 and 105.1186 minutes ($P_{min} = 91.5381$, $P_{max} = 105.1186$); these period bounds correspond to an initial altitude between 350 and 1,000 km. The transition time to the data collection phase is set at 2,872 minutes (τ=2,872).

Although the model has the flexibility to include the bounds of the longitudinal spacing, for these examples, those values are held constant. The values of t_k and Ω_k can be proportionally traded, so including both in a single model is redundant. However, depending on the mission requirements, there could be a need to hold one or the other fixed while varying the other. The more likely of the two to be held constant is the longitudinal spacing, so it held constant in the following test cases.

The scenarios are defined based on the relative spacing between the anchor satellite and the forest fire. The probabilities of all values of the relative spacing are uniformly distributed. For test cases 1–8, we define 5,184 scenarios ($|S| = 5,184$) as being all combinations of $_0$ and ν_0 in 5 steps from 0 through 355 . The model is implemented in C on a 2.9GHz Intel Core i7 processor computer with 16GB of RAM running Mac OS 10.8.5 using Gurobi.

3.4.1.1 Base Case

Test case 1 is the base case and it consists of a constellation of five satellites with a data collection phase lasting for 30 days ($|D| = 30$). The optimal initial orbital period is 97.368 minutes, which is greater than the data collection phase average period of 95.738 minutes. The greater initial period results in a westward shift of the ground track which is a reasonable trend considering the fact that the scenario parameter $_0$ is defined so that a westward shift decreases the separation between the satellite and the forest fire. The optimal objective function value is 9.454 minutes. The fuel cost, in terms of minutes, associated with the five satellites decreasing from the initial orbital period to the repeat ground track period is 8.15 minutes, so only 1.304 minutes (16.745 seconds per satellite) is used for the synchronization of the satellite orbits and the forest fire. As was mentioned above, the longitudinal spacing is held constant. The time separation for the constellation satellites are almost a complete revolution behind the anchor satellite and this delay allows for additional coasting at the initial orbital period. Due to the phasing between the satellites' periods and the Earth's rotation, there is a slight difference in the delay between the different members of the constellation.

Figure 3.4 illustrates the optimal solution for the five satellites in the constellation at epoch for a randomly chosen scenario and a forest fire in Yellowstone National Park. The orbital planes of the constellation satellites are evenly spaced and the satellites will maneuver, based on the second-stage solution so that each member of the constellation is directly overhead of the fire as it passes below and this will repeat each day.

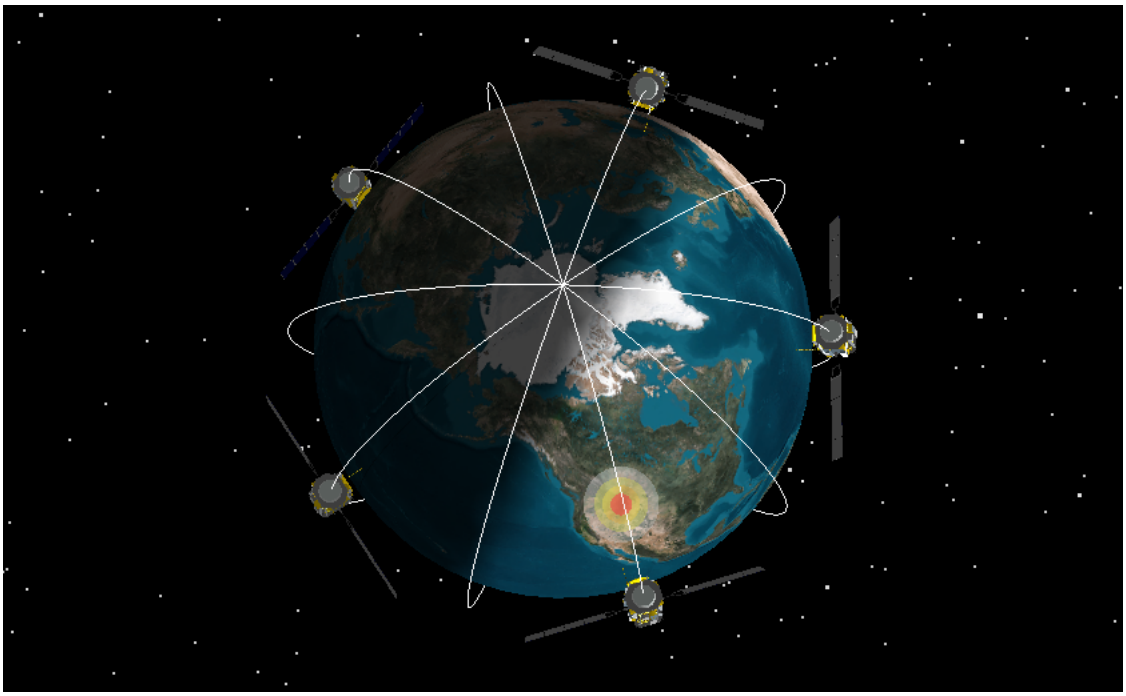

Figure 3.4

Base Case Illustration

If the initial orbital period were 95.738 minutes, then it would take 1,436.07 minutes to complete 15 revolutions and the Earth would have rotated 360 . Because the initial orbital period is 97.368 minutes, 15 revolutions will require 1,460.52 to minutes complete and in that time the Earth will have rotated 366.129 . If a satellite were directly over the Prime Meridian (0 longitude), then after the 15 revolutions it would be directly over 6.129 W. Therefore, the fact that the initial period is greater than the repeat ground track period results in a westward shift of the ground track. Each scenario defines the value of the parameter $_0$ and the model requires that the separation between the satellite and the forest fire be reduced from $_0$ at epoch to 0 at the start of the data collection phase. A westward shift of the ground track reduces this separation.

3.4.1.2 Number of Days in Data Collection Phase Comparison

To investigate the sensitivity of the model to the number of days of the data collection phase, the value of $|D|$ is adjusted and test cases 2–4 are performed. Many of the scenarios result in the satellites reaching a steady-state early in the data collection phase, so solving a larger model that includes more days is time consuming without necessarily resulting in significant change in the final solution. Reducing the value of D down to 1 day causes a small change in the optimal values for the first-stage solution and the small differences are usable considering the uncertainty in the launching of the satellites into orbit. The difference in the 30-day (test case 1) as compared to the 1-day (test case 4) solutions is a difference in P_0 of less than four seconds which corresponds to a difference in altitude of less than 4km and a roughly 1 minute difference in the satellite separation variables

Table 3.2

Base Case Results

Test Case	**1**
$\|K\|$	5
$\|D\|$ (days)	30
P_0 (min)	97.367
Ω_1 (deg)	72
t_1 (min)	94.799
Ω_2 (deg)	144
t_2 (min)	93.553
Ω_3 (deg)	216
t_3 (min)	92.118
Ω_4 (deg)	288
t_4 (min)	90.488
Run Time (sec)	13,563

which corresponds to a difference of roughly 4 of angular separation. The results from test case 4 have the advantage of solving in less than 30% of the time of the base case, but there is the disadvantage that sizing the amount of required fuel onboard the satellite is not possible. However, test case 4 provides a very reasonable solution for further planning of the mission.

3.4.1.3 Constellation Size Comparison

Test cases 5–7 investigate different size constellations as compared to the base case. Whereas with test cases 2–4 there iz minimal difference between the solutions, test cases 5–7 show significantly more difference. Comparing the initial periods between test case 5 and the base case shows a difference in P_0 of over 97 seconds that corresponds to a difference in altitude of almost 80km. The significance of these results is that they show that changing the size of the constellation after the initial design is implemented leads to a less than optimal design. Therefore, it is important for mission managers to know the number of satellites that will be launched throughout the lifetime of the mission because once a constellation has been launched, reconfiguring the constellation to one of a different size could result in orbits that are not optimal.

The initial orbital period is always more than the repeat ground track period causing a desirable westward shift. The time between satellites places the other members of the constellation roughly one complete revolution behind the anchor satellite with the amount of angular separation increasing with increasing longitudinal spacing. A key observation is seen by comparing the run times of test cases 6 and 7. Test case 6 has fewer variables

Table 3.3

Repeat ground track Size Results

Test Case	**2**	**3**	**4**
$\|K\|$	5	5	5
$\|D\|$ (days)	15	7	1
P_0 (min)	97.368	97.367	97.306
Ω_1 (deg)	72	72	72
t_1 (min)	94.802	94.781	95.833
Ω_2 (deg)	144	144	144
t_2 (min)	93.596	93.551	94.620
Ω_3 (deg)	216	216	216
t_3 (min)	92.122	92.119	93.179
Ω_4 (deg)	288	288	288
t_4 (min)	90.467	90.457	91.572
Run Time (sec)	8,021	5,897	4,312

and therefore would be expected to solve more quickly. However, the optimal solution to test case 7 is closer to the boundary and thus has faster convergence. The value of $|K|$ is dependent on the funding available for the project, and, to a certain extent, any requirements on the frequency of observations. It is not possible to solve for a smaller value of K and get generalized results that can be applied to a larger constellation size. In practice, a constellation for this type of mission would have 2 to 5 satellites. Therefore, including the base case, all reasonably sized constellations are considered.

3.4.1.4 Clustered Constellation

The final test case evaluates a mission where the five satellites of the constellation are clumped in an 180 band. This constellation design allows for heavy coverage for half of the day and then minimal coverage for the other half of the day. If the sensors on the satellites performed significantly better either during the day or the night, this type of configuration would be advisable. As is the case with the previous test cases, there is the initial orbital period causing the westward drift of the ground track. The difference between the initial orbital period for the base case and this test case results in over 50 seconds of difference corresponding to over 40km difference in altitude. The smallest time separation for test case 8 results in an angular separation of roughly 270 as compared to the minimal angular separation for the base case of almost 335 . The time between the satellites does not follow the previously observed patterns. Every other satellite is one full orbital period behind the anchor satellite while the others are roughly two-thirds of an orbital period behind; the satellites are not in decreasing time order. One complete revolution is the

Table 3.4

Constellation Size Results

Test Case	**5**	**6**	**7**
$\|K\|$	2	3	4
$\|D\|$ (days)	30	30	30
P_0 (min)	99.000	98.117	98.571
Ω_1 (deg)	180	120	90
t_1 (min)	99.000	78.192	98.571
Ω_2 (deg)	-	240	180
t_2 (min)	-	73.722	98.571
Ω_3 (deg)	-	-	270
t_3 (min)	-	-	85.336
Ω_4 (deg)	-	-	-
t_4 (min)	-	-	-
Run Time (sec)	861	4,963	11,346

bounding constraint for the time between a satellite and the anchor satellite, so the only way to achieve a greater bound is to increase the initial orbital period. However, increasing the initial orbital period potentially increases the overall cost. As a result, some of the satellites would benefit from a larger bound, but the overall cost is too significant. The other satellites would benefit from a lower initial orbital period, but tradeoff a higher initial orbital period with a quicker start to the maneuver phase. With these two forces competing, one set of satellites drives the increase in the initial orbital period and the other set correspondingly decreases the separation time.

3.4.1.5 Granularity of Scenario Grid

For test cases 9 and 10 we investigate the sensitivity of the model to the change in the number of scenarios. The angles ν_0 and $_0$ are continuous and have an infinite number of possibilities, but a finite number of scenarios is required for analysis. Test case 9 is identical to the base case with the exception being that the scenarios are defined in steps of 4 ($|S| = 8,100$ scenarios) rather than steps of 5 ($|S| = 5,184$ scenarios). Similarly, test case 10 has steps of 3 ($|S| = 14,400$ scenarios). As Table 3.6 illustrates, the results are consistent over the different granularities of the scenario grid and it can be reasoned that all three results are close to the true infinite scenario nature of the problem. Too few points of a grid will result in more significant deviation from the true value, but too many points will result in an intractable model. The results of the base case are almost identical to cases 9 and 10, but the runtime for the base case is significantly less. The choice of 5

Table 3.5

Clustered Constellation Results

Test Case	**8**
$\|K\|$	5
$\|D\|$ (days)	30
P_0 (min)	98.214
Ω_1 (deg)	36
t_1 (min)	98.214
Ω_2 (deg)	72
t_2 (min)	77.668
Ω_3 (deg)	108
t_3 (min)	98.214
Ω_4 (deg)	144
t_4 (min)	75.079
Run Time (sec)	10,340

as a base case is a compromise between these two extremes and provides a high level of model accuracy while having a reasonable runtime performance.

3.4.1.6 Run Time Results

To get an understanding of the impact of the model parameters on the run time of our approach, a test matrix is developed. The number of satellites is set to either 2 or 5, the number of days for the data collection phase is set to 15 or 30, and the number of scenarios is set to 5,184 (steps of 5) or 8,100 (steps of 4). All 8 combinations are implemented and evaluated and the results are shown in the "Enhanced L-shaped" column of Table 3.7.

Investigating the change in the number of satellites, the five satellite cases take, on average, about 16.25 times the time required for the two satellite equivalents. Increasing the number of satellites does not result in linear timing differences because more cuts are needed as part of the L-shaped method to better approximate the estimate of the second-stage cost as part of the first-stage solution.

Doubling the amount of days causes a slow-down of approximately 1.75 times the 15-day case for the equivalent 30-day case. A majority of the constraints and variables that compose the second-stage are due to the data collection phase, so doubling the length of the phase also nearly doubles the size of the model being solved, so it is reasonable to assume that it would take approximately twice as long to solve the 30-day model as compared to the 15-day model.

The ratio of the number of scenarios is 1.5625 while the timing ratio is, on average, about 1.72. If the outlier of the group is omitted, then the average ratio is 1.67. The

Table 3.6

Scenario Size Results

Test Case	9	10
$\|K\|$	5	5
$\|D\|$ (days)	30	30
P_0 (min)	97.370	97.372
Ω_1 (deg)	72	72
t_1 (min)	95.032	95.259
Ω_2 (deg)	144	144
t_2 (min)	93.835	93.971
Ω_3 (deg)	216	216
t_3 (min)	92.345	92.485
Ω_4 (deg)	288	288
t_4 (min)	90.673	90.846
Run Time (sec)	25,547	42,556

observed speedup is not linear with the number of scenarios and this fact is again due to the need for more cuts required for the first-stage approximation of the second-stage cost. The observed general trend is that the model parameters that add more refinement to the model (a longer data collection phase or a finer scenario grid) produce speed changes that are close to the ratio of the size change with there being a slight penalty in the speed due to the overhead involved with solving a larger, more complex model. On the other hand, changing the number of satellites fundamentally changes the problem and the added complexity is far greater than simply the change in the model size.

3.4.1.7 Model Performance

A first indication of the model performance is to compare the base case solution employing our solution strategy to the discrete equivalent case. Unfortunately, the discrete equivalent model is not able to converge on the optimal solution. After 219,032 seconds (roughly 2.5 days) the algorithm is terminated. The lower bound is 9.454 minutes of fuel while the upper bound is 9.455 minutes of fuel. The improvement of the bounds is not occurring rapidly, so even though the optimality gap is small, there is still potentially a significant amount of time before the algorithm converges on the optimal solution. At the same time, the results do show that our solution methodology produces the optimal result in significantly less time than the discrete equivalent solution. Because of the significant amount of time for the discrete equivalent for the base case, the methodology is not tested with additional test cases.

The model includes a penalty term to allow for relatively complete recourse (RCR). To investigate the impact of the penalty term, the model is solved without the penalty term, but with feasibility checks that resulted in cuts to the first-stage when a first-stage solution was infeasible for at least one scenario. The solution is identical for the base case, but the run time is significantly different. The base case requires 15,653 seconds while the non-penalty model requires 43,818 seconds or roughly 280% of the time. The model with the penalty term requires roughly 30% of the time and produces identical results, so the use of the penalty term is justifiable.

The solution technique of this chapter includes the concept of producing an initial set of cuts on the P_0 variable as a means of enhancing the algorithm's performance. By introducing the cuts, the algorithm starts with an initial solution that is closer to the optimal solution. As a result, fewer iterations are needed to determine the optimal solution and the total computation time is reduced. Instead of requiring 15,653 seconds to find the optimal solution with the P_0 cuts, not including the cuts resulted in 22,198 seconds required to find the optimal solution; an increase of over 40%.

A final improvement on the standard L-shaped method is to decompose the problem based on satellite and scenario instead of solely by the scenario. The equivalent to the base case with scenario only decomposition requires 31,231 seconds or roughly double the time of the base case. Therefore, including the full decomposition is a beneficial improvement to the algorithm for this problem.

Table 3.7 compares the runtime performance of our enhanced L-shaped method to the runtimes without each of our adaptions over a test matrix of 8 parameter sets. The results indicate that our enhanced L-shaped outperforms all variations over all test cases.

3.4.1.8 EVPI and VSS

As an indication of the quality of the solution based on the expected fuel cost, the expected value of perfect information (EVPI) is calculated. For this problem, it is important to define EVPI in a mathematical sense rather than a practical sense. If perfect information were in fact possible, then the satellites would be launched to monitor the *a priori* known forest fire and would not have a need to maneuver. The definition employed for EVPI is that even though it is not logical to launch the satellites into an epoch state other than directly monitoring the forest fire, it is assumed that the constellation is launched into all previously defined scenarios with equal probability. The optimal solution for each scenario is then independently calculated. The expected value with perfect information (EVWPI) is the expected value that is achieved with a solution that uses *a priori* knowledge of which disaster is going to happen and is therefore able to pick the optimal solution for the particular disaster realization. After this process described above, the EVWPI is determined to be 6.452 minutes of fuel. The EVPI is the difference between the EVWPI and the optimal value is 3.002 minutes of fuel for the base case. It is not ideal for the EVPI to be such a high percentage of the expected cost. Thus, if there were a way to predict the exact day and time of a forest fire years in advance, it would be reasonable to pay a fairly large price

Table 3.7

Model Performance Results

$\|K\|$	$\|D\|$	$\|S\|$	Discrete Equivalent	Enhanced L-Shaped	Without RCR	Without initial P_0 cuts	Without Decomposition by Satellite
2	30	5,184	–	861	10,773	1,519	2,057
5	30	5,184	¿219,032	13,563	43,818	22,198	31,231
2	15	5,184	–	511	5,768	951	1,233
5	15	5,184	–	8,021	58,428	9,745	13,671
2	30	8,100	–	1,430	17,238	2,574	3,014
5	30	8,100	–	25,547	170,469	28,481	59,927
2	15	8,100	–	852	9,250	1,537	2,011
5	15	8,100	–	13,425	87,152	19,409	22,856

for this information as a means to significantly save the amount of fuel consumed by the maneuvering of the constellation to observe the forest fire.

As a second indication of the quality of the solution, the value of the stochastic solution (VSS) is also calculated. This metric solves for the optimal solution for the midpoint of all of the scenarios (the mean-value-problem) and applies the first-stage solution of this midpoint scenario to all of the scenarios. The value of the using a first-stage solution obtained by solving the mean-value-problem for the base case is 9.564 minutes of fuel. The VSS is the difference between the mean-value-problem first-stage and the stochastic solution is 0.110 minutes of fuel. These two metrics indicate that there is a cost associated with the uncertainty represented by the EVPI, but that there is also a cost associated with not taking the stochastic nature of the problem into consideration, as represented by the VSS value. Solving the single scenario that represents the mean scenario value does produce a cost that is very close to the cost associated with solving the complete problem. However, even a 1% fuel savings is enough of an incentive to take the stochastic nature of the problem into consideration. Table 3.8 contains the VSS and EVPI values for all 8 of the timing result cases. The EVPI is greater for the cases where $|K| = 5$ while the VSS value is greater when $|K| = 2$. For the two-satellite constellation, half of the satellites can have the timing between them adjusted while for the five-satellite constellation, four-fifths of the satellites can have the timing adjusted. The greater the number of degrees of freedom for the system, the more the system can adjust to a particular scenario and thus the greater EVPI value. The scenarios are uniformly spaced, so the mean-value-problem is a decent estimate of the system as a whole; having the additional degrees of freedom allows the system to better

fit the scenario and thus to better fit the range of scenarios. As a result, the VSS value is lower for the five-satellite constellation.

Table 3.8

EVPI and VSS

$\|K\|$	$\|D\|$	$\|S\|$	EVWPI	EVPI	EVPI %	VSS	VSS %
2	30	5,184	4.191	0.643	15.33	0.265	5.47
5	30	5,184	6.452	3.002	46.52	0.110	1.16
2	15	5,184	4.191	0.643	15.33	0.265	5.47
5	15	5,184	6.452	3.002	46.52	0.110	1.16
2	30	8,100	4.198	0.643	15.32	0.261	5.39
5	30	8,100	6.467	3.000	46.39	0.114	1.20
2	15	8,100	4.198	0.643	15.32	0.261	5.39
5	15	8,100	6.467	3.000	46.39	0.114	1.20

3.4.2 Comparison With Current Practice

We show above that our methodology is able to produce a set of orbital trajectories for a constellation of satellites that minimizes the expected maneuver cost to create daily repeat ground track passes over a forest fire. However, the question remains as to whether the use of fuel for these maneuver sequences is significantly beneficial to warrant the cost. To investigate the benefits of our design, a two-satellite BLASTOFF constellation is compared

to a constellation consisting of Earth Observer 1 (EO-1) and Aura. EO-1 is a currently operational satellite that has been used to monitor forest fires and other disaster events; it is not in a repeat ground track orbit, so its ground track shifts from day-to-day. EO-1 will not achieve ideal viewing conditions on a very regular basis. It is in a nearly circular, sun-synchronous orbit with an orbital period of 98.7 minutes. Aura is the third component of NASA's Earth Observing System (EOS) and is in a similar orbit to EO-1, but with a different right ascension of the ascending node. These two satellites form a set that is similar enough to the two-satellite BLASTOFF constellation to allow for a meaningful comparison.

Systems ToolKit (STK) 10 is used to simulate a forest fire in Yellowstone National Park and retrieves the two-line element set (TLE) of the actual EO-1 and Aura orbits. The BLASTOFF constellation for the data collection phase based on the solution provided by our model is also added to the simulation. Using commercial, independent software to validate the results prevents any feedback between our model and the comparison results. The data collection opportunities for both sets of satellites of the forest fire are determined as a function of range.

Figure 3.5 shows the results of an independent simulation of the orbits of the two-satellite BLASTOFF constellation and the constellation consisting of EO-1 and Aura. During a revolution, a collection opportunity exists when the range from the satellite to the forest fire goes below a given threshold. As Figure 3.5 shows, for a range of 600 or 650 km, the BLASTOFF constellation achieves one observation opportunity per day per satellite (62 total observations over the 31 days of simulation) while neither EO-1 nor Aura are

able to achieve the threshold and had zero collection opportunities over the entire month. While our optimization model does not take the descending passes of the satellites into consideration, the simulation software does consider both the ascending- and descending-passes. At a threshold of 750 km, the descending-pass over the forest fire comes into view for the BLASTOFF constellation. For range values up to 1,250 km, the BLASTOFF constellation has more collection opportunities over the course of the month as compared to the EO-1 and Aura constellation. The lower the range from the satellite to the forest fire, the higher the resolution of the image. Therefore, the fact that BLASTOFF produces significantly more high-resolution images compared to EO-1 and Aura demonstrates the significant value of maneuvering the constellation for monitoring a forest fire as compared to waiting passively for a happenstance collection opportunities as is done with the current paradigm. The significant takeaway is that over the course of the one month of observations, the BLASTOFF constellation has more than 60 (starting at 600 km range) very high-quality imaging collections that occur on a regular basis and an additional 60 high-quality imaging collection opportunities (starting at 750 km range). At these same ranges, EO-1 and Aura have zero (600 km range) and 32 (750 km range) collection opportunities. The images collected by the BLASTOFF satellite will be of higher benefit for the various models used to predict the spread of the fire. The added detail will also help to better assign appropriate resources to appropriate locations to battle the fire.

At a range of 1,250 km, EO-1 and Aura do have three additional collection opportunity, but the amount of time of a collection opportunity is also an important consideration. A greater amount of time allows for more images to be collected. Figure 3.6 compares the

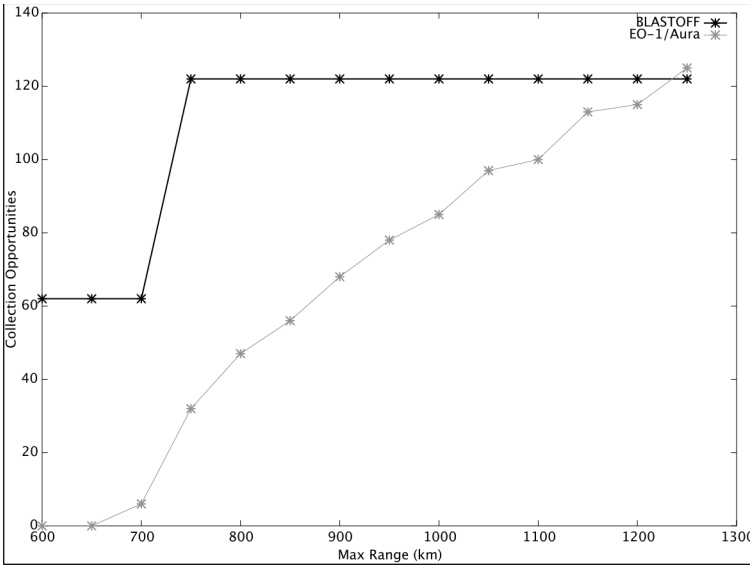

Figure 3.5

Collection Opportunity Comparison

amount of time of the collections over the 31 days as a function of range. The plot includes the minimum, maximum, and average collection times over the month for the two constellations. Two key takeaways from Figure 3.6 are that 1) the average collection time for BLASTOFF is almost always greater than the maximum EO-1 and Aura collection time and 2) the three additional collection opportunity EO-1 and Aura have at 1,250 km range only lasts about 10 seconds, so the extra collection opportunities are not very useful.

In addition to the greater number of collection opportunities, the duration of collection opportunities is also important. As a satellite is approaching a viewing opportunity, the range is decreasing smoothly until the closest approach and the range then increases smoothly as the satellite flies away from the disaster site. Therefore, the collection time

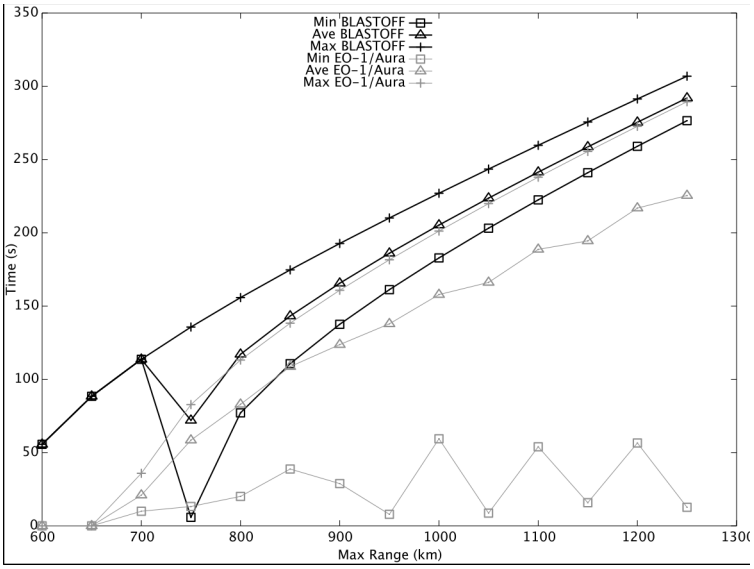

Figure 3.6

Collection Time Comparison

for an opportunity that was not available at a lower range threshold will be relatively small while the collection time for an opportunity that has been available for a number of threshold values will be available for a relatively substantial amount of time. Therefore, the BLASTOFF constellation not only has a greater number of collection opportunities for a given range threshold compared to EO-1 and Aura pair, but it also has longer collection opportunities. The greater number and longer collection opportunities will provide more images and measurements of the forest fire. With the increase in the collected data, models will be more accurate and resources will be more optimally deployed to fight the fire.

3.5 Conclusions

In this chapter, we successfully solve the combined problem of reconfiguring a satellite constellation for the observation of a forest fire as well as the optimal selection of the initial orbits to minimize the expected fuel usage. Previous researchers have decoupled these two problems, but this chapter demonstrates the value of solving the combined problem. Rather than using a metaheuristic, as is common practice in the satellite orbit design community for this class of problems, we create a model that is solved using an exact method that produces a provably optimal solution. Due to the large number of variables that are present in the discrete equivalent formulation of the model, a metaheuristic would likely have convergence difficulties in a comparable amount of time to that required by our stochastic programming approach. Our model is solved using a modified L-shaped method that includes *a priori* feasibility cuts and a deeper decomposition strategy that help to reduce the computation time for the model. To create a model with relatively complete recourse to avoid the significant time penalty associated with checking feasibility, the model includes a high cost penalty that allows for relatively complete recourse.

The results show that for the base case of a constellation of five satellites with uniformly spaced orbital planes the optimal spacing between true anomalies for the satellites is roughly 5 , with the anchor satellite behaving slightly differently. The initial orbital period is slightly above the 15 revolutions per day ground track imposed by the model for the data collection phase and this allows for smooth synchronization between the constellation and the viewing opportunities. In addition to demonstrating the use of an exact method to solve a coupled constellation orbit design and maneuver sequences for forest fire mon-

itoring, our solution is compared to the standard practice using independent simulation software. The BLASTOFF constellation achieves more high-quality observation opportunities for greater amounts of time than the currently used non-maneuvering paradigm.

The test cases indicate that reducing the number of repeat ground track days can significantly reduce computation time, while not significantly influencing the optimal first-stage solution. While the final analysis should include the more complete model, initial analysis can use a smaller problem without much loss in terms of identifying candidate solutions. In addition, if the desired monitoring were for an even greater amount of time than has been assumed in the base case, it is reasonable to assume that the solution for the longer monitoring will be very similar to the 30 day monitoring of the base case.

Satellite data is already an important tool used in monitoring disaster locations. The methodology we have presented in this chapter will allow for the collection of higher-resolution images arriving at a set cadence. The value of satellite-derived data will increase with the increase of the image quality and quantity. The use of an exact method that is provably optimal also guarantees that our maneuver cost is the globally optimal cost rather than being potentially only a locally optimal maneuver cost. Due to the significant cost of launching a satellite, it is critical that fuel usage is globally optimal.

CHAPTER 4

OPTIMIZING INITIAL ORBIT DESIGN CONSIDERING DESCENDING-PASS

4.1 Introduction

Satellite data of forest fires is a valuable asset to the crews combating the forest fire. By maximizing the amount of high-quality data collected of the forest fire, resources can be optimally used and deployed. The previous chapter examined the initial orbit design for a constellation of satellites to minimize the expected cost of maneuvering the satellites for observation of the ascending-pass over the forest fire. Collection on the descending-pass was not a part of the optimization model. The simulated example demonstrated, for that particular forest fire location, that once the allowable distance from the satellite to the forest fire was large enough, then data was collected on the descending-pass.

As is illustrated in Figure 4.1, the ascending-pass is when the satellite is flying from the south to the north and the descending-pass is when the satellite is flying from the north to the south. The results of the previous chapter demonstrated the significant increase in observational data that could be achieved by actively maneuvering the constellation to re-visit the forest fire each day. However, actively maneuvering the constellation for a second flyover each day requires significantly more fuel than a single flyover due to the fact that there is not a natural coasting orbit that readily achieves the two observations for all scenarios as was the case with the previous chapter. Maneuvering the satellite to fly directly

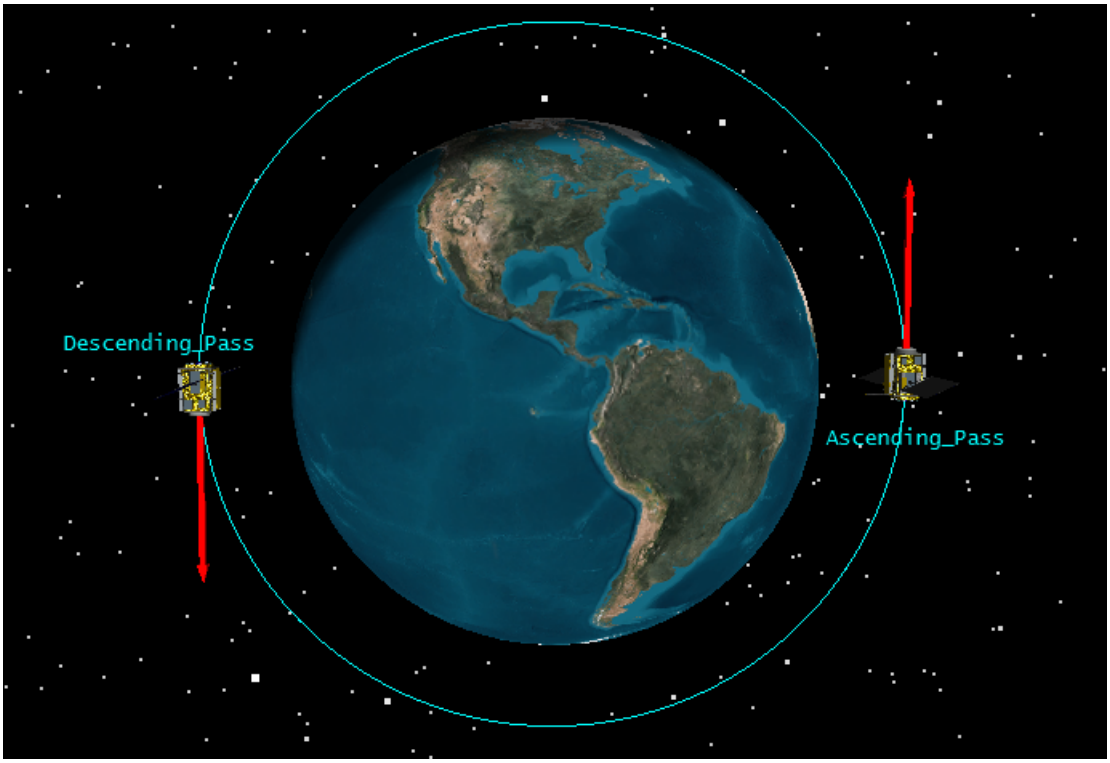

Figure 4.1

Ascending and Descending-Passes

over the forest fire twice per day rather than once per day doubles the amount of data collected at the minimum distance between the satellite and the forest fire. However, doubling the amount of collected data has the potential to be very valuable and, depending on the circumstances of the forest fire, the mission manager could decide that the second daily flyover is worth the additional fuel. Therefore, there is value in selecting the initial orbital configuration while considering the potential of actively maneuvering the constellation for a flyover on the descending-pass. On the other hand, if the mission manager were to decide not to expend the fuel for the active maneuvering to achieve the second daily flyover, then there is still the ability to maneuver for only the ascending-pass, as was done in the previous chapter.

The main goal of this chapter is to develop a methodology for constructing a model that includes both the ascending- and descending-pass flyover of the forest fire. In the process of achieving this problem-specific goal, a number of other important contributions are made. The inclusion of the descending-pass does not allow for the same linear relationships that were achievable for the ascending-pass-only formulation. As a result, additional techniques are introduced to transform the nonlinear relationships into linear representations. One of the consequences of the nonlinear relationships is that the latitude of the forest fire now impacts the model. The latitude of the forest fire adds a third scenario parameter, multiplying the number of scenarios. The L-shaped method used in the previous chapter is not computationally tractable with the significant increase in the number of discrete scenarios. Therefore, a solution technique better able to handle the very large number of scenarios is implemented. The Sample Average Approximation (SAA) technique ran-

domly samples the scenarios and uses statistical techniques to determine the optimality gap for the problem without the need to evaluate all potential scenarios.

4.2 Model Description and Formulation

The model is defined to have maneuvers only occur at apogee and perigee and to perform Hohmann-like transfers. These fuel-efficient maneuvers minimize the overall fuel cost. The ascending-pass is defined to occur at one of the maneuver locations. Because of the use of Hohmann-like transfers, the orbits remain virtually circular and the locations of apogee and perigee are not precisely defined and are left to an arbitrary definition. For our model, we define apogee as the location of the ascending-pass and perigee as being 180 away. As was assumed in the previous chapter, the location of the forest fire is unknown prior to the launch of the constellation of satellites. The two-body force model is used for the system dynamics where the only force acting on the satellite is the gravitational pull of a uniformly distributed mass Earth; this assumption is a common initial assumption in the design of satellite missions. The satellite maneuvers are assumed to be impulsive; that is, the maneuver instantaneously changes the velocity of the satellite and this is another common assumption of initial orbit design. All maneuvers occur exactly as planned; in reality, there is some error in the pointing of the satellite and the exact amount of fuel expelled, but the error is small and normally distributed, so a reasonable assumption for initial planning is that error is not present. The constellation is composed of satellites in circular orbits; a majority of satellites, especially those used for observation of the Earth's surface and climate use circular orbits, so it is a reasonable assumption. The satellites, when observing

the forest fire, will complete exactly 15 revolutions per day; the altitude corresponding to 15 revolutions per day is a reasonable selection for an Earth observing mission and completing an integer number of revolutions per day guarantees repeat flyovers of the forest fire. The satellites fly directly over the forest fire when collecting data; the satellites can collect data when they fly over a location slightly to the east or slightly to the west of the forest fire, but the image resolution is less because the distance from the satellite to the forest fire is greater than when flying directly over the forest fire. To calculate the amount of time between the ascending and descending-pass over the forest fire, four different quantities must be known: (a) the angle the forest fire will travel, (b) the angular rate of the forest fire, (c) the angle the satellite will travel, and (d) the angular rate of the satellite. The Earth rotates at a constant rate, so (b) is known. Because the satellite remains in a circular orbit, its rate is constant between pairs of maneuvers. Therefore, (d) is solved for as part of the model. The two angles, (a) and (c), are the two remaining quantities that must be determined.

4.2.1 Descending-Pass Angles Derivations

The latitude directly below a satellite at any given time can be calculated based on the z-component of its unit position vector [85].

$$\sin(\quad) = \sin(\omega)\sin(i)\cos(\nu) + \cos(\omega)\sin(i)\sin(\nu) \tag{4.1}$$

where is the latitude of the forest fire, ω is the argument of perigee, i is the inclination, and ν is the true anomaly. The latitude of the forest fire is constant, so the value of is the same for both the ascending and descending-passes. The plane of the satellite does not

change due to the maneuvers, so the values of ω and i are the same for both the ascending and descending-passes. Because our model places the ascending-pass at apogee, the value of ν for the ascending-pass is 180 . As a result of the ascending-pass being at apogee, we can calculate the value of ω in terms of i and .

$$\sin(\omega) = \frac{\sin(\ )}{\sin(i)} \tag{4.2}$$

Based on the definition of our model, the true anomaly of the descending-pass will be after apogee, $180 < \nu_d < 360$. Therefore, to avoid a quadrant ambiguity, it is best to solve equation (4.1) in terms of the cosine. The sine term is removed by using the trigonometric relationship between sine and cosine:

$$\sin(\nu) = \sqrt{1 \quad \cos^2(\nu)}. \tag{4.3}$$

Substituting equations (4.2) and (4.3) into equation (4.1) and solving for the cosine of the true anomaly of the descending-pass yields:

$$\cos(\nu_d) = 1 \quad 2\left(\frac{\sin(\ )}{\sin(i)}\right)^2 \tag{4.4}$$

$$\nu_d = \arccos \quad 1 \quad 2\left(\frac{\sin(\ )}{\sin(i)}\right)^2\Bigg) \tag{4.5}$$

To calculate the value of (a) from above, the angle the forest fire will travel, the unit vectors of the satellite positions at the ascending-, $\hat{r}_a$, and descending-, $\hat{r}_d$, passes are

projected to the equatorial plane and the dot product between the two projections provides the angular separation, $\quad_S$.

$$\left[\left(\not{\hat{Z}} \times \hat{r}_a\right) \times \hat{Z}\right] \cdot \left[\left(\not{\hat{Z}} \times \hat{r}_d\right) \times \hat{Z}\right] = \cos^2(\quad)\cos(\quad_S) \tag{4.6}$$

$$\cos(\nu_d) + \sin^2(\omega)\sin^2(i)\cos(\nu_d) + \sin^2(i)\cos(\omega)\sin(\omega)\sin(\nu_d)$$

$$= \cos^2(\quad)\cos(\quad_S) \tag{4.7}$$

By substituting equations (4.2) and (4.4) into equation (4.7) we can solve for $\quad_S$ in terms of i and $\quad$.

$$\cos(\quad_S) = \quad \frac{1}{\cos^2(\quad)} + \tan^2(\quad)\left(\frac{2}{\sin^2(i)} \quad 1\right)\left(\tag{4.8}$$

$$_S = \arccos\left(\quad \frac{1}{\cos^2(\quad)} + \tan^2(\quad)\left(\left(\frac{2}{\sin^2(i)} \quad 1\right)\right)\right)\left(\tag{4.9}$$

The value of (c) from above, the angular separation between the satellite's location at the ascending- and descending-passes, is:

$$\nu_d \quad \nu_a + \mathbb{Z} \cdot 360 \tag{4.10}$$

where ν_d is determined from equation (4.5), $\nu_a = 180$, and $\mathbb{Z}$ is an integer. The model requires the satellite to complete exactly 15 revolutions in a day and the value of ν_d provides the angle from perigee to the descending-pass location. However, the satellite will have a true anomaly equal to ν_d once per revolution, but only one of the 15 will be the instance when the forest fire is also in position. Therefore, $\mathbb{Z}$ must be included as a parameter in the model to account for the complete revolutions between the ascending- and descending-passes.

4.2.2 Determining the Integer Number of Revolutions

Equation (4.9) is used to calculate the separation angle and the angle is converted to a fraction of the day. The resulting fraction is multiplied by the amount of time in a sidereal day to arrive at the time required for the forest fire to travel from the ascending- to the descending-pass. The value of ν_d is calculated using equation (4.5) and values of $\mathbb{Z}$ between 1 and 8 are applied to calculate the total angular separation for each potential $\mathbb{Z}$ value. Taking the time the forest fire travels and dividing by the total angle of the satellite travel provides the average orbital period. If the average orbital period is above the maximum allowed orbital period or if the average orbital period is below the minimum allowed orbital period, then the value of $\mathbb{Z}$ is not feasible. The minimum orbital period is dependent on the semi-major axis of the orbit. A period of 84.489 minutes has a semi-major axis equal to the radius of the Earth and any period less than that requires the satellite to fly under the surface of the Earth. A realistic lower bound on the orbital period is 91.538 minutes which corresponds to an altitude of 350 km. There are two different ways to determine the maximum orbital period. One way is to mandate that the satellite remain below a certain altitude; for example, a maximum period of 105.119 minutes corresponds to a maximum altitude of 1,000 km. A second way is to take into the consideration that the total time of 15 revolutions is one sidereal day. By knowing the total amount of time for 15 orbits, the time and number of revolutions between the ascending- and descending-pass, then it is possible to calculate the time and the number of revolutions remaining in the day. The maximum orbital period can then be calculated so that the average time for the remaining revolutions is greater than the minimum period.

4.2.3 Model Formulation

For the model to require the satellite to fly directly over the forest fire on the descending-pass, the amount of time the satellite travels between the ascending-pass flyover and the descending-pass flyover must be equal to the time the Earth takes to rotate from one location to the other, which can be expressed as

$$\sum_{j=1}^{\mathbb{Z}} \frac{2P_{\mathcal{I}+j} + \quad {}^{+}_{\mathcal{I}+j} \quad {}_{\mathcal{I}+j}}{2} \Bigg) \Bigg(+ \frac{1}{2}P_{\mathcal{I}} + \left(\frac{1}{2} + \frac{\nu_d \quad 180}{360}\right) \Bigg(P_{\mathcal{I}+\mathbb{Z}}$$

$$= \frac{S}{360} 1,436.07 \tag{4.11}$$

where $\mathcal{I}$ is an index, P is a second-stage variable of the period for the indexed revolution, and $^{+,}$ are second-stage variables of the positive and negative components of the performed maneuvers on the indexed revolution. The constraint has two challenges when it is a part of a two-stage stochastic linear program (LP). First, both ν_d and $_S$ involve arccosine functions that are nonlinear. Second, ν_d is multiplied by $P_{\mathcal{I}+\mathbb{Z}}$, so a continuous first-stage variable is multiplied by a continuous second-stage variable, resulting in a nonconvex bilinear program. Linearization about a point is used to avoid these two issues in the model.

For notational convenience, the variable ς is introduced in equation (4.12). The orbital inclination only appears in equations (4.5) and (4.9) in this format and it is the first-stage variable for the model, thereby avoiding the sine and polynomial nonlinearities of the inclination.

$$\varsigma = \frac{1}{\sin^2(i)} \tag{4.12}$$

$$f_{sat}(\varsigma, P) = \frac{1}{2} \quad \frac{\arccos \quad 1 \quad 2\varsigma \sin^2(\ )}{360} \Bigg) \Bigg(P \tag{4.13}$$

$$f_{fire}(\varsigma) = \frac{\arccos\left(\left(\frac{1}{\cos^2(\ )} + \tan^2(\ )(2\varsigma \quad 1)\right)\right.}{360} \Bigg(1,436.07 \tag{4.14}$$

Equations (4.13) and (4.14) are the components from equation (4.11) that include the first-stage variable ς. The two equations are linearized about the point (ς_ℓ, P_ℓ) using a first-order Taylor Series approximation.

$$f_{sat}(\varsigma_\ell, P_\ell) + \frac{\partial f_{sat}}{\partial \varsigma}_{\varsigma_\ell, P_\ell} (\varsigma \quad \varsigma_\ell) + \frac{\partial f_{sat}}{\partial P}_{\varsigma_\ell, P_\ell} (P \quad P_\ell) \tag{4.15}$$

$$f_{fire}(\varsigma_\ell) + \frac{\partial f_{fire}}{\partial \varsigma}_{\varsigma_\ell} (\varsigma \quad \varsigma_\ell) \tag{4.16}$$

The linearization point is determined prior to solving the LP, so the coefficients in equations (4.15) and (4.16) can be calculated and are constant in the LP. Similarly, the terms of the slopes multiplied by the linearization component can also be calculated prior to solving the LP. As a result, the terms can be collected into a single constant term for the model with each variable having a slope. The linearized constraint is thus:

$$\begin{aligned} \sum_{j=1}^{\mathbb{Z}} \frac{2P_{\mathcal{I}+j} + \quad \overset{+}{\mathcal{I}+j} \quad \mathcal{I}+j}{2} \Bigg) + \frac{1}{2} P_{\mathcal{I}} + \quad \frac{1}{2} + \frac{\partial f_{sat}}{\partial P}_{\varsigma_\ell, P_\ell} \Bigg) P_{\mathcal{I}+\mathbb{Z}} \\ + \quad \frac{\partial f_{sat}}{\partial \varsigma}_{\varsigma_\ell, P_\ell} \quad \frac{\partial f_{fire}}{\partial \varsigma}_{\varsigma_\ell} \Bigg) \Bigg(\varsigma = f_{fire}(\varsigma_\ell) \quad f_{sat}(\varsigma_\ell, P_\ell) \\ + \quad \frac{\partial f_{sat}}{\partial \varsigma}_{\varsigma_\ell, P_\ell} \quad \frac{\partial f_{fire}}{\partial \varsigma}_{\varsigma_\ell} \Bigg) \Bigg(\varsigma_\ell + \frac{\partial f_{sat}}{\partial P}_{\varsigma_\ell, P_\ell} P_\ell \end{aligned} \tag{4.17}$$

The model from the previous chapter has additional constraints added to require the forest fire flyover on the descending-pass. In addition, the initial orbit inclination did

not impact the previous results, but as the above derivations demonstrate, the inclination does impact the descending-pass. Therefore, the model now includes the selection of the inclination as part of the first-stage.

Each revolution j is a member of the set of all revolutions J ($j \in J$). Each satellite k is a member of the set of all satellites K ($k \in K$). Each scenario s is a member of the set of all scenarios S ($s \in S$). The second-stage decision variables of the positive and negative magnitudes of the maneuvers to be performed are $^{+,}$. $\mathcal{M}$ is a very large penalty number. The second-stage variables of the amount of constraint violation are $^{+,}$. P is the second-stage variable of the orbital period, g is the index of the starting revolution for the repeat ground track phase of the model, ν_0 is a scenario parameter that defines the angular separation between the anchor satellite and the ascending-pass location at epoch, $_0$ is a scenario parameter that defines the angular separation between the longitude of the ascending-pass location and the longitude of the forest fire at epoch, Ω_k is the first-stage variable of the angular separation between satellite k and the anchor satellite, τ is a parameter of the maneuver time from epoch to the repeat ground track phase, t_k is a first-stage decision variable for the amount of time separating satellite k from the anchor satellite, and $\mathcal{I}$ is the index for the revolution of the ascending-pass over the forest fire.

$$\text{Minimize } \mathbb{E}_S \sum_{j=0}^{J} \sum_{k=1}^{K} \Bigg(\; ^{+}_{j,k}(s) + \quad _{j,k}(s) + \mathcal{M} \quad ^{+}_{k}(s) + \quad _{k}(s) \tag{4.18}$$

st

$$P_{j+1,k}(s) = P_{j,k}(s) + \quad {}^{+}_{j,k}(s) \qquad {}_{j,k}(s)$$

$$+ \quad {}^{+}_{j+1,k}(s) \qquad {}_{j+1,k}(s) \qquad \forall j \in J, k \in K, s \in S \quad (4.19)$$

$$\left(\sum_{j=1}^{g_k(s)} \frac{2P_{j,k}(s) + \quad {}^{+}_{j,k}(s) \qquad {}_{j,k}(s)}{2} \right) \left(\right.$$

$$+ \frac{1}{2} P_{g_k+1,k}(s) + \frac{\nu_0(s)}{360} P_0$$

$$\left(\quad {}_0(s) + \Omega_k \right) \frac{1,436.07}{360}$$

$$= \tau \quad t_k + \quad {}^{+}_{k}(s) \qquad {}_{k}(s) \qquad \forall k \in K, s \in S \quad (4.20)$$

$$\sum_{j=1}^{14} \frac{2P_{\mathcal{I}_k(s)+j,k}(s)}{2}$$

$$+ \frac{\left(\left({}^{+}_{\mathcal{I}_k(s)+j,k}(s) \qquad {}_{\mathcal{I}_k(s)+j,k}(s) \right) \right)}{2} \left(\right.$$

$$+ \frac{1}{2} P_{\mathcal{I}_k(s),k}(s) + \frac{1}{2} P_{\mathcal{I}_k(s)+15,k}(s) = 1,436.07 \qquad \forall k \in K, s \in S \quad (4.21)$$

$$\sum_{j=1}^{\mathbb{Z}} \frac{2P_{\mathcal{I}_k(s)+j,k}(s)}{2}$$

$$+ \frac{\left(\left({}^{+}_{\mathcal{I}_k(s)+j,k}(s) \qquad {}_{\mathcal{I}_k(s)+j,k}(s) \right) \right)}{2} \left(\right.$$

$$+ \frac{1}{2} P_{\mathcal{I}_k(s)} + \quad \frac{1}{2} + \frac{\partial f_{sat}}{\partial P} \Big)_{\varsigma_\ell, P_\ell} \left(P_{\mathcal{I}_k(s)+\mathbb{Z}} \right.$$

$$+ \quad \frac{\partial f_{sat}}{\partial \varsigma} \qquad \frac{\partial f_{fire}}{\partial \varsigma} \Big)_{\varsigma_\ell} \left(\varsigma = f_{fire}(\varsigma_\ell) \right.$$

$$f_{sat}(\varsigma_\ell, P_\ell) + \quad \frac{\partial f_{sat}}{\partial \varsigma} \qquad \frac{\partial f_{fire}}{\partial \varsigma} \Big)_{\varsigma_\ell} \left(\varsigma_\ell \right.$$

$$+ \frac{\partial f_{sat}}{\partial P} \Big)_{\varsigma_\ell, P_\ell} P_\ell \qquad \forall k \in K, s \in S \quad (4.22)$$

$$P_{min,0} \leq P_0 \leq P_{max,0} \quad (4.23)$$

$$P_{min} \leq P_{j,k}(s) \leq P_{max} \qquad \forall j \in J, k \in K, s \in S \quad (4.24)$$

$$0 \leq \quad {}^{+,}_{j,k} \ (s) \leq \quad _{max} \qquad \forall j \in J, k \in K, s \in S \quad (4.25)$$

$${}^{+,}_{j,k} \ (s) = 0 \qquad \forall j \in \mathcal{I}_k(\omega), k \in K, s \in S \quad (4.26)$$

$$0 \leq t_k < P_0 \qquad \forall k \in K \quad (4.27)$$

$$\Omega_{min,k} \leq \Omega_k \leq \Omega_{max} \qquad \forall k \in K \quad (4.28)$$

$${}^{+,}_{k} \ (\omega) \quad 0 \qquad \forall k \in K, \omega \in \xi \quad (4.29)$$

$$\varsigma_{min} \leq \varsigma \leq \varsigma_{max} \quad (4.30)$$

4.3 Solution Method

Scenarios consist of three real-valued positive parameters: ν_0, $_0$, and , resulting in an infinite scenario set. The SAA technique as presented by Santoso et al. [71] is the basis of the solution technique employed by this chapter because it finds an optimal solution without exhaustive enumeration of all scenarios.

SAA works by determining an upper and lower bound for the optimal solution. Out of all potential scenarios, n are randomly chosen and the two-stage stochastic program consisting of those n scenarios is solved. As was the implementation in [71], this chapter uses the L-shaped method to solve the sample average problem. A total of m sets of n randomly chosen scenarios are solved. The mean of the m solutions provides a lower bound of the optimal solution (as shown in equation (4.31)) and the variance, σ^2_{LB}, is calculated using equation (4.32). The confidence interval for the lower bound is calculated using equation (4.33). The student-t distribution for the desired value of α with m 1

degrees of freedom is represented as $\mathfrak{t}$. The upper bound is calculated by taking the m first-stage solutions (equation (4.34)) and calculating the cost of each of the first-stage solutions for n' scenarios (equation (4.35)) where n' is typically much larger than n and is independently sampled. The same set of n' scenarios is used to evaluate the cost of all m solutions. The mean of the m means of the n' second-stage problems provides an upper bound (equation (4.36)) to the optimal solution and the variance, σ^2_{UB}, is calculated using equation (4.37). The confidence interval for the upper bound is calculated using equation (4.38).

$$L = \frac{1}{m}\sum_{o=1}^{m}\left(\theta_o \right. \tag{4.31}$$

$$\sigma^2_{LB} = \frac{1}{m \quad 1}\sum_{o=1}^{m}\left(\theta_o \quad L\right)^2 \tag{4.32}$$

$$\left[\left(L \quad \frac{\mathfrak{t}\sigma_{LB}}{\sqrt{m}}, L + \frac{\mathfrak{t}\sigma_{LB}}{\sqrt{m}}\right.\right. \tag{4.33}$$

$$(P_0, \varsigma, \Omega, t)^*_\ell = \arg\min F_{|n|_j}(P_0, \varsigma, \Omega, t) \qquad o = 1, \ldots, m \tag{4.34}$$

$$\Theta_\ell = \frac{1}{n'}\sum^{n'}\left(F(P_0, \varsigma, \Omega, t)^*_o \right. \qquad \forall o \tag{4.35}$$

$$U = \frac{1}{m}\sum_{o=1}^{m}\left(\Theta_o \right. \tag{4.36}$$

$$\sigma^2_{UB} = \frac{1}{m \quad 1}\sum_{o=1}^{m}\left(\Theta_o \quad U\right)^2 \tag{4.37}$$

$$\left[\left(U \quad \frac{\mathfrak{t}\sigma_{UB}}{\sqrt{m}}, U + \frac{\mathfrak{t}\sigma_{UB}}{\sqrt{m}}\right.\right. \tag{4.38}$$

Algorithm 2 Implemented Sample Average Approximation

1: Create n' sample scenarios

2: Calculate linearized terms for all n' sample scenarios

3: **for** m **do**

4: Create n sample scenarios

5: Calculate linearized terms for all n sample scenarios

6: Solve L-shaped for n scenarios

7: Solve n' second-stage problems using L-shaped first-stage solution

8: Calculate mean and variance for n' costs

9: **end for**

10: Calculate mean and variance for m first-stage solutions

11: Calculate mean and variance for m n' solutions

The enhanced L-shaped method from the previous chapter was used to solve the L-shaped master problem of the SAA algorithm. The results of the sensitivity analysis from the previous chapter influenced the decision for the number of days included in the model to be two.

To guarantee relatively complete recourse, the value of ς must be bounded between feasible solutions. Equations (4.9) and (4.10) as well as the value of $\mathbb{Z}$ can be combined to require that the amount of time the for the forest fire to reach the descending-pass observation location is the same as the amount of time for the satellite as seen in equation (4.39). The resulting function includes terms for and ς and an offset, $\mathcal{O}$ that is dependent on the maximum allowable maneuver magnitude to bound the time to be feasible. Two Golden Ratio searchers are performed using as the independent variable and ς as the dependent variable with one search minimizing and the other maximizing; the minimizing corresponds to subtracting the offset while the maximizing corresponds to adding the offset. The two values bound the feasible region of ς.

$$_{S}\frac{1,436.07}{360} = \left(\frac{1,436.07}{360} \pm \mathcal{O}\right)\left(\mathbb{Z} + \frac{\nu_d}{360}\right) \tag{4.39}$$

4.4 Numerical Results

First, the value of $\mathbb{Z}$ is determined to ensure relatively complete recourse for all 395 forest fires the National Park Service (NPS) combatted between 1980 and 2014 that consumed at least 5,000 acres. Once this model parameter is determined, it is then possible to solve the model. The model is solved with different sampling approaches to investigate

Algorithm 3 Descending-Pass Algorithm

1: Read in problem parameters

2: Calculate ς bounds using Golden Ratio algorithm

3: Calculate $P_{min,0}$ and $P_{max,0}$

4: Use Algorithm 4.1 to determine solution

the performance of the model with respect to the sampling scheme. The optimal solution to the problem will also be analyzed to determine its behavior.

4.4.1 Calculating the Number of Complete Revolutions Between the Ascending- and Descending-Passes

A constant value for $\mathbb{Z}$ is beneficial for model development because the number of variables in the constraint necessitating the descending-pass flyover of the forest fire is directly related to the value of $\mathbb{Z}$. The maximum latitude of the ground track is equal to the orbit's inclination and it is only achieved once per revolution. The latitude a very small amount less than the orbit's inclination is reached twice per revolution, but the two occurrences are virtually instantaneous. The two crossings of the equator are 180 apart and, for a circular orbit, are one half of the orbital period separated in time. As a result of this geometry, locations closer to the poles will have a smaller range of feasible inclinations for a given $\mathbb{Z}$ value, but will have more feasible $\mathbb{Z}$ values. On the other hand, locations closer to the equator will have a larger feasible range of inclinations for a given $\mathbb{Z}$ value, but will have fewer feasible $\mathbb{Z}$ values. Because of the desire for a constant $\mathbb{Z}$ and the need for all 395 forest fires to have a feasible solution, examining the forest fire at the lowest latitude will eliminate the greatest number of $\mathbb{Z}$ values. The lowest latitude of the set is 19.31 , $= 19.31$; this

latitude is the latitude of a forest fire in Hawaii. Table 4.1 calculates the average orbital periods for the Hawaii forest fire for different combinations of i and $\mathbb{Z}$. For $i = 70$, the corresponding value of $_S$ is 165.35 or 45.9% of the day (659.576 minutes) and the value of ν_d is 318.791 or a separation from the ascending-pass of 138.791 . If the value of $\mathbb{Z}$ is one, then the first complete revolution plus the next 138.791 must take 659.576 minutes resulting in an average period of 476.046 minutes. This average period corresponds to an altitude of 13,817.593 km. In addition, the remaining 13 full orbits plus 221.209 must be completed with an average orbital period of 57.034 minutes corresponding to an altitude of $5,777.125$ km. Because this altitude requires the satellite to fly below the surface of the Earth, it is not feasible for the forest fire in Hawaii to be observed on both the ascending- and descending-passes with an inclination of 70 and a $\mathbb{Z}$ value of 1. Similarly, all inclinations are infeasible for the Hawaii fire with a $\mathbb{Z}$ value of 1 through 6. A $\mathbb{Z}$ of 8 results in a negative altitude during the revolutions between the ascending- and descending-passes over the forest fire (the previous analysis has a positive altitude for the revolutions between the ascending and descending-passes over the forest fire, but has a negative altitude on the revolutions between the descending and ascending-passes over the forest fire). The lower inclinations for $\mathbb{Z} = 7$ still result in the satellite needing to reenter the atmosphere. However, the higher inclinations are feasible. Therefore, in order for the model to support a descending-pass flyover for a forest fire occurring at the southern boundary of the scenario definitions, the value of $\mathbb{Z}$ must be 7.

Table 4.1

$\mathbb{Z}$ Feasibility

$i(\ )$	$\mathbb{Z}=1$	$\mathbb{Z}=2$	$\mathbb{Z}=3$	$\mathbb{Z}=4$	$\mathbb{Z}=5$	$\mathbb{Z}=6$	$\mathbb{Z}=7$	$\mathbb{Z}=8$
70	476.046	276.490	194.822	150.398	122.472	103.292	89.307	78.656
72.5	481.103	279.576	197.039	152.128	123.889	104.493	90.348	79.576
75	486.078	282.594	199.203	153.813	125.270	105.662	91.362	80.471
77.5	490.997	285.560	201.324	155.464	126.621	106.806	92.353	81.345
80	495.885	288.49	203.413	157.088	127.949	107.929	93.326	82.204
82.5	500.764	291.393	205.481	158.693	129.260	109.037	94.286	83.051
85	505.655	294.287	207.535	160.285	130.560	110.136	95.237	83.889
87.5	510.581	297.182	209.585	161.872	131.855	111.229	96.183	84.722
90	515.564	300.092	211.640	163.460	133.149	112.321	97.127	85.555

4.4.2 Problem Instances

There are three parameters for every scenario: ν_0, $\ _0$, and $\ $. The location of the satellite on its orbital path and the relative spacing between the forest fire and the satellite are unknown at the epoch of the forest fire. However, the Earth and satellite both have constant angular velocities, so the likelihood of the values of ν_0 and $\ _0$ are uniformly distributed between 0 and 360 ($0 \ \leq \nu_0 < 360 \ $ and $0 \ \leq \ _0 < 360 \ $). The latitude of the forest fire is also assumed to be uniformly distributed. However, the minimum and maximum latitudes of NPS forest fires from 1980 through 2014 of greater than 5,000 acres are used as bounds ($19.311 \ \leq \ < 68.175 \ $).

Model parameters include the minimum orbital period of $P_{min} = 91.538$ minutes (an altitude of 350 km) and the maximum orbital period of $P_{max} = 105.119$ minutes (an altitude of 1,000 km). These altitudes are consistent with current Low Earth Orbit (LEO) satellite missions. The maximum maneuver magnitude is $\ = 0.25$ minutes is also consistent with reasonably sized impulsive maneuvers. Two sidereal days ($\tau = 2,872$ minutes) are allotted for transitioning to the data collection phase.

The variables Ω_k and t_k both both only appear in the second-stage model in the transition constraint. Therefore, there are multiple solutions with the same objective value that tradeoff Ω_k and t_k to satisfy the constraints. To simplify the search process, the values of Ω_k are set to constant values. Of the two, it is more likely that Ω_k would be held constant because that set of variables controls the relative time between observations of the forest fire by the constellation. A mission manager would thus be able to control the cadence at which data are collected. If the values of t_k were fixed, then the spacing between the col-

lection opportunities would vary depending on the values of Ω_k associated with the optimal solution.

Two different constellation designs are considered: a two-satellite and a five-satellite constellation. For the two-satellite constellation, the value of Ω_2 is constrained to be 90 . The two ascending-passes are therefore at 0 and 90 and the two descending-passes are at approximately 180 and 270 . Spacing the observations of the forest fire to be roughly once every six hours is a likely choice for a mission manager to make because it results in a fairly constant data cadence. Similarly, the ascending-passes for the five-satellite constellation are separated by 36 providing for approximately equal spacing of all 10 observation opportunities.

The descending-pass constraint is linearized using the point $\varsigma_\ell = 1.0014$ ($i = 87.85$), $P_\ell = 95.738$ minutes. The period portion of the linearization is chosen to be the repeat ground track period for the required 15 revolutions per day; the average period over the day is equal to this linearization point. The inclination portion of the linearization is found by creating tables similar to Table 4.1 for multiple latitudes and calculating the average inclination where the corresponding period with a $\mathbb{Z}$ value of 7 is the repeat ground track period. The SAA parameters are $n = 2^{12} = 4,096$, $m = 2^5 = 32$, and $n' = 2^{17} = 131,072$.

To compare the results to current operating procedures, the orbital information for two operational satellites (Earth Observing 1 and Aura) is downloaded and the two satellites are simulated using Systems Toolkit (STK) 10. The maneuvers of the data collection phase of the constellation found by this research are also simulated. The amount of observation

opportunities and the duration of the observation opportunities are compared for these two different satellite constellations. The maneuvering costs for the two-satellite and five-satellite constellations are compared to the results of the previous chapter to analyze the amount of additional data collected by having each satellite directly fly over the forest fire on both the ascending- and descending-passes and the associated costs of the maneuvers.

4.4.2.1 Analysis of Sampling Approaches

There are multiple ways to sample the potential scenarios. One approach is stratified sampling. For a stratified sampling approach, a grid is created with each scenario parameter as an axis. Each grid cell spans a range of values. A scenario is sampled from each cell. This methodology ensures that all regions are sampled, but provides variation between different sets. For this problem, each scenario parameter is split into 16 equal partitions. As an example, the first partition of $_0$ is $0 \leq {}_0 < 22.5$, the second partition is $22.5 \leq {}_0 < 45$, etc. The 4,096 equally spaced cells each contributes one scenario to each of the m first-stage problems. For the n' second-stage problems, each cell contributes 32 scenarios. The results for the stratified sampling are presented in Table 4.2. The optimality gap is less than 0.25% in all instances and the 95% confidence intervals, for all instances, are overlapping.

As an alternative sampling approach, Latin Hypercube sampling is used. Rather than splitting each parameter into 16 partitions, this method splits each parameter into 4,096 partitions. However, once a cell is sampled, no remaining cells with that same partition value can be chosen. For example, the first partition of $_0$ is $0 \leq {}_0 < 0.088$ and

once a scenario is created that has $_0 < 0.088$, no future scenarios have $_0 < 0.088$. As a comparison, in the stratified sampling approach, there are 256 scenarios with values of $_0$ from the first partition. The Latin Hypercube sampling approach helps to reduce variability by guaranteeing that there is some dispersion of the samples. The results of the Latin Hypercube sampling are included in Table 4.2. The optimal solutions for the two sampling methodologies are virtually identical. In addition, with a stochastic solution approach for a problem with continuous variables it is not likely to find identical optimal solutions with each run of the software; therefore, two solutions that are close to being identical does not validate the accuracy of one method over the other.

4.4.2.2 Physical Insights

For both the two-satellite and five-satellite constellations, the initial orbital period (P_0) is greater than the 95.738 minutes corresponding to an orbit that completes exactly 15 revolutions in a single day. Because the orbital period is greater, there is a resulting westward shift in the ground track. A westward shift in the ground track is beneficial because $_0$ is defined as the angular distance from the forest fire to the satellite's ascending-pass location and the westward shift reduces the separation as is needed to allow for the satellite to fly directly over the forest fire at the completion of the two-day transition phase. The inclination is 87.851 . If the inclination were 90 , then the ascending- and descending-passes would be separated by exactly half a day, and a forest fire on the equator would have a direct flyover without any need to maneuver. For an inclination less than 90 , the time between the ascending- and descending-passes is less than half a day. The orbital angular

Table 4.2

Sampling Results

	Stratified Sampling		Latin Hypercube Sampling	
$\|K\|$	2	5	2	5
Lower Bound (minutes of fuel)	10.222	24.409	10.249	24.438
95% Confidence	10.200,10.244	24.359,24.459	10.229,10.270	24.393,24.483
Upper Bound (minutes of fuel)	10.246	24.451	10.249	24.476
95% Confidence	10.244,10.248	24.447,24.454	10.247,10.252	24.472,24.480
Gap %	0.23	0.17	0.00	0.16
P_0 (minutes)	99.417	98.670	99.451	98.688
ς	1.001	1.001	1.001	1.001
i ( )	87.851	87.851	87.851	87.851
Ω ( )	90	36, 72, 108, 144	90	36, 72, 108, 144
t (minutes)	99.417	97.020, 45.811, 91.878, 40.355	99.451	97.219, 46.100, 92.095, 40.517
Computation Time (minutes)	312	2,028	315	1,925

separation between the ascending- and descending-passes will be less than 180° for forest fires not located on the equator. Decreasing the inclination from 90° causes a greater decrease in the time the forest fire requires to move from the ascending-pass location to the descending-pass location than the time required for the satellite, so an inclination less than 90° is expected. However, the decrease in the time required for the forest fire to move from the ascending-pass location to the descending-pass location can become too significant at the higher latitudes resulting in the the need for orbital periods where the satellites fly under the surface of the Earth. The value of 87.851° balances the need of the lower latitude fires to have a lower inclination and the higher latitude fires need to have the rotation time significant enough to allow for seven complete revolutions between the ascending- and descending-passes.

The second satellite of the two-satellite constellation is a complete revolution behind the anchor satellite. This geometry provides for an increase in the transition time and a longer transition time allows for smaller early maneuvers to have a greater impact at a relatively low cost. The second and fourth satellites of the five-satellite constellation demonstrate this same trailing behavior. The third and fifth satellite, on the other hand, are about half a revolution behind the anchor satellite. The satellites can be, at most, one complete revolution behind the anchor satellite. The model trades off the phasing of the Earth and satellite rotation rates to achieve the direct flyovers and the phasing of the satellites in the constellation relative to each other. For a given satellite, the cost would be lower to increase the initial orbital period to allow for more time for the transitioning. However, all of the satellites in the constellation need to use more fuel to transition from the higher

orbital period to the observational orbital period. The added costs of the constellation can outweigh the advantages of a single satellite changing the initial orbital period. As a result, there is a tradeoff in between the initial orbital period and the time between the anchor satellite and the constellation satellite and for the third and fifth satellites, the time was optimal at roughly half an orbital period.

The cost for the two-satellite constellation is approximately 10.25 minutes of fuel. The five-satellite base case of the previous chapter requires 9.454 minutes of fuel. Therefore, the two-satellite constellation including the descending-pass requires more fuel than the five-satellite constellation for only the ascending-pass. The five-satellite constellation including the descending-pass requires roughly 250% of the fuel that the five-satellite ascending-pass-only solution requires. In addition, the cost of the ascending-pass-only solution is fairly constant regardless of the length of the observing of the forest fire because once the satellite achieves a repeat ground track altitude, it can passively meet the constraint of flying over the forest fire once per day. In contrast, the ascending- and descending-pass solution increases in cost as the length of the observing of the forest fire increases because maneuvers need to be performed between the observation passes to synchronize the satellite and Earth rotational phases.

Table 4.3 compares the amount of time in seconds observing a forest fire in Yellowstone National Park for three different constellation designs as a function of the maximum range from the satellite to the forest fire. The maximum range is incremented by 50 km from one row to the next; the amount of time in the subsequent three columns is the amount of time during the day that the range from the satellite to the forest fire is less than the maximum

range. The two direct flyovers column contains the results for a two-satellite constellation based on the methodology of this chapter. The ascending-pass-only column contains the results of the previous chapter's two-satellite constellation. The EO-1/Aurora column contains the results based on two operational satellites that follow the current operational paradigm of not maneuvering. Both of the maneuvering constellations significantly outperform the non-maneuvering constellation; data are collected at all ranges with maneuvering and the amount of collection time is significantly greater even at the largest range. As is expected, flying directly over the forest fire twice per day results in more collection time than flying directly over the forest fire once per day. At lower range limits, the amount of collection time more than doubles. The reason it does not simply double is that the difference in the inclinations of the two constellations leads to a difference in the amount of collection time. In addition, the different orbital periods between the two constellations result in different angular rates. However, at the maximum range limit, the difference between the two constellations is less than seventy seconds. If data is needed from 600 km, then maneuvering for the second direct flyover provides significantly more data. On the other hand, if data from 1,250 km is of sufficient quality, then the additional fuel cost might not warrant maneuvering for the second opportunity.

4.5 Conclusions

A model to include a flyover of the forest fire on the descending-pass observation opportunity is developed. In practice, the advantage of this approach is that each satellite will collect very high-resolution images of the forest fire twice per day instead of only one per

Table 4.3

Simulation Comparison of Constellations

Max Range (km)	Two Direct Flyovers (s)	Ascending-Pass-Only (s)	EO-1 / Aurora (s)
600	257.102	111.348	0
650	377.156	176.906	0
700	473.466	227.392	20.967
750	558.638	283.072	116.935
800	637.206	465.826	165.724
850	711.394	570.66	217.354
900	782.446	660.548	247.286
950	851.152	742.614	275.777
1,000	918.036	819.708	315.636
1,050	983.484	893.304	332.437
1,100	1,047.77	964.322	377.408
1,150	1,111.082	1,033.332	388.957
1,200	1,173.608	1,100.744	433.771
1,250	1,235.454	1,166.858	450.82

day. The increase in high-quality data will increase the accuracy of the models used by the crew battling the forest fire. However, there is a significant increase in the amount of fuel required to maneuver for the second collection opportunity. The significant increase is due to the fact that for the ascending-pass-only solution, the satellites maneuver to a repeat ground track orbit and then coast without fuel usage for the entire data collection phase. In contrast, the natural motion of the satellite does not guarantee both direct flyovers and, as a result, fuel is used to create the desired relative motion.

Although the expected cost for maneuvering the constellation to observe on the descending-pass is relatively high, the results are valuable for three main contributions. First, it is feasible to monitor the forest fire and if the additional collected data is deemed to be of significantly high value, then the additional fuel costs would be warranted. Second, the ascending-pass-only solution is insensitive to the inclination of the orbit, but the constellation's orbits will have an inclination. The methodology presented in this chapter provides a reasonable means to select an appropriate inclination for the constellation. Third, while the expected cost for including the descending-pass is high, there are instances where the natural motion of the satellite in the repeat ground track orbit will provide the two direct flyovers each day without needing any maneuvering and other instances that will not require much maneuvering. If the forest fire happened to be at a latitude that encouraged a minimally maneuvering solution to include the descending-pass, then using the solution based on this chapter would result in the greatest amount of collected data. If the forest fire does not happen to be at a latitude associated with a minimally maneuvering solution, then

the mission manager can opt to not maneuver for the descending-pass and instead only collect data during the ascending-pass.

The inclusion of the descending-pass does not permit the linear relationships between all points of interest in the model. Therefore, linearization using a first-order Taylor Series approximation about a reasonable point is used to transform the nonlinear relationship into a linear relationship. The nonlinear relationship is dependent on the latitude of the forest fire, so a third scenario parameter is required. For the discretized representation of the scenarios for the ascending-pass problem, a significant number of scenarios are required. Adding an additional scenario parameter results in a polynomial increase in the number of scenarios and, as a consequence, the L-shaped method is not tractable. SAA provides the ability to randomly sample the large search space to find the optimal solution.

Two different sampling strategies, stratified sampling and Latin Hypercubes, are both used to solve the problem. The two sampling methods perform virtually identically. The stratified sampling solves the two-satellite constellation faster, but solves the five-satellite constellation slower. The spans of the confidence intervals are all small and both sampling methods have instances of a smaller span and instances of a larger span when comparing the two sets of results. The optimality gaps are all reasonable and the better performance switches between the two methods. The returned solutions of both the two-satellite and five-satellite constellations are very similar for the two sampling methods. The uncertainties in the physical system are larger than the differences between the two methodologies. Both sampling methods perform well and equivalently.

CHAPTER 5

GROUND STATION LOCATION SELECTION

5.1 Introduction

5.1.1 Motivation

Satellite data can provide significant and valuable information related to natural disasters, from data to assist relief efforts [37] to data that helps with the forecast of weather events [49, 78]. In order for the data to get to relief personnel, the satellite must fly over the disaster site, collect data, and then download the data through a ground station. The amount of data capacity of a ground station differs on a revolution-by-revolution basis. Simply choosing the ground stations with the largest average amount of download capacity is not necessarily optimal because some of the capacity could be overlapping and, in addition to the amount of capacity, the timing of the available capacity is an important consideration. Each disaster produces a different amount of data on a revolution-by-revolution basis. Depending on the quantity of data produced and the timing of data collection, different combinations of ground stations will provide optimal capacity and timeliness. Thus, with appropriately positioned ground stations, the quantity of data collected and disseminated will increase and this information will allow for a more prompt response.

Ensuring a satellite collects high-quality data is not a trivial task. A geostationary (GEO) satellite is always in the same relative position, so it can constantly collect and

directly download data, but the geostationary altitude reduces the resolution of the data. Low Earth orbit (LEO) satellites can collect higher-resolution data and can collect data from the entire globe, but there is a limit in their ability to download collected data because it is not reasonable for a ground station to be continuously in view of the satellite. This is because ground stations are expensive to construct. As a result, the intelligent placement of ground stations is a critical step in ensuring a satellite is able to collect high-quality data after a disaster.

The selection of ground station locations occurs before the launch of the satellite, but the disaster site is unknown until after the disaster has occurred and the satellite has launched. Hence, the problem falls in the domain of optimization under uncertainty. This chapter investigates optimizing the location of ground stations with an uncertain disaster location while maximizing the amount of data downloaded. The same approach can extend to the observation of any object on the Earth's surface where data quantity is critical (such as monitoring a facility being built in a hostile nation).

The inclusion of ground stations into the problem of satellite data collection becomes more complicated because ground stations are scarce resources that are carefully scheduled [57]. In addition, the routing of satellite data is a non-trivial problem [33]. Because of these complications, most researchers who study satellite motion optimization do not include ground station placement as part of their model.

Not including ground stations in the satellite data collection problem is a valid assumption if the satellite has access to a ground station whenever it is desired and for high-priority satellites, this assumption is usually valid. However, in actuality, there is no guarantee that

all of the ground stations around the world will be tasked for the disaster that is of interest; for example, if there was the need to download data from one satellite about a hurricane heading for Miami and there was simultaneously the need to download data about an earthquake in San Francisco, only one satellite would be able to download data through the ground station. It is also standard practice to lock down the schedule of ground stations one week in advance [18]; if a high-priority satellite is already scheduled to be downloading to a ground station, then the satellite that collected data about the disaster may not be granted access to download its data. For instance, the Air Force Satellite Control Network (AFSCN) consists of nine heavily tasked sites that can rarely accommodate every user request [4].

Therefore, optimal placement of mission specific ground stations, based on the expected mission requirements, would avoid having to rely on other resources being available. Because the operator need not be located at the ground station [8], it is feasible for a mission to have ground stations in place before a disaster that are not co-located with mission headquarters. It is beyond the scope of this dissertation to consider any factors other than geographic location, but the placement of ground stations in urban areas can pose unique challenges [11]. Political considerations can also influence where ground stations are located. Finally, there are also logistical concerns (e.g., file distribution, scheduling of concurrent download opportunities) that arise as the number of ground stations increases [69].

5.1.2 Contributions

Although there have been many advances in satellite motion optimization and facility location in disaster settings, important gaps remain. To begin with, an often cited reason for not using an exact method to solve problems concerning satellite motion is the complex dynamics of the system. To address this difficulty, this chapter uses simulation tools to gather information to generate the coefficients of a mathematical program, thereby incorporating the complex dynamics into the optimization model without requiring the inclusion complex and nonlinear satellite motion equations. Because of this approach, this chapter is able to employ an exact solution method that results in a provably optimal solution that can be used as a benchmark. If a particular satellite ground station location problem is too complicated to fit into the type of model presented in this chapter, then this research still provides a means of bounding the problem to allow a researcher to achieve a better understanding of the true quality of their solution. The primary builders and operators of satellite ground stations are government agencies as well as universities and having a technique to optimally place ground stations given a list of candidate locations will increase data received from satellites and potentially reduce costs by being able to download the same amount of data using fewer ground stations. As well, disaster relief efforts will be enhanced through more data helping to better forecast disasters as well as assist in recovery efforts.

The major contributions of this chapter, which is the first mathematically rigorous study of the satellite ground station location problem, include the following: 1) a demonstration of the ability to convert output from commercial satellite simulation software into

a mixed-integer linear stochastic programming (MILP) model, 2) the development of an MILP model to solve the satellite ground station location problem accompanied by an L-shaped algorithmic approach that significantly outperforms solving the discrete equivalent problem directly, 3) sensitivity analysis that demonstrates that the model is very robust to uncertain scenarios and to variations in model parameter values, and 4) a validation of current National Oceanic and Atmospheric Administration (NOAA) ground station locations with analysis of additional ground stations.

5.2 Problem Description and Model

Our problem assumes that a satellite is in orbit and has the ability to collect data about a natural disaster; the data can be visual images, infrared images, or any similar data of importance to the relief personnel. As the data is being collected, it is stored in a storage-limited buffer onboard the satellite. When the satellite is in range with a ground station, the satellite transmits data to the ground station for processing and dissemination.

Figures 5.1 and 5.2 shows the very basic notion of the problem. The example assumes a forest fire in Yellowstone National Park with a ground station built at Poker Flat in Alaska. First, in Figure 5.1, the satellite flies within range of Yellowstone and collects data on the forest fire. Second, at some later time in Figure 5.2, the satellite downloads the data to the ground station at Poker Flat. The complete problem consists of a number of different potential forest fire locations and multiple potential ground station locations. In this simple example, the satellite was able to download the data at Poker Flat because it was chosen to be built. However, while Poker Flat could be a good ground station for the scenario

in which a disaster occurs at Yellowstone, it may not be desirable in the scenario that a disaster occurs at a different site. In the problem studied in this chapter, the selection of where to build the ground stations occurs before knowing the disaster location. The selection of ground station locations maximizes the expected amount of data downloaded over all potential disaster scenarios.

5.2.1 Initial Model Formulation

The problem formulation consists of a two-stage stochastic program. The first-stage consists of binary variables that determine whether to utilize each potential ground station location. There is a limit on the number of ground stations constructed because 1) there are costs associated with building, maintaining, and operating the facilities and 2) there are issues with data fusion with too many ground stations. The second-stage is the realization of a natural disaster; the latitude and longitude are different for the different disaster scenarios and the disaster scenarios can have time-dependent latitude and longitude (e.g. a hurricane's location that changes with time). The second-stage decision variables are when to collect data and when to transmit data to the ground stations. Data can only be collected when the satellite has an appropriate line-of-sight to the disaster location and data can only be transmitted to the ground when the satellite has an appropriate line-of-sight with a ground station that was constructed.

Because of the time dependencies of the model due to the system dynamics, we break the orbits in the model into time segments based on when a line-of-sight first becomes available and then when a line-of-sight becomes unavailable. Figure 5.3 illustrates the

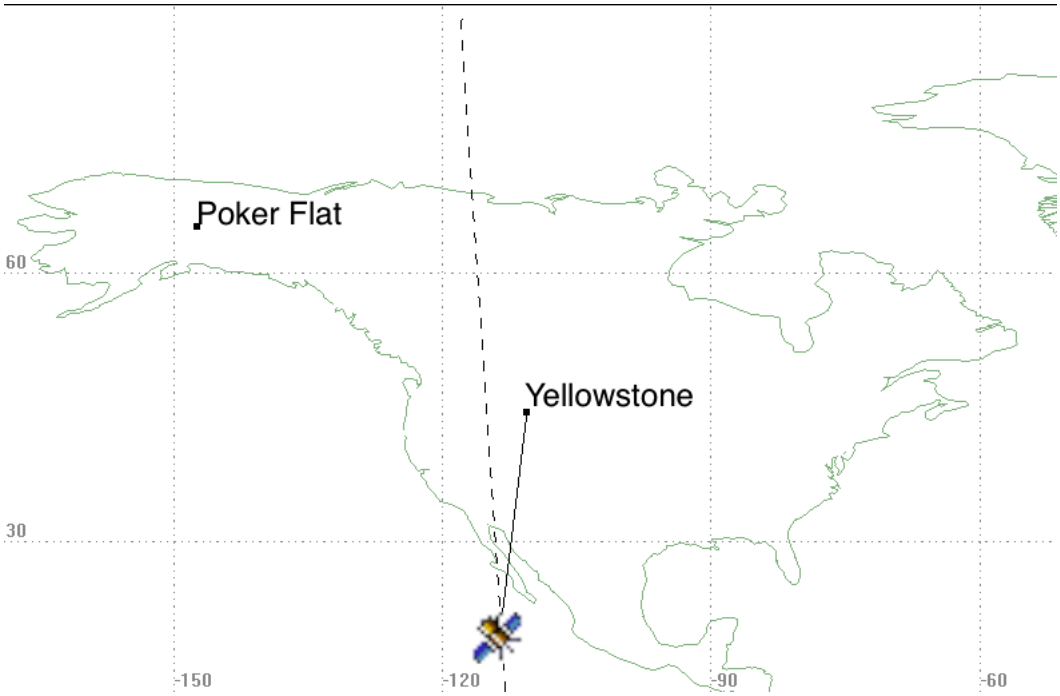

Figure 5.1

Satellite Uploads Disaster Data from Yellowstone Disaster Site.

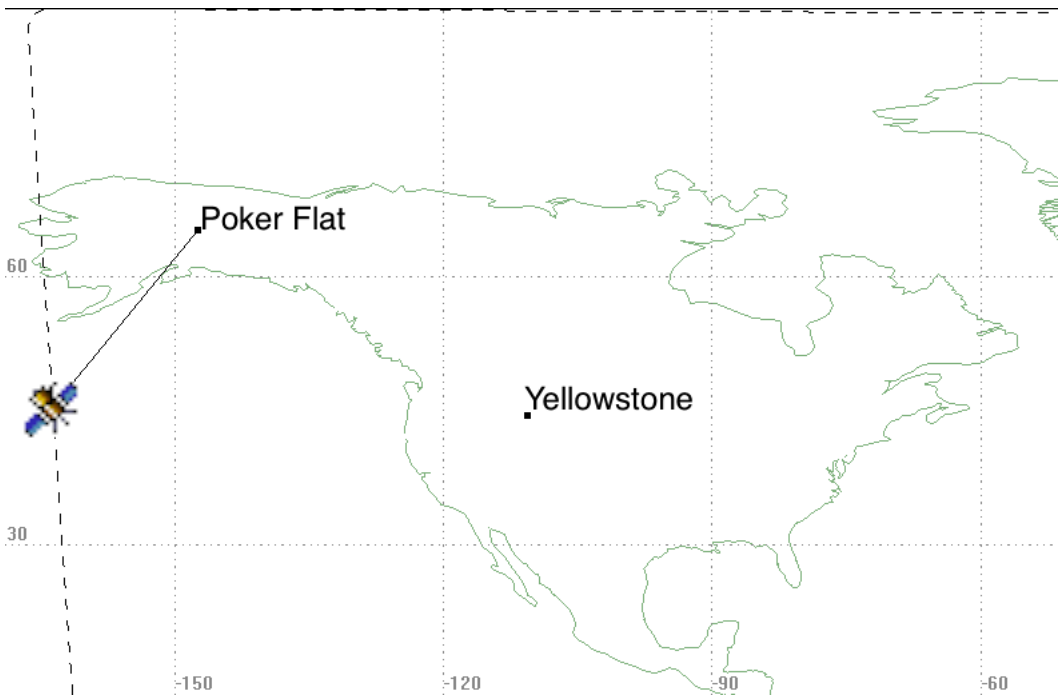

Figure 5.2

Satellite Downloads Data to Poker Flat Ground Station.

time segments. The numbered diagonal lines in the figure are the paths along the ground the satellite is following as it is orbiting the Earth; the paths are three consecutive revolutions. Each thin, black line segment is a time segment where there is no line-of-sight for collection or downloading. The thick, black line segments are the time segments when there is only a download opportunity (to Poker Flat). The thick, gray line segments are the time segments where there is only a collection opportunity (from Yellowstone). Finally, the dashed line segments are the time segments where the satellite can either collect from Yellowstone or download to Poker Flat. An important takeaway from the figure is that the time segments are not of equal length, but are defined based on when a line-of-sight is no longer present or when a line-of-sight is newly available.

Defining the model notation, the set of all time segments is I ($i \in I$), the set of all potential ground stations is J ($j \in J$), and the set of all potential disaster scenarios is S ($s \in S$). Whether ground station j is built is defined by the binary decision variable g_j. The maximum amount of data collected during time segment i in scenario s is the parameter $d_i(s)$. The maximum amount of data that can be downloaded on time segment i to ground station j is $c_{i,j}$, the proportion of the available download utilized on time segment i to ground station j in scenario s is represented as the decision variable $\rho_{i,j}(s)$, and the proportion of data collected during time segment i in scenario s is the decision variable $\rho_{i,d}(s)$.

At most, κ data packets can be in storage at a given time and no more than η ground stations can be built. Using this notation, the initial two-stage stochastic programming formulation is as follows:

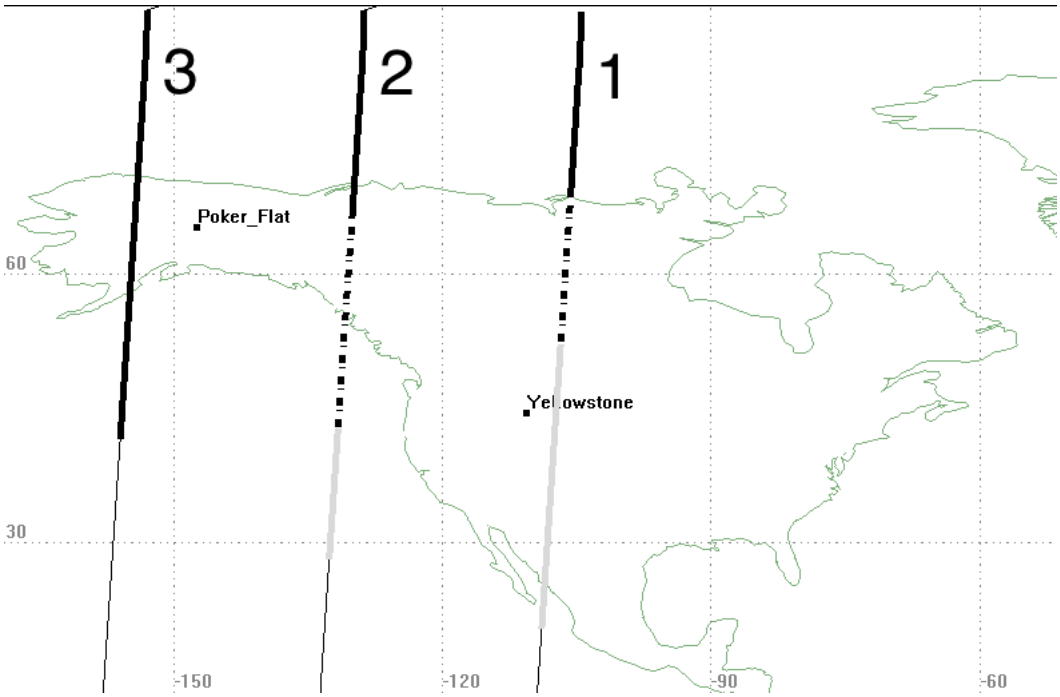

Figure 5.3

Time Segment Illustration

$$\text{Maximize } \mathbb{E}_S \quad \sum_i \sum_j \left(c_{i,j} \rho_{i,j}(s) \right) \left(\right. \tag{5.1}$$

st

$$\sum_{\ell=0}^{i} \left(d_\ell(s)\, \rho_{\ell,d}(s) \quad \sum_j \left(c_{\ell,j} \rho_{\ell,j}(s) \right) \right) \left(\right. \quad 0 \qquad \forall i \in I, s \in S \tag{5.2}$$

$$\sum_{\ell=0}^{i} \left(d_\ell(s)\, \rho_{\ell,d}(s) \quad \sum_j \left(c_{\ell,j} \rho_{\ell,j}(s) \right) \right) \left(\right. \leq \kappa \qquad \forall i \in I, s \in S \tag{5.3}$$

$$\rho_{i,d}(s) + \sum_j \left(\rho_{i,j}(s) \right. \leq 1 \qquad \forall i \in I, s \in S \tag{5.4}$$

$$0 \leq \rho_{i,d}(s) \qquad \forall i \in I, s \in S \tag{5.5}$$

$$0 \leq \rho_{i,j}(s) \leq g_j \qquad \forall i \in I, j \in J, s \in S \tag{5.6}$$

$$\sum_j \left(g_j \right. \leq \eta \tag{5.7}$$

$$g_j \in \{0, 1\} \qquad \forall j \tag{5.8}$$

The objective function (5.1) seeks to maximize the expected value of the amount of data downloaded. The amount of data downloaded is the download capacity multiplied by the proportion utilized. Constraints (5.2) and (5.3) enforce that the amount of data in storage never goes below 0 and never goes above κ. The amount of data in storage at the end of time segment i is the sum of all data collected through the end of the time segment minus all downloaded data.

The definition of the time segments are based on a sorted list of all of the starting and ending times of collection and download opportunities based on results of an orbital simulation. Because of this construction, a collection or download opportunity is either

0% of a particular time segment or 100%. At the same time, there is no restriction on the number of ground stations that are within view of the satellite during a time segment nor is there a restriction preventing a ground station from being in view at the same time as a disaster location. However, the satellite can only be pointed towards one location at any given moment, so it is not possible to simultaneously collect and download data, nor is it possible to simultaneously download to multiple ground stations. Thus, the utilization of the time segment is at most 100%. Constraint (5.4) enforces this requirement.

The minimum amount of collected data is 0 and constraint (5.5) enforces this limitation. Due to constraint (5.4), it is not possible to collect more than 100% of the data from a disaster location nor is it possible to download more than 100% of the capacity of a ground station. However, the model needs to account for the fact that a station that is not constructed does not have any capacity. Constraint (5.6) requires that the percentage of the capacity utilized is 0 if the ground station is not constructed and is at most 100% otherwise. Finally, constraint (5.7) limits the number of built ground stations to at most η.

5.2.2 Alternate Formulation

In this chapter, we also investigate an alternate formulation of the model. The model is augmented to include the auxiliary variables $\mathcal{B}_i$ that contain the amount of data in the storage buffer at the beginning of time segment i. The inclusion of the auxiliary variables increases the number of columns of the constraint matrix, but significantly decreases the number of non-zero values in the constraint matrix.

$$\text{Maximize } \mathbb{E}_S \quad \sum_i \sum_j \left(c_{i,j} \rho_{i,j}(s) \right) \left(\right. \tag{5.9}$$

st

$$d_i(s)\,\rho_{i,d}(s) \quad \sum_j \left(c_{i,j} \rho_{i,j}(s) + \mathcal{B}_i(s) = \mathcal{B}_{i+1}(s) \qquad \forall i \in I, s \in S \right. \tag{5.10}$$

$$\rho_{i,d}(s) + \sum_j \left(\rho_{i,j}(s) \leq 1 \qquad \forall i \in I, s \in S \right. \tag{5.11}$$

$$0 \leq \rho_{i,d}(s) \qquad \forall i \in I, s \in S \tag{5.12}$$

$$0 \leq \rho_{i,j}(s) \leq g_j \qquad \forall i \in I, j \in J, s \in S \tag{5.13}$$

$$\mathcal{B}_0(s) = 0 \qquad \forall s \in S \tag{5.14}$$

$$0 \leq \mathcal{B}_i(s) \leq \kappa \qquad \forall i > 0, s \in S \tag{5.15}$$

$$\sum_j \left(g_j \leq \eta \right. \tag{5.16}$$

$$g_j \in \{0, 1\} \qquad \forall j \tag{5.17}$$

The model is nearly identical to initial model, but this model uses constraint (5.10) to calculate the amount of data in storage for each time segment and uses constraints (5.14) and (5.15) to enforce the physical limitations. Although this model has more variables, the resulting constraint matrix is significantly sparser. For example, consider the comparison between constraint (5.2) and (5.10). As an example, if there are 25 potential ground station locations, then there are at most 28 non-zero coefficients in constraint (5.10) for time segment 1,000. As a comparison, constraint (5.2) potentially contains 26,000 non-zero coefficients for time segment 1,000. While adding a large number of variables will increase

the computation time, more zero coefficients in the constraint matrix will expedite computation time. Part of our forthcoming analysis compares the performance of these two models that tradeoff the sparsity and number of columns in the constraint matrix.

5.3 Solution Methodology

The L-shaped method solves the problem through a decomposition of the problem into a first-stage problem including an upper bound estimate of the second-stage cost (θ) followed by solving a second-stage model for each scenario based on the first-stage solution. The first-stage model has cuts added based on the simplex multipliers of the second-stage problems. The process iterates until convergence on the optimal solution. The first-stage model is

$$\text{Maximize } \theta \tag{5.18}$$

st

$$\sum_j \left(g_j \leq \eta \right. \tag{5.19}$$

$$E_\ell g + \theta \quad e_\ell \qquad \forall \ell \tag{5.20}$$

$$g_j \in \{0,1\} \qquad \forall j \tag{5.21}$$

where the values of E_ℓ and e_ℓ depend on the second-stage Simplex multipliers.

The second-stage model depends on which of the two formulations is used. The solution of the second-stage model for all $s \in S$ is independently determined.

The second-stage model for the initial formulation in Section 5.2.1 is the following:

$$\text{Maximize} \sum_i \sum_j \left(c_{i,j}\rho_{i,j} \right. \tag{5.22}$$

st

$$\sum_{\ell=0}^{i} \quad d_\ell \rho_{\ell,d} \quad \sum_j \left(c_{\ell,j}\rho_{\ell,j} \right) \left(\right. \quad 0 \qquad \forall i \in I \tag{5.23}$$

$$\sum_{\ell=0}^{i} \quad d_\ell \rho_{\ell,d} \quad \sum_j \left(c_{\ell,j}\rho_{\ell,j} \right) \left(\right. \leq \kappa \qquad \forall i \in I \tag{5.24}$$

$$\rho_{i,d} + \sum_j \left(\rho_{i,j} \right. \leq 1 \qquad \forall i \in I \tag{5.25}$$

$$0 \leq \rho_{i,d} \qquad \forall i \in I \tag{5.26}$$

$$0 \leq \rho_{i,j} \leq g_j \qquad \forall i \in I, j \in J \tag{5.27}$$

Similarly, the second-stage model for the alternate formulation is:

$$\text{Maximize} \sum_i \sum_j \left(c_{i,j}\rho_{i,j} \right. \tag{5.28}$$

st

$$d_i \rho_{i,d} \quad \sum_j \left(c_{i,j}\rho_{i,j} + \mathcal{B}_i = \mathcal{B}_{i+1} \right. \qquad \forall i \in I \tag{5.29}$$

$$\rho_{i,d} + \sum_j \left(\rho_{i,j} \right. \leq 1 \qquad \forall i \in I \tag{5.30}$$

$$0 \leq \rho_{i,d} \qquad \forall i \in I \tag{5.31}$$

$$0 \leq \rho_{i,j} \leq g_j \qquad \forall i \in I, j \in J \tag{5.32}$$

$$\mathcal{B}_0 = 0 \tag{5.33}$$

$$0 \leq \mathcal{B}_i \leq \kappa \qquad \forall i > 0 \tag{5.34}$$

The second-stage model is comprised of a recourse matrix (W) that includes all coefficients for the second-stage variables, a technology matrix (T) that includes the coefficients of the first-stage variables included in the second-stage model, and a righthand-side vector (h) that includes all of the constant terms in the constraint equations. The simplex multipliers for the optimal solution of the second-stage problem are π. Below is the condensed formulation for the first formulation of the second-stage. The alternate formulation includes columns for the $\mathcal{B}$ variables in the W matrix and multiplies the W matrix by the second-stage variables for that formulation.

$$\text{Maximize} \sum_i \sum_j c_{i,j}\rho_{i,j} \tag{5.35}$$

st

$$W\rho = h \quad Tg \tag{5.36}$$

Algorithm 4 contains pseudo code for the implementation of our L-shaped method.

There are four different categories of time segments and if only three of the categories exist for a particular set of parameters, then a simple algorithm can be used to solve the second-stage problem by inspection and save computational time. However, if the fourth category is present, then a linear program (LP) needs to solve the problem. The first three categories are 1) there are no collection or download opportunities ($d_i + \sum_j c_{i,j} = 0$), 2) there are only collection opportunities ($d_i > 0, \sum_j c_{i,j} = 0$), and 3) there are only download opportunities ($d_i = 0, \sum_j c_{i,j} > 0$). If all time segments fall into one of these three categories, then the algorithm collects data whenever possible and downloads data whenever possible; when collecting data $\rho_{i,d} = \min\left\{1, \frac{\kappa \ \mathcal{B}_i}{d_i}\right\}$ and when downloading

Algorithm 4 L-shaped Method

1: $a = v = 0$

2: Set $v = v + 1$

3: Solve first-stage

4: Define first-stage solution as g^v

5: **for** $s \in S$ **do**

6: Solve second-stage

7: Determine second-stage simplex multipliers $\pi^v(\omega)$

8: **end for**

9: Set $E_{a+1} = \frac{1}{|S|} \sum_{s=1}^{|S|} \pi^v(s) T(s)$

10: Set $e_{a+1} = \frac{1}{|S|} \sum_{s=1}^{|S|} \pi^v(s) h(s)$

11: Set $w^v = e_{a+1} \quad E_{a+1} g^v$

12: **if** $\theta^v \quad w^v$ **then**

13: Stop; have optimal solution

14: **else**

15: Set $a = a + 1$

16: GOTO 2

17: **end if**

all $\rho_{i,j}$ are set to zero other than $\rho_{i,j*} = \min\left\{1, \frac{\mathcal{B}_i}{c_{i,j*}}\right\}$ (where $j* = \arg\max\left\{\frac{\mathcal{B}_i}{c_{i,j}}\right\}$. (The fourth category is when there are both collection and download opportunities during a time segment ($d_i > 0, \sum_j c_{i,j} > 0$). When a category four time segment is present, then there is not necessarily a clear-cut decision as to how to proportion the time segment between the two activities.

5.4 Computational Results

5.4.1 Experimental Setup

The amount of data that can be collected from each disaster site and the amount of data that can be downloaded to each ground station is determined by using the Access Tool inside of System Tool Kit (STK) 10 . (STK is a commercial simulation and analysis software package for dynamical systems such as satellites, aircraft, and ground vehicles.) Using this general simulation package provides ample opportunities for future analysis using our model because it is possible to simulate non-circular orbits or to make the amount of data collected time dependent. The simulation is of a 600 km altitude polar orbiting satellite with a simulation period of one week. The first sets of test cases are the locations of class 7 fires (those fires consuming 5,000 or more acres) from 1980 through 2014 by the National Parks Service (NPS). The latitude and longitude pairs for all 395 NPS forest fires define the scenarios ($|S| = 395$). The data was downloaded from the Federal Fire Occurrence website. Figure 5.4 shows the locations of the fires. Although forest fires are unlikely to occur in the exact same position as they have in the past, this dataset provides realistic scenarios of where forest fires are more likely to occur. All 395 fire scenarios are equally likely to occur. The potential ground station locations are all radar tracking sites

that have been in operation in the United States. Table 5.1 lists the 25 potential ground station locations ($|J| = 25$).

Table 5.1:

Potential Ground Stations

Name	Latitude (N)	Longitude (E)
Poker Flat	65.13	-147.47
Arecibo	18.34	-66.75
Beale AFB	39.14	-121.35
Cape Cod	41.75	-70.54
Cavalier	40.72	-97.90
Clear	64.30	-149.19
Cobra Dane	52.74	174.09
Eglin	30.57	-86.21
Eldorado	30.98	-100.55
Elephant Butte	33.44	-107.00
Gila River	33.11	-112.03
HAARP	62.39	-145.15
Hawkinsville	32.29	-83.54
Haystack	42.62	-71.49
Jordan Lake	32.66	-86.26
Kaena Point	21.57	-158.27
Lake Kickapoo	33.55	-98.76

Table 5.1:
Potential Ground Stations

Name	Latitude (N)	Longitude (E)
Mickelsen	48.59	-98.36
Millstone Hill	42.62	-71.49
Red River	33.33	-93.55
Robins	32.58	-83.57
San Diego	32.58	-116.97
Silver Lake	33.15	-91.02
Tattnall	32.04	-81.93
Zenith	42.62	-71.49

The minimum elevation for observing the disaster site is 20 and the minimum elevation for download is 0 for all test cases. However, the number of constructed ground stations (η) varies between 1 and 4 and the maximum buffer size (κ) varies as being either 500, 600, or 1,000.

To solve the test cases, software, written in C, made use of Gurobi to solve the two-stage stochastic mixed integer linear program (MILP). The software is run on a 2.9GHz Intel Core i7 processor computer with 16GB of RAM running Mac OS 10.8.5.

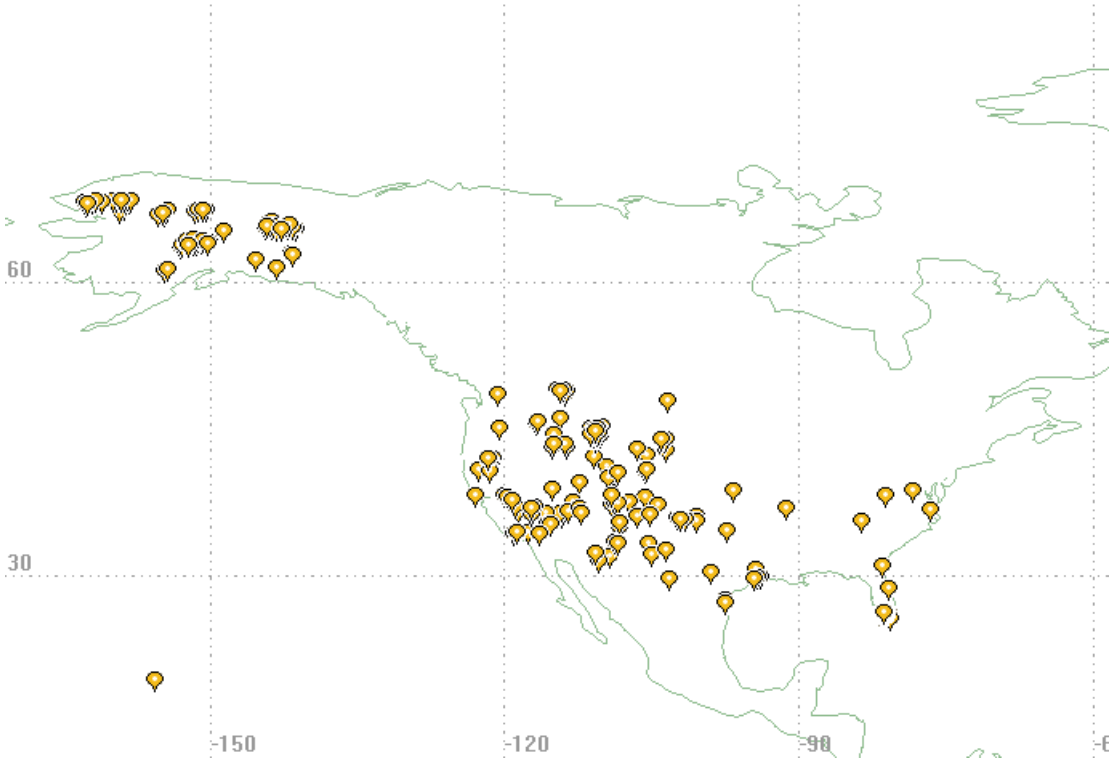

Figure 5.4

NPS Fires

5.4.2 Numerical Results

5.4.2.1 Model Comparison

The L-shaped method solves both versions of the model using the same concrete base case. The number of constructed ground stations is 1 ($\eta = 1$) and the maximum buffer size is 500 ($\kappa = 500$). The model formulation not including the auxiliary variables (see Section 5.2.1) solves in 34,303 seconds. In comparison, the model including the auxiliary variables (see Section 5.2.2) solves in 217 seconds. Because of the two-orders of magnitude difference in the amount of time required to solve the problem, the remainder of the analysis does not include the first model; all of the results presented in the next sections use the alternative model that includes the auxiliary variables.

5.4.2.2 Test Results

The test cases include twelve different parameter combinations. The number of ground stations varies between 1 and 4 and the buffer size limit can be 500, 600, or 1,000. Table 5.2 includes the results of the 12 test cases.

Poker Flat is the northern most of the potential ground sites and, due to the fact that the satellite passes over the poles each revolution, Poker Flat has the greatest available capacity and has frequent opportunities. Therefore, it is the optimal choice when one ground station is constructed; in fact, it is included as part of the solution for all test cases.

When a second ground station exists, two different ground station locations are optimal depending on the buffer sizing. For the smaller buffer, Kaena Point is optimal; this Hawaiian location has independent time segments from Poker Flat, so there is no lost total capacity due to shared time segments. The satellite's orbit also has it traveling from east to

west, Kaena Point is the western-most candidate ground station, so its available capacity is always after data has been collected from a disaster location. This location allows the satellite to download data and avoid losing data due to the buffer overflowing. Zenith is located in the northeastern United States and its northern location along with its separation from Poker Flat provides for larger amount of download capacity. Because the buffer is larger, there is less lost data than is seen with the smaller buffer case, so the greater total capacity is preferred over the more timely download capacity.

The third and fourth stations do not have a significant impact on the objective value. For some of the test cases there are multiple optimal solutions. The general trend is that northern locations provide more total capacity while southern locations can provide timely capacity.

5.4.2.3 Discrete Equivalent

The L-shaped method solves a set of smaller subproblems rather than the single, large problem. The smaller problems are easier to solve than the large problem, but there is additional computational costs associated with the handling of the subproblems. The twelve combinations of parameters for the NPS fires are solved using the discrete equivalent model with the auxiliary buffer variables instead of the L-shaped method. Table 5.3 compares the timing results for the two methods. As can be seen, the discrete equivalent solution always requires significantly more time with the worst performance being a 75-fold increase in the amount of required time. Thus, the L-shaped method is a very effective method for solving this problem.

Table 5.2

Test Case Results

η	κ	Ground Stations	Cost
1	500	Poker Flat	5,013.407
1	600	Poker Flat	5,035.023
1	1,000	Poker Flat	5,035.453
2	500	Poker Flat, Kaena Point	5,191.073
2	600	Poker Flat, Zenith	5,233.810
2	1,000	Poker Flat, Zenith	5,235.038
3	500	Poker Flat, Kaena Point, Zenith	5,238.797
3	600	Poker Flat, Kaena Point, Zenith	5,241.671
3	1,000	Poker Flat, Arecibo, Mickelsen	5,242.076
4	500	Poker Flat, Haystack, Kaena Point, Mickelsen	5,242.954
4	600	Poker Flat, Arecibo, Cavalier, Kaena Point	5,244.886
4	1,000	Poker Flat, Haystack, Kaena Point, Mickelsen	5,244.886

Table 5.3

Discrete Equivalent Timing Results

η	κ	L-shaped (sec)	Discrete Equivalent (sec)	Increase Factor
1	500	227	5,807	25.58
1	600	226	4,285	18.96
1	1,000	229	6,528	28.51
2	500	695	13,664	19.66
2	600	486	2,730	5.62
2	1,000	562	3,940	7.01
3	500	953	14,291	15.00
3	600	1,455	16,887	11.61
3	1,000	1,380	19,238	13.94
4	500	1,291	39,842	30.86
4	600	1,305	71,055	54.45
4	1,000	1,066	80,247	75.28

5.4.3 Sensitivity Analysis

5.4.3.1 Expected Value With Perfect Information

As a means of evaluating the solutions to our stochastic programming model, we calculate the expected value with perfect information (EVWPI) and the resulting expected value of perfect information (EVPI) for each of the test cases. The EVWPI is calculated by solving the "wait-and-see" problem for each scenario (the entire problem, including the first-stage variables, is solved given that the random realization is known) and calculating the weighted average of the objective values of the deterministic solutions, equation (5.37) is the EVWPI value and the EVPI value is the difference between the EVWPI and the two-stage optimal objective value; it is calculated with (5.38).

$$EVWPI = \mathbb{E}\left[\left(\text{Maximize } \sum_i \left(\sum_j \left(c_{i,j}(s)y_{i,j}(s) \qquad z_i(s)\right)\right)\right]\left(\right. \tag{5.37}$$

$$EVPI = EVWPI \quad Cost \tag{5.38}$$

$$\%Difference = \frac{EVPI}{EVWPI} \tag{5.39}$$

Table 5.4 shows the EVWPI and EVPI for the twelve test cases as well as the percent difference between the two-stage optimal solution and the EVWPI solution calculated using equation (5.39).

The EVWPI provides an upper bound on the solution value. Without perfect knowledge, the ground stations built provide the greatest expected return. As the table shows, the difference between the EVPI and stochastic programming solution is often quite small, indicating that it is possible to select a robust set of ground stations that performs almost

as well as in the situation of perfect information. In all cases, the objective value of the stochastic problem is at least 99% of the EVWPI.

The largest EVPI are associated with the three test cases involving a single ground stations and the test case of two ground stations with the smallest buffer capacity. For the single ground stations, there are instances where fires in Alaska can better tradeoff collecting and downloading when there is more geographical separation between the forest fire and the Poker Flat ground station. For these disasters, selecting a different ground station results in more data collected for that particular scenario as compared to the Poker Flat station. As a result, the EVPI increases because of these situations. For the test case of two ground station with a 500 buffer, there are many instances where Zenith as the second ground station provides better results than Kaena Point, but over all scenarios the expected value is better with Kaena Point being selected.

For the test cases with four ground stations and the two larger buffer sizes, the EVPI is zero. There is more data capacity and the buffer is large enough to prevent the loss of data due to the buffer overflowing its capacity. Because there is excess capacity, there are multiple optimal solutions and the system is able to optimally handle all scenarios.

5.4.3.2 Value of the Stochastic Solution

The value of the stochastic solution (VSS) is calculated by creating a single scenario that is the average of all of the scenarios (the mean-value-problem) and determining the optimal set of first-stage variables for that single scenario. Next, the expected cost over all scenarios using those first-stage variable values is calculated. The VSS is the differ-

ence between that expected value and the expected value of the complete problem. For the NPS forest fires fires, the average latitude and longitude of the forest fires are calculated (40.102 N, 109.376 W), i.e., not the location of any of the 395 NPS fires. If only one ground station is built, then the optimal choice is Poker Flat and that is the same as the solution when taking all scenarios into consideration, so the VSS is 0. However, as is seen in Table 5.5, once additional ground stations are constructed, there is value in considering the stochastic nature of the problem. The four ground station case has a significant difference because there are multiple first-stage combinations with equal, optimal objective values for the mean-value-problem and the software arbitrarily selects one of the first-stage combinations. However, the chosen first-stage combination is not a good solution when all scenarios are considered. For the particular orbit used in this chapter with the particular ground station locations, taking the stochastic nature of the problem into consideration is significant when the number of ground stations constructed allows multiple combinations of first-stage variables to produce equal objective values and when the total amount of storage capacity is limited. If the combination of orbit and ground station locations results in a greater variety of optimal ground station locations for the scenarios, then the VSS would likely be greater in all cases.

5.4.3.3 Parameter Variation

Throughout the chapter, results comparing the number of ground stations and the buffer size demonstrate the sensitivity of the model to these parameters. An additional model parameter is the number of scenarios. As a means of increasing the number of test cases, all

major Atlantic hurricane tracks from 1854 through 2014 are included as additional disasters. These disaster locations change with time; unlike the forest fires that are assumed to be stationary. In addition to the 395 forest fires, there are 367 hurricanes virtually doubling the number of scenarios. Table 5.6 shows the run times for the twelve sets of parameter values with the additional scenarios. Comparing Tables 5.3 and 5.6, it can be observed that the runtimes increase by, on average, more than 14 times. Thus, we observe that the solution time is sensitive to the number of scenarios. However, for the two sets of scenarios discussed in this chapter (NPS forest fires and a combination of NPS forest fires and Atlantic Hurricanes), the runtimes are still reasonable. That said, if a significantly larger number of scenarios were evaluated, then a different methodological solution approach might be necessary.

5.4.4 Comparison with Current NOAA Ground Station Locations

The NOAA Office of Satellite and Product Operations (OSPO) operates three ground station locations (Suitland, MD, Wallops, VA, and Fairbanks, AK). To compare the current OSPO locations with the locations prescribed by our model, the 395 scenarios of NPS forest fires are simulated with the three NOAA ground stations. Table 5.7 compares the costs of the ground stations selected through our methodology compared to the costs of the NOAA ground stations for the three-ground stations test cases ($\eta = 3$); the three test cases included examine the sensitivity to the size of the data storage buffer (κ). The results confirm that the NOAA stations are wisely selected; placing one of the three stations

in Fairbanks, AK provides significant coverage in the same manner that Poker Flat, AK provides significant coverage for our set of three ground stations.

One benefit of our optimization model is that it can be used to help decide where to locate additional ground stations. Table 5.8 shows the ground station solutions generated by our model with the added constraint that the ground stations in the current OSPO plan are opened and the 25 candidate locations from Table 5.1 are being considered. For the cases of added stations to the OSPO network, a buffer capacity of 500 ($\kappa = 500$) is used. The 395 scenarios of NPS forest fires are used for the investigation of the added ground stations. The stations added fill in missing geographical coverage. Kaena Point adds coverage outside of the continental United States, Cavalier is a northern station that is between the stations in Alaska and on the East Coast, and San Diego adds in a ground station in the southern continental United States.

5.5 Conclusion

Natural disasters can strike any place at any time. When such events do occur, satellite data can be an invaluable tool for the relief efforts. Unfortunately, the satellite cannot be launched at a moment's notice and the supporting ground stations placed to optimize for the disaster. Instead, the ground stations have to be in place before the disaster occurs. Thus, it is important to find a set of ground station locations that hedge against the uncertainty in the disaster location. The need to make a decision with uncertainty can be well handled by a stochastic programming approach, as we demonstrate in this chapter.

This chapter presents an example problem that optimally places ground stations from a list of twenty-five candidates given the major forest fires battled by the NPS as well as Atlantic Ocean hurricanes. The methodology of this chapter allows mission designers to tradeoff not only the location and quantity of ground stations, but also the potential size of onboard data storage. Commercial software simulates the complex dynamics of the satellite motion and the results of the simulation, along with a MILP solver and the L-shaped method, efficiently solve the problem. The runtimes are reasonable even when the set of scenarios includes decades of forest fire locations and over a century of hurricane tracks. The EVPI analysis indicates that the optimal solution found performs very well regardless of the scenario that becomes realized. The VSS indicates that as the ground station selection becomes varied between the scenarios, then there is a penalty to considering only the midpoint solution and not considering the true stochastic nature of the problem.

Three different formulations are compared: 1) L-shaped without auxiliary variables, 2) L-shaped with auxiliary variables, and 3) discrete equivalent with auxiliary variables. The L-shaped with auxiliary variables significantly outperforms the other two formulations.

One implication of this chapter is that mission-specific ground stations are advantageous to ensure that download capacity is available for the satellite. Having sufficient capacity to download as much data as possible about a natural disaster will enable relief personnel to make the best choices about the distribution of the resources at their disposal. This chapter presents a methodology for optimally selecting ground station locations from a set of candidate choices using an exact method while considering the uncertainty of where a natural disaster will occur.

Table 5.4

EVPI

η	κ	Cost	EVWPI	EVPI	% Difference
1	500	5,013.407	5,035.526	22.119	0.44%
1	600	5,035.023	5,057.762	22.739	0.45%
1	1,000	5,035.453	5,058.952	23.499	0.46%
2	500	5,191.073	5,230.833	39.759	0.76%
2	600	5,233.810	5,234.668	0.858	0.02%
2	1,000	5,235.038	5,235.516	0.478	0.01%
3	500	5,238.797	5,244.886	6.089	0.12%
3	600	5,241.671	5,244.886	3.215	0.06%
3	1,000	5,242.076	5,244.886	2.810	0.05%
4	500	5,242.954	5,244.886	1.932	0.04%
4	600	5,244.886	5,244.886	0.000	0.00%
4	1,000	5,244.886	5,244.886	0.000	0.00%

Table 5.5

VSS

η	κ	Cost	VSS	VSS/Cost %
1	500	5,013.407	0.000	0.000
1	600	5,035.023	0.000	0.000
1	1,000	5,035.453	0.000	0.000
2	500	5,191.073	53.160	1.02
2	600	5,233.810	47.635	0.91
2	1,000	5,235.038	48.572	0.93
3	500	5,238.797	40.445	0.77
3	600	5,241.671	40.446	0.77
3	1,000	5,242.076	40.851	0.78
4	500	5,242.954	327.108	6.24
4	600	5,244.886	157.175	3.00
4	1,000	5,244.886	119.278	2.27

Table 5.6

NPS Fires and Atlantic Hurricanes

η	κ	Ground Stations	Cost	Time (sec)
1	500	Poker Flat	4,329.876	3,603
1	600	Poker Flat	4,341.081	3,606
1	1,000	Poker Flat	4,341.304	3,609
2	500	Poker Flat, Millstone Hill	4,471.022	7,603
2	600	Poker Flat, Haystack	4,509.073	8,725
2	1,000	Poker Flat, Zenith	4,509.710	8,732
3	500	Poker Flat, Haystack, Kaena Point	4,511.659	12,460
3	600	Poker Flat, Arecibo, Mickelson	4,516.732	18,669
3	1,000	Poker Flat, Arecibo, Mickelson	4,517.369	19,799
4	500	Poker Flat, Arecibo, Cavalier, Kaena Point	4,517.824	15,341
4	600	Poker Flat, Arecibo, Cape Cod, Mickelson	4,520.525	21,465
4	1,000	Poker Flat, Arecibo, Cavalier, Haystack	4,521.161	12,685

Table 5.7

NOAA Ground Station Results

κ	L-shaped	NOAA	Difference	% Different
500	5,238.797	5,155.376	83.422	1.59
600	5,241.671	5,228.696	12.975	0.25
1,000	5,242.076	5,229.924	12.152	0.23

Table 5.8

Optimal Ground Station Solutions as Additional Ground Stations are Added

Solution	Ground Stations	Cost
Current OSPO locations	Suitland, MD; Wallops, VA; Fairbanks, AK	5,155.376
Optimal solution with 1 station added	Suitland, MD; Wallops, VA; Fairbanks, AK; Kaena Point, HI	5,235.582
Optimal solution with 2 stations added	Suitland, MD; Wallops, VA; Fairbanks, AK; Kaena Point, HI; Cavalier, ND	5,242.954
Optimal solution with 3 stations added	Suitland, MD; Wallops, VA; Fairbanks, AK; Kaena Point, HI; Cavalier, ND; San Diego, CA	5,244.886

CHAPTER 6

CONCLUSIONS

6.1 Summary

It has not been a full century since the first satellite was launched, but society's reliance on satellites has grown to the point where they are an intricate component of our daily lives. Science has also used satellites to monitor and investigate areas that would otherwise go unobserved. Response and recovery from natural disasters, including forest fires, depends on satellite data providing current conditions of the situation. Although satellite data is valuable during a forest fire, there are often shortcomings in the data. One such shortcoming is the fact that high-resolution images of the forest fire are not always made readily available by existing collection methods. A second shortcoming is the ability to download the collected data from the satellite in a timely manner due to a lack of resources on the ground.

This dissertation addresses these two shortcomings. To increase the collection of high-resolution data, a methodology is developed whereby a constellation of satellites maneuvers so as to fly directly over the forest fire once per day. The methodology is then expanded to increase the direct flyover of the forest fire from once per day to twice per day. The shortcoming of a lack of ground station resources is addressed by developing a

methodology to optimally place ground stations to collect data from an unknown forest fire.

The methodologies of this dissertation provide for the ability to design a complete system for the monitoring of a forest fire by a constellation of satellites. The implementation of the methodologies of this dissertation will increase the amount of high-quality satellite data collected for forest fires and will minimize the costs associated with building and maintaining ground stations.

The collection of satellite data using the methodology of this dissertation is compared to the current operating practices of not maneuvering satellites. The orbits of current operational satellites are simulated using independent software and the orbits for a constellation using the methodology of this dissertation are also simulated. The results indicated that there is a significant increase in the collection of high-quality data using the maneuver strategy as compared to passively collecting data. The expected fuel cost is also kept reasonable by optimally selecting the initial orbit so as to minimize the expected maneuver costs for an *a priori* unknown forest fire. This paradigm has the ability to significantly enhance the efforts in combating forest fires by increasing both the quantity and quality of the data that is being collected.

The analysis also investigates the sensitivity of the model to various parameters such as the size of the constellation, the number of days included in the model, and the number of scenarios. There is a significant dependence on the size of the constellation, so the size of the constellation must be determined before launch because changing the size of the constellation after launch will have a significant impact on the optimal design. For some satel-

lite constellations, additional satellites have been added to the constellation over the lifetime of the constellation. However, for a satellite constellation designed with the methodology of this dissertation, the number of satellites must be determined prior to launch in order to achieve optimal performance of the constellation. The model is insensitive to the number of days included in the data collection phase of the ascending-pass-only problem. Therefore, initial trade-studies can be performed with a small number of days without significantly impacting the results. Knowing this insensitivity allows for less computation time being required by a mission designer and allows for the computational savings to be put towards considering a wider variety of potential solutions.

The model includes a number of modifications that help to speed up performance. The use of a penalty term allows for relatively complete recourse which in turn allows for the use of standard solution techniques. The most significant model modification is the inclusion of additional variables to convert the absolute value objective function from a nonlinear equation to a linear equation. These two approaches are beneficial for any researcher investigating a similar model. The ability to use a standard solution technique generalizes the problem and allows for easier modification for expanded research. For example, the constellation collecting data both on the ascending- and descending-passes is built around the core solution techniques of the ascending-pass-only model. If a more customized solution technique had been required, then it might not be feasible to expand the model to include the descending-pass observation opportunity.

Including the descending-pass increases the amount of collected data, but also significantly increases the fuel cost. A mission manager will need to decide if the additional

fuel cost is worth the additional observation opportunity or not, but an optimal initial orbit developed through the presented methodology at least provides the mission manager with a choice as to whether or not the additional fuel cost is worthwhile. The ascending-pass-only example problem does include data collection opportunities on the descending-pass, but the satellites does not fly directly over the forest fire. If the forest fire had occurred at a different location than the one example, then there might not have been an opportunity on a descending-pass. Two options for the mission manager are to either maneuver the constellation for only ascending-pass data collection or select to maneuver the constellation to collect on both the ascending- and descending-passes. The increase in the quantity and quality of the data collected as well as the additional fuel cost will need to be determined for the mission manager to decide on the best course of action.

The descending-pass portion of the dissertation also includes a shift in the solution strategy, Rather than partitioning the continuous search space into a discrete search space, a sampling approach is employed to determine the optimal solution. In addition, the non-linear equations that contain both first and second-stage variables are linearized to allow for more efficient solution techniques. Preprocessing is again used to eliminate infeasible solutions to decrease solution convergence time. The addition of a third scenario parameter causes a polynomial increase in the number of required discrete scenarios. By changing from a discrete search space to a stochastic search space, the computation time is more tractable. In addition, removing the assumed discrete scenarios makes the problem a better representation of the actual situation.

A mathematically rigorous methodology for optimally placing ground stations is not present in the literature prior to this dissertation. The cost and complexity of satellite ground stations requires careful selection of locations. While ad hoc procedures have produced descent results, as can be seen by the fact that the current NOAA ground stations are well placed, there is significant value in having a formal way to prove that the selection is optimal. In addition, it provides an easy mechanism for determining future sites if the need arises to increase the number of ground stations. Introducing a mathematically rigorous methodology for selecting ground station selection sites will help to ensure that funds are appropriately spent for the construction of new ground stations and will enable engineers to easily justify the sites that are selected for ground stations.

Commercial software is used to simulate the complex motion of the satellites and hurricane ground tracks, but the results of the simulation are parsed to allow for an efficient linear solution technique. This interplay between simulation and solution algorithms is an important link for the solving of complex dynamic problems. As an example, a similar problem of where relief supplies should be placed would be determined by simulating potential possible hurricane paths and then using the results of those simulations to build a facility location model for the locations of the relief supplies. Simulating health facility usage and feeding that information back to a linear model would be a means of optimizing scheduling of resources. As a third additional example, simulating weather patterns to determine crop yields can be used to build a linear model to determine the optimal growing scheme for a farmer to employ.

6.2 Future Work

6.2.1 Ascending- and Descending-Pass Data Collection

One of the most significant assumptions made is that the two-body force model describes the forces acting on the satellite. As a first approximation, this is a good assumption. However, there are a variety of forces that are acting on the satellite. The most significant of these perturbing forces is the Earth oblateness. The magnitude of the perturbing force is dependent on the orbit's inclination. Since the descending-pass model presents a means of including the inclination in the model, this work could be extended to include the J_2 and J_4 terms; these terms are the first two terms of the series of terms that account for the fact that the Earth's mass is not uniformly distributed. Over the course of a day or two, there will be little impact from the perturbations due to the Earth's oblateness. On the other hand, over the course of a month, the impact will be significantly greater. Forces such as atmospheric drag and solar radiation pressure can be modeled approximately, but the exact magnitudes are unknown beforehand.

A second significant assumption is that the satellite needs to fly directly over the forest fire. The image resolution is maximized when the satellite flies directly overhead, but if the satellite is one foot to the east or west, the resulting resolution is virtually identical. Therefore, in actuality, there is an acceptable range of distances where the resolution would still be considered "good enough". The model could be modified to constrain the satellite to remain within the allowable time window rather than needing to fly directly overhead. A significant challenge to that model design is constructing the objective function. Flying directly overhead is ideal, but how much additional fuel is worth flying directly overhead

instead of one foot to the west? Is the relationship between the tradeoff in fuel and distance linear or nonlinear? The objective function would need to be constructed so as to appropriately tradeoff fuel and image resolution.

The fact that the forest fire is stationary is a third significant assumption. Having the forest fire move greatly increases the number of scenarios because there is the current large set of scenarios multiplied by every potential movement of the forest fire. However, the SAA approach has been shown to work for the problem, so there is a proven means of reducing the number of evaluated scenarios through sampling. A more significant challenge would be incorporating the forest fire movement into the model. Movement to the east or west is relatively easy to include because this motion is linearly related to the rotation rate of the Earth and could thus be added to the model. Any movement with a north or south component is nonlinear and depends on both the latitude of the forest fire as well as the inclination of the orbit and the orbital period.

While this study focusses on forest fires, the model only requires the latitude and longitude of the point on the Earth that is being observed. Therefore, the work could be extended to a variety of Earth surveillance contexts including monitoring a dam during flooding conditions, monitoring crops during a drought, or observing a city after an earthquake. In addition, the model could be extended to cover occurrences other than natural disasters. As an example, the constellation could be maneuvered to monitor and provide communications during a military operation. Image scheduling could also be added to the model. Ideally, the scheduling of image collection could be done in real-time [90]

and combining the planning of the collection of images in conjunction with the maneuver sequences would be an avenue of future work.

6.2.2 Ground Station Locations

The most significant additional work in the ground station location problem would be the inclusion of data holding cost. The data has a time relevance; getting images of the conditions of a forest fire a week delayed is not of significant benefit, but getting the same images in realtime has significant benefit. Expanding the model to include a holding cost would place more value on more recent data and less value on stale data. This addition would also necessitate establishing whether the data download followed a first-in-first-out (FIFO) or first-in-last-out (FILO) paradigm. There would also be the added complexity of tracking not only the quantity of data, but the arrival time of the data. Overcoming these challenges would provide for a design better suited for response to a natural disaster.

In addition, all of the ground station sites are restricted to the United States; however, a set of worldwide locations could provide for more continuous availability of ground station resources and a design better able to have the timely capacity needed by the satellites. At the same time, the disaster scenarios should also be expanded to include worldwide disasters because the satellites would likely be tasked for natural disasters that occurred outside of the United States.

Data collection in this study is assumed to be time insensitive. However, some measurements can only be taken during daylight hours and some can only be taken during darkness. Including time dependence in the data collection simulation has the potential

to be required by some satellite instruments and has the potential to change the optimal solution of the model.

6.2.3 Holistic System Design

An additional area of future work would be the combination of the entire system (satellites and ground stations) into a single problem. The objective function of such a problem would need to be tuned because there is the question of how much extra fuel expense is the equivalent of an extra packet of collected data. In addition, this combined problem would add significant complexity because of the required feedback between the simulation model used to create the input for the ground station selection and the linear program (LP) for the orbit design. However, the ability to use a simulation model as a component of a stochastic program would be beneficial to problem domains outside of satellite collection of forest fire data.

A first approach might be to leave the two problems decoupled in terms of optimization. The maneuvers for the constellation could first be determined. The maneuver sequence for each scenario could be recorded and simulated for the corresponding fire location. The resulting simulation results could be paired with the set of ground station location choices and the subsequent model solved. This methodology is the equivalent of a combined objective function having an infinite weight on the fuel cost compared to the amount of downloaded data.

As a significantly different approach of combing the two problems, the decoupling could occur in the opposite sense. The ground stations could be selected based on the his-

torical record as was presented in this study. The constellation could then be maneuvered to fly directly over the ground station or to fly a specified distance to the east on one revolution and then a specified distance to the west on the following revolution. This approach would put an infinite weight on the download capacity component of the objective function as compared to the fuel component.

The two approaches from above are the two extremes where one component of the cost function is set to zero. An iterative approach that uses the solutions from the methodologies above to add cuts to the model and solves each of the sets of problems (satellites and ground stations) iteratively until convergence is achieved would be an alternative. However, such an iterative approach could prove to be computationally intractable because of the complexity involved with each iteration.

REFERENCES

[1] O. Abdelkhalik and A. Gad, "Optimization of space orbits design for Earth orbiting missions," *Acta Astronautica*, vol. 68, no. 7, April-May 2011, pp. 1307–1317.

[2] L. Appel, M. Guelman, and D. Mishne, "Optimization of satellite constellation reconfiguration maneuvers," *Acta Astronautica*, vol. 99, June–July 2014, pp. 166–174.

[3] I. Averbakh and O. Berman, "Minimax regret p-center location on a network with demand uncertainty," *Location Science*, vol. 5, no. 4, December 1997, pp. 247–254.

[4] L. Barbulescu, A. Howe, and D. Whitley, "AFSCN scheduling: How the problem and solution have evolved," *Mathematical and Computer Modelling*, vol. 43, no. 9, May 2006, pp. 1023–1037.

[5] C. F. Barnes, H. Fritz, and J. Yoo, "Hurricane Disaster Assessments With Image-Driven Data Mining in High-Resolution Satellite Imagery," *IEEE Transactions on Geoscience and Remote Sensing*, vol. 45, no. 6, May 2007, pp. 1631–1640.

[6] O. Berman, D. Krass, and M. B. C. Menezes, "Facility Reliability Issues in Network p-Median Problems: Strategic Centralization and Co-Location Effects," *Operations Research*, vol. 55, no. 2, March–April 2007, pp. 332–350.

[7] O. Berman, D. Krass, and M. B. C. Menezes, "Locating Facilities in the Presence of Disruptions and Incomplete Information," *Decision Sciences*, vol. 40, no. 4, November 2009, pp. 845–868.

[8] S. Bernier and M. Barbeau, "A Virtual Ground Station Based on Distributed Components for Satellite Communications," *Small Satellite Conference*, Logan, UT, 2001, AIAA/Utah State University.

[9] N. Bianchess, J.-F. Cordeau, J. Desrosiers, and G. Laporte, "A heuristic for the multi-satellite, multi-orbit and multi-user management of Earth observation satellites," *European Journal of Operational Research*, vol. 177, no. 2, March 2007, pp. 750–762.

[10] N. Bogdos and E. S. Manolakos, "A tool for simulation and geo-animation of wildfires with fuel editing and hotspot monitoring capabilities," *Environmental Modelling and Software*, vol. 46, August 2013, pp. 182–195.

[11] S. Cakaj and K. Malarić, "Rigorous analysis on performance of LEO satellite ground station in urban environment," *International Journal of Satellite Communications and Networking*, vol. 25, no. 6, November/December 2007, pp. 619–643.

[12] N. Chen, Z. Chen, and L. Di, "An Efficient Method for Near-Real-Time On-Demand Retrieval of Remote Sensing Observations," *IEEE Journal of Selected Topics in Applied Earth Observations and Remote Sensing*, vol. 4, no. 3, September 2011, pp. 615–625.

[13] Y. Chen, V. Mahalec, Y. Chen, and R. He, "Optimal Satellite Orbit Design for Prioritized Multiple Targets with Threshold Observation Time Using Self-Adaptive Differential Evolution," *Journal of Aerospace Engineering*, vol. 28, no. 2, March 2015.

[14] Y. Chen, V. Mahalec, Y. Chen, X. Liu, R. He, and K. Sun, "Reconfiguration of satellite orbit for cooperative observation using variable-size multi-objective differential evolution," *European Journal of Operational Research*, vol. 242, no. 1, April 2015, pp. 10–20.

[15] C. Circi, E. Ortore, and F. Bunkheila, "Satellite constellations in sliding ground track orbits," *Aerospace Science and Technology*, vol. 39, December 2014, pp. 395–402.

[16] J. Cloud, "Imaging the World in a Barrel CORONA and the Clandestine Convergence of the Earth Sciences," *Social Studies of Science*, vol. 31, no. 2, April 2001, pp. 231–251.

[17] T. C. Co, C. Zagaris, and J. T. Black, "Responsive Satellites Through Ground Track Manipulation Using Existing Technology," *Journal of Spacecraft and Rockets*, vol. 50, no. 1, January–February 2013, pp. 206–216.

[18] S. Damiani, H. Dreihahn, J. Noll, M. Niézette, and G. P. Calzolari, "A Planning and Scheduling System to Allocate ESA Ground Station Network Services," *The International Conference on Automated Planning and Scheduling*. American Association for Artificial Intelligence, September 2007.

[19] D. K. Davies, S. Ilavajhala, and M. M. Wong, "Fire Information for Resource Management System: Archiving and Distributing MODIS Active Fire Data," *IEEE Transactions on Geoscience and Remote Sensing*, vol. 47, no. 1, January 2009, pp. 72–79.

[20] Z. Drezner, "Heuristic Solution Methods for Two Location Problems with Unreliable Facilities," *Journal of the Operational Research Society*, vol. 38, no. 6, June 1987, pp. 509–514.

[21] H. earl Park, S.-Y. Park, and K.-H. Choi, "Satellite formation reconfiguration and station-keeping using state-dependent Riccati equation technique," *Aerospace Science and Technology*, vol. 15, no. 6, September 2011, pp. 440–452.

[22] M. P. Ferringer and D. B. Spencer, "Satellite Constellation Design Tradeoffs Using Multiple-Objective Evolutionary Computation," *Journal of Spacecraft and Rockets*, vol. 43, no. 6, November–December 2006, pp. 1404–1411.

[23] M. P. Ferringer, D. B. Spencer, and P. Reed, "Many-objective reconfiguration of operational satellite constellations with the Large-Cluster Epsilon Non-dominated Sorting Genetic Algorithm-II," *2009 IEEE Congress on Evolutionary Computation*. IEEE, May 2009.

[24] A. Forghani, S. Kazemi, and L. Ge, "Wildland Fire Behaviour Simulations Employing an Integrated Weather-Topographical-Fuel Datasets and Satellite Remote Sensing," *International Journal Of Geoinformatics*, vol. 10, no. 4, December 2014, pp. 35–44.

[25] N. H. F. French, W. J. de Groot, L. K. Jenkins, B. M. Rogers, E. Alvarado, B. Amiro, B. de Jong, S. Goetz, E. Hoy, E. Hyer, R. Keane, B. E. Law, D. McKenzie, S. G. McNulty, R. Ottmar, D. R. Pérez-Salicrup, J. Randerson, K. M. Robertson, and M. Turetsky, "Model comparisons for estimating carbon emissions from North American wildland fire," *Journal of Geophysical Research: Biogeosciences*, vol. 116, no. G4, December 2011.

[26] X. Fu, M. Wu, and Y. Tang, "Design and Maintenance of Low-Earth Repeat-Ground-Track Successive-Coverage Orbits," *Journal of Guidance, Control, and Dynamics*, vol. 35, no. 2, March–April 2012, pp. 686–691.

[27] V. Gabrel, "Strengthened 0-1 linear formulation for the daily satellite mission planning," *Journal of Combinatorial Optimization*, vol. 11, no. 3, May 2006, pp. 341–346.

[28] V. Gabrel and D. Vanderpooten, "Enumeration and interactive selection of efficient paths in a multiple criteria graph for scheduling an earth observing satellite," *European Journal of Operational Research*, vol. 139, no. 3, June 2002, pp. 533–542.

[29] A. Gad and O. Abdelkhalik, "Repeated Shadow Track Orbits for Space-SunSetter Missions," *International Journal of Aerospace Engineering*, 2009.

[30] G. Galindo and R. Batta, "Prepositioning of supplies in preparation for a hurricane under potential destruction of prepositioned supplies," *Socio-Economic Planning Sciences*, vol. 47, no. 1, March 2013, pp. 20–37.

[31] I. Galindo, P. López-Pérez, and M. Evangelista-Salazar, "Real-time AVHRR forest fire detection in Mexico (1998-2000)," *International Journal Of Remote Sensing*, vol. 24, no. 1, 2003, pp. 9–22.

[32] B. S. Gottfried, "Technical Note—A Stopping Criterion for the Golden-Ratio Search," *Operations Research*, vol. 23, no. 3, May–June 1975, pp. 553–555.

[33] V. V. Gounder, R. Prakash, and HosameAbu-Amara, "Routing in LEO-based satellite networks," *1999 IEEE Emerging Technologies Symposium. Wireless Communications and Systems*. IEEE, 1999.

[34] W. Hohmann, *Die Erreichbarkeit der Himmelskörper*, Verlag Oldenbourg, München, Germany, 1925.

[35] A. B. Hoskins and E. M. Atkins, "Satellite Formation Mission Optimization with a Multi-Impulse Design," *Journal of Spacecraft and Rockets*, vol. 44, no. 2, March–April 2007, pp. 425–433.

[36] R. Huang, S. Kim, and M. B. C. Menezes, "Facility location for large-scale emergencies," *Annals of Operations Research*, vol. 181, no. 1, December 2010, pp. 271–286.

[37] A. Iwasaki, S. Miyatani, and S. Nakasuka, "Satellite Contributions to Disaster Monitoring - Japanese Earthquake and Tsunami Case in 2011," *Small Satellite Conference*, Logan, UT, 2012, AIAA/Utah State University.

[38] J. Jang, J. Choi, H.-J. Bae, and I.-C. Choi, "Image collection planning for KOrea Multi-Purpose SATellite-2," *European Journal of Operational Research*, vol. 230, no. 1, October 2013, pp. 190–199.

[39] H. Jia, F. Ordóñez, and M. M. Dessouky, "Solution approaches for facility location of medical supplies for large-scale emergencies," *Computers and Industrial Engineering*, vol. 52, no. 2, March 2007, pp. 257–276.

[40] J. F. A. Jónsson, R. Morris, and D. E. Smith, "Planning and scheduling for fleets of earth observing satellites," *The 6th International Symposium on Artificial Intelligence, Robotics, Automation and Space*, Montreal, June 2002.

[41] E. J. L. Jr., K. N. Ballard, and C. H. Song, "Pre-positioning hurricane supplies in a commercial supply chain," *Socio-Economic Planning Sciences*, vol. 46, no. 4, December 2012, pp. 291–305.

[42] R. E. Keane, J. M. Herynk, C. Toney, S. P. Urbanski, D. C. Lutes, and R. D. Ottmar, "Evaluating the performance and mapping of three fuel classification systems using Forest Inventory and Analysis surface fuel measurements," *Forest Ecology and Management*, vol. 305, no. 1, October 2013, pp. 248–263.

[43] N. Kerle and C. Oppenheimer, "Satellite Remote Sensing as a Tool in Lahar Disaster Management," *Disasters*, vol. 26, no. 2, June 2002, pp. 140–160.

[44] H.-D. Kim, H. Bang, and O.-C. Jung, "Genetic Design of Target Orbits for a Temporary Reconnaissance Mission," *Journal of Spacecraft and Rockets*, vol. 46, no. 3, May–June 2009, pp. 725–728.

[45] S.-R. Kim, W.-K. Lee, D.-A. Kwak, G. S. Biging, P. Gong, J.-H. Lee, and H.-K. Cho, "Forest cover classification by optimal segmentation of high resolution satellite imagery," *Sensors*, vol. 11, no. 2, February 2011, pp. 1943–1958.

[46] N. Kussul, A. Shelestov, and S. Skakun, *Grid and Cloud Database Management*, chapter Grid Technologies for Satellite Data Processing and Management Within International Disaster Monitoring Projects, Springer, 2011, pp. 279–305.

[47] N. N. Kussul, A. Y. Shelestov, and S. V. Skakun, "The Wide Area Grid Testbed for Flood Monitoring Using Earth Observation Data," *IEEE Journal of Selected Topics in Applied Earth Observations and Remote Sensing*, vol. 5, no. 6, December 2012, pp. 1746–1751.

[48] A. M. Leigh and J. T. Black, "Navigation solution to maneuver a spacecraft relative to multiple satellites and ground locations," *Acta Astronautica*, vol. 109, April–May 2015, pp. 1–13.

[49] L. M. Leslie, J. F. LeMarshall, R. P. Morison, C. Spinoso, R. J. Purser, N. Pescod, and R. Seecamp, "Improved hurricane track forecasting from the continuous assimilation of high quality satellite wind data," *Monthly Weather Review*, vol. 126, no. 5, May 1998, pp. 1248–1258.

[50] H. Li and B. Wu, "Adaptive geo-information processing service evolution: reuse and local modification method," *ISPRS Journal of Photogrammetry and Remote Sensing*, vol. 83, September 2013, pp. 165–183.

[51] T. Li, J. Xiang, Z. Wang, and Y. Zhang, "Circular revisit orbits design for responsive mission over a single target," *Acta Astronautica*, vol. 127, October–November 2016, pp. 219–225.

[52] S. Liu and M. E. Hodgson, "Optimizing large area coverage from multiple satellite-sensors," *GIScience and Remote Sensing*, vol. 50, no. 6, 2013, pp. 652–666.

[53] C.-C. Lu and J.-B. Sheu, "Robust vertex p-center model for locating urgent relief distribution centers," *Computers and Operations Research*, vol. 40, no. 8, August 2013, pp. 2128–2137.

[54] X. Luo, M. Wang, G. Dai, and Z. Song, "Constellation Design for Earth Observation based on the Characteristics of the Satellite Ground Track," *Advances in Space Research*, 2017.

[55] D. Mandl, "Experimenting with sensor Webs using Earth Observing 1," *2004 IEEE Aerospace Conference*. IEEE, March 2004, vol. 1.

[56] M. A. Mansour and M. M. Dessouky, "A genetic algorithm approach for solving the daily photograph selection problem of the SPOT5 satellite," *Computers and Industrial Engineering*, vol. 58, no. 3, April 2010, pp. 509–520.

[57] F. Marinelli, S. Nocella, F. Rossi, and S. Smriglio, "A Lagrangian heuristic for satellite range scheduling with resource constraints," *Computers and Operations Research*, vol. 38, no. 11, November 2011, pp. 1572–1583.

[58] X. U. Ming and T. A. N. Tian, "A New Constellation Architecture for Practical Responsive Revisiting," *Transactions of the Japan Society for Aeronautical and Space Sciences*, vol. 57, no. 3, 2014, pp. 134–142.

[59] M. Mu, J. T. Randerson, G. R. van der Werf, L. Giglio, P. Kasibhatla, D. Morton, G. J. Collatz, R. S. DeFries, E. J. Hyer, E. M. Prins, D. W. T. Griffith, D. Wunch, G. C. Toon, V. Sherlock, and P. O. Wennberg, "Daily and 3-hourly variability in global fire emissions and consequences for atmospheric model predictions of carbon monoxide," *Journal of Geophysical Research: Atmospheres*, vol. 116, no. D24, December 2011.

[60] P. Murali, F. Ordóñez, and M. M. Dessouky, "Facility location under demand uncertainty: Response to a large-scale bio-terror attack," *Socio-Economic Planning Sciences*, vol. 46, no. 1, March 2012, pp. 78–87.

[61] M. J. Nadoushan and N. Assadian, "Repeat ground track orbit design with desired revisit time and optimal tilt," *Aerospace Science and Technology*, vol. 40, January 2015, pp. 200–208.

[62] G. G. Pacheco and R. Batta, "Forecast-driven model for prepositioning supplies in preparation for a foreseen hurricane," *Journal of the Operational Research Society*, vol. 67, no. 1, January 2016, pp. 98–113.

[63] M. Pontani and P. Teofilatto, "Satellite constellations for continuous and early warning observation: A correlation-based approach," *Journal of Guidance, Control, and Dynamics*, vol. 30, no. 4, July–August 2007, pp. 910–921.

[64] J. T. Randerson, Y. Chen, G. R. van der Werf, B. M. Rogers, and D. C. Morton, "Global burned area and biomass burning emissions from small fires," *Journal of Geophysical Research: Biogeosciences*, vol. 117, no. G4, December 2012.

[65] C. G. Rawls and M. A. Turnquist, "Pre-positioning and dynamic delivery planning for short-term response following a natural disaster," *Socio-Economic Planning Sciences*, vol. 46, no. 1, March 2012, pp. 46–54.

[66] Y. N. Razoumny, "Fundamentals of the route theory for satellite constellation design for Earth discontinuous coverage. Part 1: Analytic emulation of the Earth coverage," *Acta Astronautica*, vol. 128, November–December 2016, pp. 722–740.

[67] Y. N. Razoumny, "Fundamentals of the route theory for satellite constellation design for Earth discontinuous coverage. Part 2: Synthesis of satellite orbits and constellations," *Acta Astronautica*, vol. 128, November–December 2016, pp. 741–758.

[68] A. Rejaie and M. Shinozuka, "Reconnaissance of Golcuk 1999 earthquake damage using satellite images," *Journal of Aerospace Engineering*, vol. 17, no. 1, 2004, pp. 20–25.

[69] C. W. Rose and J. R. Wirthlin, "Using M and S to maximize space satellite data collection with multiple ground stations," *Procedia Computer Science*, vol. 8, 2012, pp. 124–129.

[70] B. Saboori, A. M. Bidgoli, and B. Saboori, "Multiobjective optimization in repeating sun-synchronous orbits design for remote-sensing satellites," *Journal of Aerospace Engineering*, vol. 27, no. 5, September 2014.

[71] T. Santoso, S. Ahmed, M. Goetschalckx, and A. Shapiro, "A stochastic programming approach for supply chain network design under uncertainty," *European Journal of Operational Research*, vol. 167, no. 1, November 2005, pp. 96–115.

[72] S. Sarno, M. D. Graziano, and M. D'Errico, "Polar constellations design for discontinuous coverage," *Acta Astronautica*, vol. 127, October–November 2016, pp. 367–374.

[73] W. Schroeder, E. Prins, L. Giglio, I. Csiszar, C. Schmidt, J. Morisette, and D. Morton, "alidation of GOES and MODIS active fire detection products using ASTER and ETM+ data," *Remote Sensing of Environment*, vol. 112, no. 5, May 2008, pp. 2711–2726.

[74] P. Sengupta, S. R. Vadali, and K. T. Alfriend, "Satellite orbit design and maintenance for terrestrial coverage," *Journal of Spacecraft and Rockets*, vol. 47, no. 1, January–February 2010, pp. 177–187.

[75] H. D. Sherali, T. B. Carter, and A. G. Hobeika, "A location-allocation model and algorithm for evacuation planning under hurricane/flood conditions," *Transportation Research Part B: Methodological*, vol. 25, no. 6, December 1991, pp. 439–452.

[76] R. Sherwood, S. Chien, R. Castano, and G. Rabideau, "Autonomous Planning and Scheduling on the TechSat 21 Mission," *AI 2002: Advances in Artificial Intelligence*, B. McKay and J. Slaney, eds. November 2002, vol. 2557 of *Lecture Notes in Computer Science*, pp. 213–224, Springer.

[77] D. J. Showalter and J. T. Black, "Responsive Theater Maneuvers via Particle Swarm Optimization," *Journal of Spacecraft and Rockets*, vol. 51, no. 6, November 2014, pp. 1976–1985.

[78] B. J. Soden, C. S. Velden, and R. E. Tuleya, "The impact of satellite winds on experimental GFDL hurricane model forecasts," *Monthly Weather Review*, vol. 129, no. 4, April 2001, pp. 835–852.

[79] M. Sofiev, R. Vankevich, M. Lotjonen, M. Prank, V. Petukhov, T. Ermakova, J. Koskinen, and J. Kukkonen, "An operational system for the assimilation of the satellite information on wild-land fires for the needs of air quality modelling and forecasting," *Atmospheric Chemistry and Physics*, vol. 9, no. 18, September 2009, pp. 6833–6847.

[80] D. Spiller, L. Ansalone, and F. Curti, "Particle Swarm Optimization for Time-Optimal Spacecraft Reorientation with Keep-Out Cones," *Journal of Guidance, Control, and Dynamics*, vol. 39, no. 2, February 2016, pp. 312–325.

[81] R. Sridharan, "The capacitated plant location problem," *European Journal of Operational Research*, vol. 87, no. 2, December 1995, pp. 203–213.

[82] P. Tangpattanakul, N. Jozefowiez, and P. Lopez, "A multi-objective local search heuristic for scheduling Earth observations taken by an agile satellite," *European Journal of Operational Research*, vol. 245, no. 2, September 2015, pp. 542–554.

[83] K. E. Tsiolkovsky, "Exploration of the universe with reaction machines," *The Science Review*, vol. 5, 1903.

[84] Y. Ulybyshev, "Geometric analysis and design method for discontinuous coverage satellite constellations," *Journal of Guidance, Control, and Dynamics*, vol. 37, no. 2, March 2014, pp. 549–557.

[85] D. A. Vallado, *Fundamentals of Astrodynamics and Applications*, second edition, Microcosm Press, El Segundo, California, 2001.

[86] T. L. van Zyl, I. Simonis, and G. McFerren, "The Sensor Web: systems of sensor systems," *International Journal Of Digital Earth*, vol. 2, no. 1, March 2009, pp. 16–30.

[87] R. M. VanSlyke and R. Wets, "L-Shaped Linear Programs with Applications to Optimal Control and Stochastic Programming," *SIAM Journal on Applied Mathematics*, vol. 17, no. 4, 1969, pp. 638–663.

[88] S. Vtipil and B. Newman, "Determining an Earth Observation Repeat Ground Track Orbit for an Optimization Methodology," *Journal of Spacecraft and Rockets*, vol. 49, no. 1, January 2012, pp. 157–164.

[89] J. Wang, X. Zhu, D. Qiu, and L. T. Yang, "Dynamic Scheduling for Emergency Tasks on Distributed Imaging Satellites with Task Merging," *IEEE Transactions on Parallel and Distributed Systems*, vol. 25, no. 9, September 2014, pp. 2275–2285.

[90] J. Wang, X. Zhu, L. T. Yang, J. Zhu, and M. Ma, "Towards dynamic real-time scheduling for multiple earth observation satellites," *Journal of Computer and System Sciences*, vol. 81, no. 1, February 2015, pp. 110–124.

[91] M. Wang, G. Dai, and M. Vasile, "Heuristic Scheduling Algorithm Oriented Dynamic Tasks for Imaging Satellites," *Mathematical Problems in Engineering*, 2014.

[92] P. Wang, G. Reinelt, P. Gao, and Y. Tan, "A model, a heuristic and a decision support system to solve the scheduling problem of an earth observing satellite constellation," *Computers and Industrial Engineering*, vol. 61, no. 2, September 2011, pp. 322–335.

[93] X.-W. Wang, Z. Chen, and C. Han, "Scheduling for single agile satellite, redundant targets problem using complex networks theory," *Chaos, Solitons and Fractals*, vol. 83, February 2016, pp. 125–132.

[94] E. A. Williams, W. A. Crossley, and T. J. Lang, "Average and maximum revisit time trade studies for satellite constellations using a multiobjective genetic algorithm," *The Journal of the Astronautical Sciences*, vol. 49, no. 3, 2001, pp. 385–400.

[95] W. J. Wolfe and S. E. Sorensen, "Three Scheduling Algorithms Applied to the Earth Observing Systems Domain," *Management Science*, vol. 46, no. 1, January 2000, pp. 148–166.

[96] G. Wu, J. Liu, M. Ma, and D. Qiu, "A two-phase scheduling method with the consideration of task clustering for earth observing satellites," *Computers and Operations Research*, vol. 40, no. 7, July 2013, pp. 1884–1894.

[97] G. Wu, M. Ma, J. Zhu, and D. Qiu, "Multi-satellite observation integrated scheduling method oriented to emergency tasks and common tasks," *Journal of Systems Engineering and Electronics*, vol. 23, no. 5, October 2012, pp. 723–733.

[98] G. Wu, W. Pedrycz, H. Li, M. Ma, and J. Liu, "Coordinated Planning of Heterogeneous Earth Observation Resources," *IEEE Transactions on Systems, Man, and Cybernetics: Systems*, vol. 46, no. 1, January 2016, pp. 109–125.

[99] L. Xiaolu, B. Baocun, C. Yingwu, and Y. Feng, "Multi satellites scheduling algorithm based on task merging mechanism," *Applied Mathematics and Computation*, vol. 230, March 2014, pp. 687–700.

[100] R. Xu, H. Chen, X. Liang, and H. Wang, "Priority-based constructive algorithms for scheduling agile earth observation satellites with total priority maximization," *Expert Systems with Applications*, vol. 51, June 2016, pp. 195–206.

[101] F. Yamazaki, M. Matsuoka, P. Warnitchai, S. Polngam, and S. Ghosh, "Tsunami Reconnaissance Survey in Thailand Using Satellite Images and GPS," *Asian Journal of Geoinformatics*, vol. 5, no. 2, May 2005, pp. 53–61.

[102] X. Zhai, X. Niu, H. Tang, L. Wu, and Y. Shen, "Robust Satellite Scheduling Approach for Dynamic Emergency Tasks," *Mathematical Problems in Engineering*, 2015.

[103] X. Zhang, N. Chen, and Z. Chen, "Spatial Pattern and Temporal Variation Law-Based Multi-Sensor Collaboration Method for Improving Regional Soil Moisture Monitoring Capabilities," *Remote Sensing*, vol. 6, no. 12, December 2014, pp. 12309–12333.

[104] K.-J. Zhu, J.-F. Li, and H.-X. Baoyin, "Satellite scheduling considering maximum observation coverage time and minimum orbital transfer fuel cost," *Acta Astronautica*, vol. 66, no. 1, February 2010, pp. 220–229.